

A&A manuscript no.

(will be inserted by hand later)

Your thesaurus codes are:

06 (08.01.1; 08.06.3; 08.08.2; 08.16.4; 08.22.3 10.08.1;

ASTRONOMY
AND
ASTROPHYSICS

A spectroscopic study of field BHB star candidates^{*,**}

T. Kinman¹, F. Castelli², C. Cacciari³, A. Bragaglia³, D. Harmer¹, and F. Valdes¹

¹ Kitt Peak National Observatory, National Optical Astronomy Observatories, Box 26732, Tucson, AZ 85726-6732, U.S.A.
email: kinman@noao.edu

² CNR-Gruppo Nazionale Astronomia and Osservatorio Astronomico di Trieste, v. Tiepolo 11, I-34131 Trieste, Italy.
email: castelli@ts.astro.it

³ Osservatorio Astronomico di Bologna, v. Ranzani 1, I-40127 Bologna, Italy.
email: cacciari@bo.astro.it, angela@bo.astro.it

Received 23 February 2000 / Accepted 7 June 2000

Abstract. New spectroscopic observations are presented for a sample of thirty-one blue horizontal branch (BHB) star candidates that are sufficiently nearby to have reliable proper motions. Comments are given on a further twenty-five stars that have previously been suggested as BHB star candidates but which were not included in our sample. Moderately high-resolution spectra ($\lambda/\Delta\lambda \approx 15000$) of twenty five of our program stars were taken with the coude feed spectrograph at Kitt Peak. Twelve of the program stars were also observed with the CAT spectrograph at ESO. Six of these program stars were observed from both hemispheres. IUE low-resolution spectra are available for most of our candidates and were used, in addition to other methods, in the determination of their T_{eff} and reddening. A compilation of the visual photometry for these stars (including new photometry obtained at Kitt Peak) is also given. Abundances were obtained from these spectra using models computed by Castelli with an updated version of the ATLAS9 code (Kurucz 1993a).

All thirty one candidates are halo stars. Of these, twenty eight are classified as BHB stars because:

- (1) they lie close to the ZAHB (in a similar position to the BHB stars in globular clusters) in the T_{eff} versus $\log g$ plot. For all but one of these stars, far-UV data were available which were consistent with other data (Strömgren photometry, energy distributions, $H\gamma$ profiles) for deriving T_{eff} and $\log g$.
- (2) they have a distribution of $v \sin i$ ($\leq 40 \text{ km s}^{-1}$) that is similar to that found for the BHB in globular clusters. Peterson et al. (1995) and Cohen & McCarthy (1997) have shown that the BHB stars in the globular clusters M13 and M92 have a higher $v \sin i$ ($\leq 40 \text{ km s}^{-1}$) than

those in M3 and NGC 288 ($\leq 20 \text{ km s}^{-1}$). The mean deprojected rotational velocity (\overline{v}) was calculated for both the two globular clusters and the nearby BHB star samples. A comparison of these suggests that both globular cluster $v \sin i$ types are present in our nearby sample. No obvious trend is seen between $v \sin i$ and either $(B - V)_0$ or $[\text{Fe}/\text{H}]$.

- (3) they have $-0.99 \geq [\text{Fe}/\text{H}] \geq -2.95$ (mean $[\text{Fe}/\text{H}] -1.67$; dispersion 0.42 dex), which is similar to that found for field halo RR Lyrae and red HB stars. These local halo field stars appear (on average) to be more metal-poor than the halo globular clusters. The local sample of red giant stars given by Chiba & Yoshii (1998) contains a greater fraction of metal-poor stars than either our halo samples or the halo globular clusters. The stars in our sample that have a T_{eff} that exceeds about 8500 K show the He I ($\lambda 4471$) line with a strength that corresponds to the solar helium abundance.
- (4) they show a similar enhancement of the α -elements ($\langle [\text{Mg}/\text{Fe}] \rangle = +0.43 \pm 0.04$ and also $\langle [\text{Ti}/\text{Fe}] \rangle = +0.44 \pm 0.02$) to that found for other halo field stars of similar metallicity.

Key words: Stars: abundances – Stars: fundamental parameters – Stars: horizontal branch – Stars: AGB and post-AGB – Stars: variables: RR Lyrae – Galaxy: halo

1. Introduction

The *field* blue horizontal branch (BHB) stars have often been used to trace the galactic halo. Recent surveys of *distant BHB stars* include those of Pier (1983), Sommer-Larsen & Christensen (1986), Flynn & Sommer-Larsen (1988), Sommer-Larsen et al. (1989), Preston et al. (1991), Arnold & Gilmore (1992), Kinman et al. (1994, hereafter KSK), Beers et al. (1996) and Sluis & Arnold (1998).

The *nearby BHB stars* have been discovered sporadically over the past sixty years – the majority by Strömgren 4-colour photometry. Pre-eminent among the

Send offprint requests to: T. Kinman

* Based on observations obtained at KPNO, operated by the Association of Universities for Research in Astronomy, Inc., under contract with the National Science Foundation, and the European Southern Observatory, Chile.

** Tables 4 and 5 are only available in electronic form at the CDS via anonymous ftp to cdsarc.u-strasbg.fr

discoverers have been A. G. Davis Philip (Philip 1994) and Stetson (1991). The only attempt, however, to obtain a complete sample of the nearby BHB stars (and hence a local space density) appears to be that by Green & Morrison (1993). Following Philip et al. (1990), they showed that a BHB star must not only have the appropriate Strömgren ($b-y$) and c_1 indices, but must also show little or no rotational broadening in high-resolution spectra. This criterion must now be somewhat modified since Peterson et al. (1995) found BHB stars with $v \sin i$ as large as 40 km s^{-1} in the globular cluster M13. Philip et al. also considered that a BHB star must have an appropriate location in the $C(19-V)_0$ vs. $(b-y)_0$ diagram¹. In the solar neighbourhood, disk stars greatly outnumber halo stars and there is a relatively high probability of finding disk objects whose Strömgren indices are close to those of BHB stars. To emphasize this, we give, in the Appendix A, a non-exhaustive list of stars whose colours resemble those of BHB stars but which most probably do not belong to this category. *The use of high-resolution spectra is mandatory for the selection of BHB stars in the solar neighbourhood since both accurate abundances and $v \sin i$ are needed as criteria.*

High resolution studies of nearby RR Lyrae stars have been made by Clementini et al. (1995) and by Lambert et al. (1996). Both the RR Lyrae and BHB stars may be expected to have similar galactic kinematics. There are, however, *disk* RR Lyrae stars in the nearby field, but there are (as far as we know) no corresponding nearby field BHB stars that have disk kinematics².

While it is known that the field BHB stars generally show the low metal abundances that characterize halo stars, early determinations of these abundances show a rather wide scatter (see Table A27 in KSK). The first reliable determination was probably that based on the co-added photographic spectra of HD 161817 by Adelman et al. (1987). The metallic lines in the visible spectra of BHB stars are relatively weak and early photographic spectra did not have adequate signal-to-noise to measure these lines with sufficient accuracy. Also, until relatively recently, it was not known with certainty whether or not the evolution from the tip of the giant branch to the blue end of the horizontal branch (with significant mass-loss) would change the composition in the stellar atmospheres and whether diffusion effects would be present. Glaspey et al. (1989) observed two HB stars in the globular cluster NGC 6752. The hotter (16 000 K) showed low rotation, a strong overabundance of iron and a helium deficiency.

The cooler (10 000 K) showed a higher rotation and no abundance anomalies compared to the red giants in the cluster. An example of a hot (16 430 K) field HB star is Feige 86 which was analyzed by Bonifacio et al. (1995). They found overabundances of the heavy elements and other peculiarities which might be attributed to diffusion. Lambert et al. (1992) used an echelle spectrograph with a CCD detector to obtain moderately high-resolution spectra ($\lambda/\Delta\lambda \approx 18\,000$) of two BHB stars (with $T_{\text{eff}} \leq 10\,000 \text{ K}$) in the globular clusters M4 and NGC 6397. They found that their metallicities agreed well with those found previously for the red giants in these clusters. Caloi (1999) proposed that the gap observed in the HB sequence in many globular clusters at a $(B-V)$ of about zero is a surface phenomenon and that stars with $T_{\text{eff}} > 10\,000 \text{ K}$ will show peculiar chemical compositions. Grundahl et al. (1999) have noted that a jump in both Strömgren u and $\log g$ occurs for stars hotter than $T_{\text{eff}} = 11\,500 \text{ K}$ in the EHB of globular clusters and suggest that this marks the onset of radiative levitation. This would explain the results of Glaspey et al. (1989) and the more recent discoveries of strong overabundances of Fe in these hotter stars in the globular clusters NGC 6752 (Moehler et al. 1999) and M13 (Behr et al. 1999). Behr et al. (2000) find that the HB stars in M13 that are cooler than $T_{\text{eff}} = 11\,000 \text{ K}$ have high rotation ($v \sin i \sim 40 \text{ km s}^{-1}$) while the hotter stars have a low rotation as might be expected if radiative levitation is operating.

All stars in our sample are cooler than 11 000 K because hotter stars cannot easily be identified as BHB stars by their Strömgren indices. We should therefore expect them to have chemical abundances that are similar to those of other halo field stars such as halo RR Lyrae stars and halo red giants. We should not expect abundance anomalies to be present, and none have been reported, in the cooler field BHB stars that have previously been observed. In addition to HD 161817 (Adelman & Hill 1987), abundances have been derived from CCD spectra for ten other nearby field BHB stars (Adelman & Philip 1990, 1992, 1994, 1996a, 1996c). We consider that the abundances of BHB stars based on photographic spectra by Klochkova & Panchuk (1990) are less accurate because of the poor agreement of their equivalent widths with those obtained from CCD spectra.

The aim of the present study is to provide data for a reliable sample of the BHB stars in the solar neighbourhood. This includes the colour distribution, the reddenings, the stellar parameters, the projected stellar rotations ($v \sin i$) and the abundance ratios. These data can be compared with data for BHB in globular clusters and in other parts of the galaxy. The galactic orbits of about half the stars in our present sample have recently been calculated and analyzed by Altmann & de Boer (2000). It is intended, in a future paper, to derive the galactic orbits not only for this BHB sample but also for other local samples of halo stars so that these may be compared. These samples can

¹ The $C(19-V)$ index is derived from the magnitude at 1900\AA in IUE spectra and the V magnitude of the star.

² One BHB star is known in the old metal-rich galactic cluster NGC 6791 (Green et al. 1996) and extended blue horizontal branches have been found in the two disk metal-rich globular clusters NGC 6388 and NGC 6441 by Rich et al. (1997). A search for metal-rich BHB stars in the galactic bulge has been started by Terndrup et al. (1999).

help us to determine a better overall definition of the local halo and determine to what extent it may be distinguished from the disk populations³.

2. The Selection of Candidates: notes on the individual objects

Green & Morrison (1993) found 10 BHB stars among the 23 candidates that they studied and considered that their sample was incomplete for BHB stars with $V > 8.5$. Many *nearby* BHB stars have been identified among high proper motion stars and so any sample of them will have kinematic bias. Thus Stetson (1991) made 4-colour observations of high proper motion early-type stars taken from the SAO Catalogue. More bright BHB stars might well be discovered by using a more recent source of proper motions such as the PPM Star Catalogue (Röser & Bastian 1991) in which a larger fraction of the stars have spectral types. To do this, even for a part of the sky, would be a large undertaking and we have therefore chosen to limit our observations to previously identified BHB star candidates. Strömgren photometry can only be used to distinguish BHB stars that are redder than $(b - y) \sim -0.01$ mag, so that the hotter stars (belonging to the extended horizontal branch) are excluded. This paper enlarges the local sample of definite BHB stars, but does not affect our knowledge of the local BHB space density because this depends only on the number of the very brightest of these stars. Our sample is limited to stars that are brighter than $V = 10.9$; these stars are near enough to have significant proper motions and bright enough for their high-resolution spectra to be obtainable with the Kitt Peak coude feed spectrograph and with the ESO-CAT spectrograph.

Thirty-one nearby BHB candidates were selected from the literature. BD +00 0145 was listed by Huenemoerder et al. (1984). Twelve candidates were described by Philip (1984) who gave finding charts and some references to their original identification. These same stars and a (FHB) numbering system are also given in a more recent compilation and discussion of BHB star candidates by Gray et al. (1996). The remaining eighteen candidates were identified as possible HB stars by Stetson (1991) as a result of his 4-colour photometry of high proper motion A stars; some of these had been identified earlier as BHB stars as noted below.

HD 2857 (FHB No. 61) Noted by Oke et al. (1966).

HD 4850 Stetson (1991).

BD +00 0145 Noted by Cowley (1958). Kilkenny (1984) classified it as A0 from his 4-colour photometry. Our

colours ($(B - V) = +0.04$, $(u - B)_K = +1.83$) would not make it a BHB star if the reddening given by the maps of Schlegel et al. (1998, hereafter SFD) ($E(B - V) = 0.028$) is correct. Huenemoerder et al. (1984) included it in their list of HB stars but derived a high gravity ($\log g = 3.9$) for this star. We find a similar gravity that is too high for it to be a BHB star.

HD 8376 Stetson (1991).

HD 13780 Stetson (1991).

HD 14829 (FHB No. 23) Philip (1969).

HD 16456 Stetson (1991). This is the type c RR Lyrae star CS Eri which was discovered by Przybylski (1970).

HD 31943 Stetson (1991).

HD 252940 Stetson (1991).

HD 60778 (FHB No. 47). Noted by Roman (1955a).

HD 74721 (FHB No. 48). Noted by Roman (1955a). Adelman & Philip (1996a) give $[\text{Fe}/\text{H}] = -1.40$ (see Sect. 10.1).

HD 78913 Stetson (1991).

HD 86986 (FHB No. 66). Noted by Oke et al. (1966). Adelman & Philip (1996a) give $[\text{Fe}/\text{H}] = -1.80$ (see Sect. 10.1).

HD 87047 Stetson (1991).

HD 87112 Stetson (1991).

HD 93329 Stetson (1991). Adelman & Philip (1996a) give $[\text{Fe}/\text{H}] = -1.40$ (see Sect. 10.1).

BD +32 2188 (FHB No. 1) Originally noted by Slettebak & Stock (1959), Gray et al. (1996) described this star as “UV bright” or “above horizontal branch”. Mitchell et al. (1998) refer to this star as SBS 10. They derive $T_{\text{eff}} = 11\,200$ K and $\log g = 2.2$ from c_1 and the equivalent widths of $\text{H}\gamma$ & $\text{H}\delta$ and $T_{\text{eff}} = 10\,700$ K and $\log g = 2.28$ from a fit of the observed high-resolution spectrum to a grid of synthetic spectra. They classify it as a post-AGB star in their T_{eff} vs $\log g$ diagram in which the star lies close to the track for a $0.546 M_{\odot}$ post-AGB star (Schönberner 1983). Our results agree with this classification.

HD 106304 Stetson (1991). This star had previously been classified as a metal-poor HB star by Przybylski (1971).

BD +42 2309 (FHB No. 03). Identified as a BHB star by Philip (1967).

HD 109995 (FHB No. 67). Originally noted by Slettebak, Bahner & Stock (1961), an early abundance analysis was made by Wallerstein & Hunziker (1964). Adelman & Philip (1994) give $[\text{Fe}/\text{H}] = -1.89$ (see Sect. 10.1).

BD +25 2602 Stetson (1991). Identified as an HB star by Hill et al. (1982).

HD 117880 (FHB No. 49). Noted by Roman (1955a, 1955b) whose radial velocity (-44.6 km s^{-1}) differs completely from that given by Greenstein & Sargent (1974: $+141 \text{ km s}^{-1}$) and by Kilkenny & Muller (1989) with which our velocity agrees. Adelman & Philip (1992) observed this star but only give an abundance from two Si II lines.

³ For instance Majewski (1999) questions whether there is any difference between populations that have been identified as “Intermediate Population II” and as the “Flat halo”. If the concept of stellar populations is to be useful, there is a continual need to refine the definitions of each population so that misunderstandings are less likely to occur.

HD 128801 Stetson (1991). Adelman & Philip (1996a) give $[\text{Fe}/\text{H}] = -1.26$ (see Sect. 10.1). The $[\text{Ca}/\text{Fe}]$ ratio which they derive (-1.03) is very low.

HD 130095 (FHB No. 68). First suggested to be a halo star by Luyten (1957) (as CoD -26 10505) and later by Greenstein & Eggen (1966). Found to be a velocity variable by Przybylski & Kennedy (1965b) and also Hill (1971). It does not, however, show light variations (ESA Hipparcos Catalogue 1997) nor was it found to be a photometric binary by Carney (1983). Adelman & Philip (1996a) give $[\text{Fe}/\text{H}] = -2.03$ (see Sect. 10.1). HD 130201 Stetson (1991).

HD 139961 Stetson (1991). This star was first noted as an HB star by Graham & Doremus (1968). It is NSV 7204 in the New Catalogue of Suspected Variable stars (1982). Corben et al. (1972) found a range of 0.08 magnitudes in V over six observations. It does not appear to be variable according to the ESA Hipparcos Catalogue (1997).

HD 161817 (FHB No. 69). Albitzky (1933) took the first spectrum of HD 161817 and noted its large radial velocity. Slettebak (1952) gives a referenced account of the early spectroscopic observations of this star. Burbidge & Burbidge (1956) were the first to show that it was a metal-weak Population II star. Other early abundance determinations are mentioned by Takeda & Sadakane (1997) who made a non-LTE study of its C, N, O and S abundances. They adopted $T_{\text{eff}} = 7500$ K and $\log g = 3.0$ and found $v \sin i$ from between 14.3 km s $^{-1}$ and 15.9 km s $^{-1}$. Their re-analysis of Adelman & Philips (1994) data leads to $[\text{Fe}/\text{H}] \simeq -1.5$; Adelman & Philip (1994) and Adelman & Philip (1996a) derived $[\text{Fe}/\text{H}] = -1.74$ and $[\text{Fe}/\text{H}] = -1.66$ respectively (see also Sect. 10.1)

HD 167105 Stetson (1991). Adelman & Philip (1996a) give $[\text{Fe}/\text{H}] = -1.80$ (see Sect. 10.1).

HD 180903 Stetson (1991).

HD 202759 (FHB No. 70). Noted by MacConnell et al. (1971) as a probable HB star. It was shown by Przybylski & Bessell (1974) to have a very low V amplitude (0.075 mag) with a period of 11.5 hours; it is classified as a type c RR Lyrae star (AW Mic). Przybylski & Bessell deduced from its colour that this star must be very close to the blue edge of the instability strip; they derived a T_{eff} of 7400 K and $\log g = 3.1$ in good agreement with the values derived by us. It was confirmed spectroscopically as an HB star by Kodaira & Philip (1984). Adelman & Philip (1990) give $[\text{Fe}/\text{H}] = -2.36$ (see Sect. 10.1)

HD 213468 Stetson (1991). The large radial velocity was discovered by Przybylski & Kennedy (1965a) and it was noted as a probable HB star by MacConnell et al. (1971).

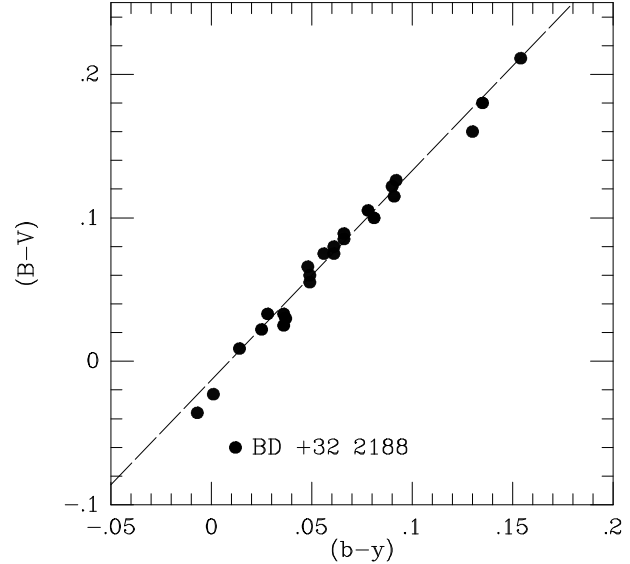


Fig. 1. A plot of $(B - V)$ against $(b - y)$ for the program BHB star candidates. These colours show a close linear relationship except for the PAGB star BD +32 2188.

3. Photometric observations in the visible spectrum

Table 1 is a compilation of both existing and new photometry for all our BHB candidates except for the RR Lyrae variable HD 016456⁴. The final adopted photometry is given in boldface.

The new photometric observations were made by Kinman with the Mk III photometer on the Kitt Peak 1.3-m telescope (with chopping secondary) on the $(uBV)_K$ system as described by KSK. Additional $(uBV)_K$ observations were also made with the Kitt Peak 0.9-m telescope using a 512×512 CCD under control of the CCDPHOT program; details of this observing system are given by Kinman (1998). The $(uBV)_K$ photometry gives $(B - V)$ on the Johnson system and a hybrid $(u - B)_K$ index from the Strömgren u filter and the Johnson B filter. The $(u - B)_K$ vs $(B - V)$ diagram can be used to separate BHB from other stellar types as described by KSK. A $(u - B)_K$ vs $(B - V)$ diagram using the most recent data is shown in Fig. 3 of Kinman (1998). There is a satisfactory separation of the BHB stars and RR Lyrae stars with $(B - V) \geq 0.00$, but bluer than this the separation becomes rapidly more difficult. The $(u - B)_K$ vs $(B - V)$ diagram gives a satisfactory way of distinguishing fainter BHB stars at high galactic latitudes because the risk of confusion with other types of early-type stars is not too severe and the integration times are smaller than for the

⁴ The amplitude of this RR Lyrae is large enough ($\Delta V \sim 0.5$ mag) for its colours to be quite variable. Although Strömgren photometry for this star is given by Gray & Olsen (1991) and Stetson (1991), there are not enough individual observations (with phases) to determine the stellar parameters.

Table 1. Summary of Photometric Data for Horizontal Branch Star Candidates

No.	Object	V	$(B - V)$	$(u - B)_K$	$(b - y)$	β	m_1	c_1	$(V - K)$	Source [‡]
(1)	(2)	(3)	(4)	(5)	(6)	(7)	(8)	(9)	(10)	(11)
1	HD 2857	9.990 9.990	+0.180 +0.180	2.094 2.094	... +0.135	2.787 2.787	... 0.113	... 1.212	... 0.67	K(19,27,4) (1)
2	HD 4850	9.619	+0.066	...	0.048	2.846	0.132	1.282	...	(2)(3)
3	BD +00 0145	10.58 10.58	+0.040 +0.040	1.831 1.831	... +0.023	2.897 2.897	... 0.154	... 1.032	K(7,8,3) (4)(5)
4	HD 8376	9.640 9.655	+0.126 +0.126	2.123 2.123	... +0.092	2.820 2.835	... 0.104	... 1.273	K(11,15,7) (3)
5	HD 13780	9.811	+0.088	2.816	0.119	1.285	...	(3)
6	HD 14829	10.29 10.306	+0.033 +0.033	2.004 2.004	... +0.036	2.858 2.858	... 0.135	... 1.241	... 0.15	K(11,11,6) (2) (6)
7	HD 31943	8.262	+0.083	2.814	0.142	1.226	...	(1) (3)
8	HD 252940	9.090 9.098	+0.211 +0.211	2.115 2.115	... +0.159	2.769 2.768	... 0.091	... 1.215	K(14,17,8) (1) (3)
9	HD 60778	9.090 9.103	+0.104 +0.105	2.104 2.104	... +0.078	2.833 2.834	... 0.118	... 1.294	... 0.41	K(8,8,6) (1) (3)
10	HD 74721	8.700 8.713	+0.033 +0.033	2.028 2.028	... +0.028	2.857 2.859	... 0.127	... 1.273	... 0.20	K(12,12,6) (1) (3)
11	HD 78913	9.285	+0.089	...	+0.066	2.842	0.118	1.281	...	(1) (3)
12	HD 86986	8.000 8.000	+0.121 +0.122	2.103 2.103	... +0.092	2.809 2.825	... 0.109	... 1.278	... 0.48	K(11,5,4) (1) (3)
13	HD 87047	9.740 9.752	+0.112 +0.115	2.084 2.084	... +0.091	2.796 2.797	... 0.105	... 1.273	K(6,12,8) (3)
14	HD 87112	9.710 9.717	-0.023 -0.023	1.860 1.860	... +0.001	2.839 2.840	... 0.115	... 1.161	K(7,10,6) (3)
15	HD 93329	8.780 8.790	+0.080 +0.080 +0.060	2.814 2.825	... 0.123	... 1.315	K(3,9,5) (1)(3)(8)
16	BD +32 2188	10.750 10.756	-0.050 -0.060 +0.012	... 2.633**	... 0.069	... 0.921	K(1,2) (1)
17	HD 106304	9.069	+0.022	...	+0.025	2.845	0.114	1.162	...	(1) (3)
18	BD +42 2309	10.771	+0.030	...	+0.037	2.844*	0.134	1.259	...	(1)(3)
19	HD 109995	7.630 7.602	+0.052 +0.055	2.083 2.083	... +0.049	... 2.848	... 0.117	... 1.305	... 0.30	K(1,4) (1)(3)

Table 1. Summary of Photometric Data for Horizontal Branch Star Candidates (continued)

No.	Object	V	$(B - V)$	$(u - B)_K$	$(b - y)$	β	m_1	c_1	$(V - K)$	Source [‡]
(1)	(2)	(3)	(4)	(5)	(6)	(7)	(8)	(9)	(10)	(11)
20	BD +25 2602	10.120 10.120	+0.070 +0.060	2.056 2.056	... +0.048	... 2.850	... 0.128	... 1.298	K(1,1) (1)(3)
21	HD 117880	9.064	+0.075	...	+0.056	2.855	0.125	1.207	0.25	(1) (3)
22	HD 128801	8.730 8.738	-0.036 -0.036	1.745 1.745	... -0.005	... 2.816	... 0.109	... 1.056	K(5,11) (1)(3)
23	HD 130095	8.128	+0.085	...	+0.065	2.855	0.108	1.256	0.31	(1)(3)
24	HD 130201	10.110	+0.075	...	+0.061	2.860	0.109	1.245	...	(1)(3)
25	HD 139961	8.860	+0.100	...	+0.078	2.858	0.115	1.298	...	(1)(3)
26	HD 161817	6.976	+0.160	...	+0.127	2.746	0.100	1.197	0.61	(1)(3)
27	HD 167105	8.966	+0.025	...	+0.036	2.849	0.120	1.260	...	(1)(3)(8)
28	HD 180903	9.568	+0.174	2.800	0.095	1.255	...	(1)(3)
29	HD 202759	09.09v	+0.178	2.770	0.082	1.164	...	(1)(3)
30	HD 212468	10.926	+0.009	...	+0.018	2.849	0.126	1.246	...	(1)(3)

[‡] (K)(m,n,o): new observations by Kinman where m and n are the number of nights and the total number of BV observations and o is the total number of observations of β .

Other sources used to form adopted values (columns 3 to 9):

(1) Hauck & Mermilliod (1998); (2) Alexander & Carter 1971; (3) Stetson 1991; (4) Klemola 1962; (5) Kilkeny 1984; (6) Gray et al. 1996; (7) Cousins 1972; (8) Oja 1987; (9) ESA Hipparcos Catalogue, 1997 (for V magnitudes) ($V - K$) (column 10) are from Arribas & Martinez Roger (1987).

[†] The value of β is derived from observations by Philip & Tift (1971) only.

^{**} Mean of Hauck & Mermilliod catalogue value and single observation by Kinman (2.644 ± 0.010)

^{*} Mean of Hauck & Mermilliod catalogue value and single observation by Kinman (2.873 ± 0.015)

Strömgren photometry; this is an important consideration for faint stars. In the solar neighbourhood, however, there is a wide variety of early-type stars and these diagrams can only be used to provide BHB candidates.

Some idea of the accuracy of the adopted photometric data can be appreciated from the plots of $(b - y)$ against $(B - V)$ shown in Fig. 1. With the exception of the Post-AGB star (BD +32 2188), which has a lower gravity than the remaining stars, the BHB star candidates approximately follow the linear relationship:

$$B - V = 1.459(b - y) - 0.013$$

which is shown by the dashed line in Fig 1. None of the BHB stars depart from this relation by more than 0.01 mag in $(b - y)$. This suggests that these quantities

are not likely to be in error by more than one or two hundredths of a magnitude.

Hipparcos magnitudes (which are of high accuracy and on a very homogeneous system) are available for twenty one of the thirty stars given in Table 1. It was found that the difference (ΔV) between the Hipparcos magnitude and the mean V magnitude⁵ for our BHB star candidates could be expressed as the following linear function of $(B - V)$:

$$\Delta V = 0.002 + 0.275(B - V)$$

The Hipparcos Catalogue (Vol. 1) (1997) gives values of ΔV for various $(V - I)$ in Table 1.3.5 and values of $(V - I)$ for different $(B - V)$ in Table 1.3.7. Thus the catalogue values of ΔV may be obtained for various $(B - V)$. These

⁵ The observations of Stetson (1991) were given double weight in forming these means.

Table 2. Journal of KPNO spectra of BHB star candidates

Star	RA (J2000)	Dec (J2000)	V	Date	Start	T	S/N	Rad. Vel.	no. of	σ
(1)	(2)	(3)	(4)	(UT)	(UT)	(min.)	(8)	(km s ⁻¹)	lines	(km s ⁻¹)
HD 2857	00:31:53.8	-05:15:43	9.99	1994 Sep 06	06:41	60	124	-155.7	9	0.9
BD +00 0145	00:56:26.9	+01:43:45	10.58	1994 Sep 06	07:47	60	...	-261.0	1	...
HD 8376	01:23:27.8	+31:47:13	9.66	1994 Sep 06	09:01	60	114	+143.8	7	1.1
HD 14829	02:23:09.2	-10:40:38	10.30	1995 Jan 01	03:18	60	...	-177.0	1	...
HD 16456 ^{a,b}	02:37:05.8	-42:57:48	9.0v	1995 Jan 09	02:05	60	063	-139.8	7	0.4
HD 31943 ^b	04:57:40.7	-43:01:58	8.26	1995 Jan 09	04:22	45	092	+088.2	11	0.8
				1995 Jan 09	05:08	45	104	+088.7	11	0.7
HD 252940	06:11:37.2	+26:27:30	9.10	1995 Jan 07	04:25	40	100	+160.5	8	0.7
				1995 Jan 09	03:10	40	106	+159.4	9	0.8
HD 60778	07:36:11.7	-00:08:16	9.10	1995 Jan 07	07:24	50	121	+041.1	11	0.7
HD 74721	08:45:59.2	+13:15:49	8.71	1995 Jan 07	08:23	22	108	+030.7	9	0.6
HD 86986	10:02:29.6	+14:33:26	8.00	1995 Jan 07	08:49	12	096	+009.3	9	0.7
HD 87047	10:03:12.8	+31:03:19	9.75	1995 Jan 07	09:05	60	105	+137.2	7	0.4
HD 87112	10:04:38.8	+57:49:56	9.71	1995 Jan 07	10:11	60	086	-171.9	7	0.9
HD 93329	10:46:36.7	+11:11:03	8.79	1995 Jan 09	11:20	60	108	+205.2	8	0.7
BD +32 2188	11:47:00.5	+31:50:09	10.74	1995 May 04	04:13	67	072	+091.6	11	1.5
BD +42 2309	12:28:22.2	+41:38:53	10.77	1995 May 02	04:00	60	078	-145.3	8	1.7
HD 109995	12:38:47.6	+39:18:32	7.60	1995 May 03	03:18	20	136	-129.0	8	0.9
				1995 May 03	03:40	20	175	-130.1	7	1.1
BD +25 2602	13:09:25.6	+24:19:25	10.12	1995 May 03	04:06	60	099	-067.0	8	1.4
HD 117880	13:33:29.8	-18:30:54	9.06	1995 May 04	06:25	60	137	+144.7	6	0.5
HD 128801	14:38:48.1	+07:54:40	8.74	1995 May 04	07:28	40	171	-081.1	6	0.9
HD 130095 ^b	14:46:51.9	-27:14:50	8.13	1995 May 03	07:08	30	130	+066.0	5	0.7
HD 139961 ^b	15:42:52.9	-44:56:41	8.86v	1995 May 03	08:24	50	097	+145.3	5	0.5
				1995 May 04	08:27	60	100	+143.2	9	2.2
HD 161817	17:46:40.6	+25:44:57	6.97	1994 Sep 06	02:30	10	205	-363.8	10	0.6
				1995 May 03	10:22	20	203	-362.7	10	0.6
HD 167105	18:11:06.4	+50:47:32	8.96	1995 May 04	09:38	50	183	-173.6	10	2.0
HD 180903 ^b	19:19:16.3	-24:23:11	9.57	1995 May 04	10:37	60	100	+103.7	11	0.8
HD 202759 ^{a,b}	21:19:05.9	-33:55:08	9.09v	1994 Sep 06	05:08	60	108	+021.3	8	0.6

^a RR Lyrae variable.^b Also observed with ESO-CAT.

ΔV agree well with our linear relation at a $(B - V)$ of 0.00 and 0.22 but are up to 0.01 magnitudes larger at intermediate $(B - V)$. The catalogue ΔV are for “early type stars” and we have preferred our relation because it refers to the specific class of stars that we are studying. Our linear relation was therefore used to convert the Hipparcos magnitudes to V magnitudes and these are our adopted magnitudes. If no Hipparcos magnitude is available, the weighted mean V magnitude was adopted.

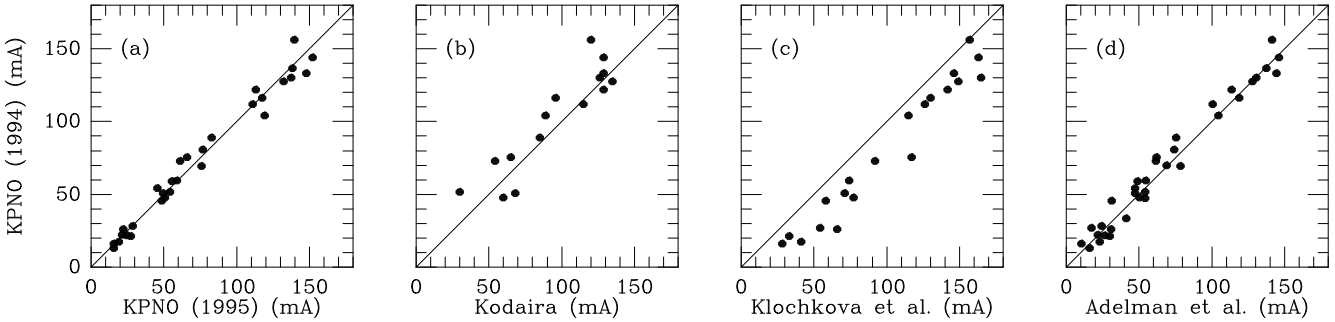
Significant systematic differences exist between values of the Strömgren β -index made by different observers (Joner & Taylor 1997). Fortunately, many of the BHB candidates have been observed by Stetson (1991) and were therefore on one system. New β observations of a selection of our candidates were made using BHB (and other stars of similar colour that were observed by Stetson) as stan-

dards so as to be on his system⁶. These new β values are given in the first line of Table 1, when the source K(n,m,o) is given. It should be noted that the large radial velocities of BHB stars can cause their $H\beta$ line to be shifted (in the case of HD 161817 by as much as 6 Å) from the rest wavelength. The FWHM of the narrow $H\beta$ filter is only 30 Å, so that small inaccuracies may be expected from this cause. As a check, synthetic β indices were determined by measuring the “magnitudes” of the $H\gamma$ -line through 30Å and 150Å bandpasses in our spectra (which do not include $H\beta$) using the *magband* routine in the CTIO package of IRAF. It was found that these synthetic β indices (on the

⁶ The Strömgren β index is very valuable because it is not changed by interstellar extinction but it does require measuring to a high accuracy to be useful. The central wavelength of the narrow $H\beta$ filter undoubtedly shifts with temperature and this means that careful calibration is needed in order to get onto the standard system.

Table 3. Journal of ESO-CAT spectra of BHB star candidates.

Star	RA(J2000)	Dec(J2000)	V	Date	Start	T	S/N	Rad. Vel.	no. of	σ
(1)	(2)	(3)	(4)	(5)	(6)	(7)	(8)	(9)	(10)	(11)
HD 4850	00:49:59.7	-47:17:34	9.62	1995 Sep 09	04:38	70	60	-041.7	10	0.6
				1995 Sep 09	07:39	60	60	-041.8	8	0.6
HD 13780	02:12:51.4	-49:03:17	9.80	1995 Sep 09	05:52	45	50	+025.4	9	1.0
				1995 Sep 09	06:40	45	40	+025.4	9	1.0
HD 16456 ^{a,b}	02:37:05.8	-42:57:48	9.0v	1995 Sep 09	09:43	30	65	-158.9	9	0.8
HD 31943 ^b	04:57:40.7	-43:01:58	8.26	1995 Sep 09	08:50	40	80	+084.9	12	3.5
HD 78913	09:06:55.0	-68:29:22	9.28	1995 Apr 29	00:26	70	105	+316.8	7	0.7
HD 106304	12:13:53.6	-40:52:25	9.07	1995 Apr 29	01:48	60	85	+115.4	3	1.0
HD 130095 ^b	14:46:51.9	-27:14:50	8.13	1995 Apr 29	02:58	20	65	+065.6	3	0.8
HD 130201	14:48:19.9	-45:40:12	10.11	1995 Apr 29	03:46	60	45	+069.7	2	1.0
				1995 Apr 29	04:49	60	40	+069.3	2	1.0
HD 139961 ^b	15:42:52.9	-44:56:41	8.86v	1995 Apr 29	06:12	40	65	+142.6	4	0.8
HD 180903 ^b	19:19:16.3	-24:23:11	9.57	1995 Apr 29	09:19	45	45	+105.6	9	1.1
HD 202759 ^{a,b}	21:19:05.9	-33:55:08	9.09v	1995 Apr 29	07:03	40	55	+027.5	5	1.0
				1995 Sep 09	00:08	60	65	+018.5	10	0.7
HD 213468	22:32:17.3	-42:34:49	10.92	1995 Sep 09	02:12	60	25	-174.3	3	0.8
				1995 Sep 09	03:15	60	35	-173.6	5	0.5

^a RR Lyrae variable.^b Also observed at Kitt Peak.**Fig. 2.** Comparison of the equivalent widths of the lines in HD 161817 in a KPNO spectrum taken in 1994 with **a** those from a KPNO spectrum taken in 1995; **b** those given by Kodaira (1964); **c** those given by Klochkova and Panchuk (1990) and **d** those given by Adelman et al. (1987).

photoelectric system) could be derived as a linear function of the difference between the broad and narrow $H\gamma$ “magnitudes”; these synthetic indices are given in column 5 of Table 15. In general, these synthetic β agree well with the mean photoelectric values of β taken from Hauck & Mermilliod (1998) and given in Table 1 and with our adopted values that are also given in Table 16. The *rms* difference between our synthetic β and the adopted photoelectric values for the BHB stars is ± 0.009 if we omit HD 161817 for which the difference is 0.031.

Photometric data both from the far ultraviolet and from the infrared can also be used for the determination of the interstellar reddening and stellar parameters. These data are discussed in Sects 5.4 and 7.5 respectively.

4. Spectroscopic observations

High resolution spectra of the thirty-one candidates were obtained either with the Kitt Peak coude feed spectrograph or with the ESO-CAT spectrograph at La Silla, Chile; six stars were observed at both observatories. The journals of the observations are given in Table 2 and Table 3 for Kitt Peak and ESO respectively. These tables contain the coordinates (columns 2 and 3) and *V* magnitude (column 4) of each star. The UT date, starting time and duration of each integration is given in columns 5, 6 and 7. The S/N of each spectrum (column 8) was determined by using the IRAF *splot* task which determined the $(\sqrt{\text{mean signal}})/\text{rms}$ near the $\lambda 4481$ Mg II line in each spectrum. The measured heliocentric radial velocities and their *rms* errors are given in columns 9 and 11 and the number of lines used is in column 10. The agree-

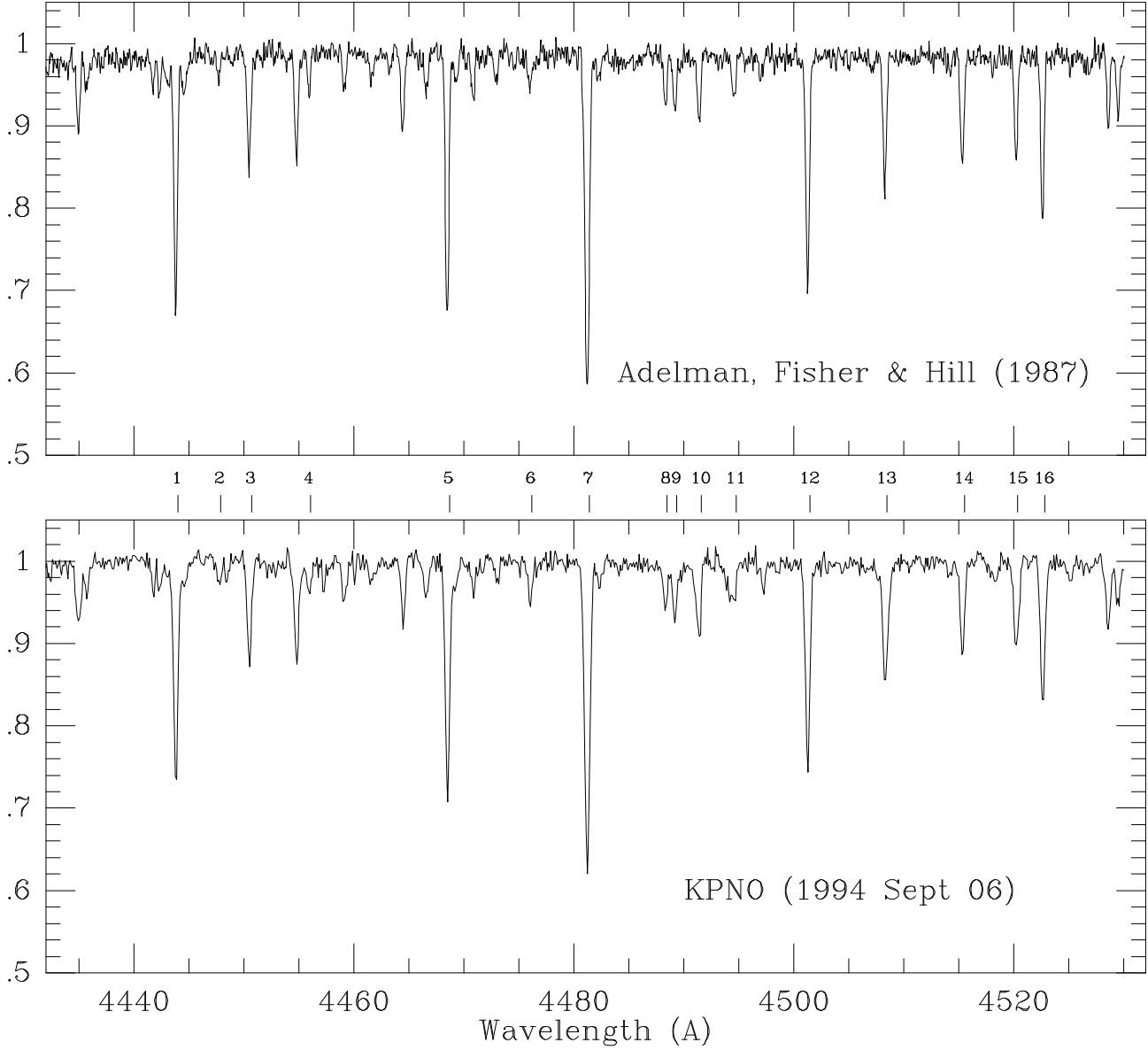


Fig. 3. Comparison of the spectrum of HD 161817 by Adelman et al. (1987) (above) with that taken at the Kitt Peak Coudé Feed telescope on 1999 Sept 06 UT (below). Line identifications: (1) 4443.8 (Ti II), (2) 4447.7 (Fe I), (3) 4450.5 (Ti II), (4) 4455.9 (Ca I), (5) 4468.5 (Ti II), (6) 4476.0 (Fe I), (7) 4481.2 (Mg II), (8) 4488.3 (Ti II), (9) 4489.2 (Fe II), (10) 4491.4 (Fe II), (11) 4494.6 (Fe I), (12) 4501.3 (Ti II), (13) 4508.3 (Fe II), (14) 4515.3 (Fe II), (15) 4520.2 (Fe II) and (16) 4522.6 (Fe II).

ment between the two sets of observations for the stars in common is satisfactory if we consider the number of lines that were available and also that three of these stars (HD 16456, HD 202759 and possibly HD 139961) are variable. The spectra of BD +00 0145 and HD 014829 have a significantly poorer quality than the others and were not used for a complete abundance analysis. We were able, however, to measure the equivalent width of the $\lambda 4481$ Mg II line in these spectra and so derive an approximate [Fe/H] for these stars as explained in Sect. 8.2.

4.1. KPNO Observations

The spectroscopic observations of the northern BHB candidates were made by Kinman and Harmer using the Kitt Peak 0.9 m coudé feed spectrograph. The long collimator (F/31.2; focal length 10.11 m) and camera 5 (F/3.6; focal length 108.0 cm) were used with grating A (632 grooves/mm) in the second order with a Corning 4-96 blocking filter. This gives a 300 \AA bandpass covering $\lambda\lambda 4260\text{--}4560$ which includes both H γ , the Mg II $\lambda 4481$ -line and a selection of Fe I, Fe II and Ti II lines. The detector was a Ford 3KB chip (3072×1024 pixels) with a pixel size

of 15 microns. This gives a 3-pixel resolution of approximately 0.3\AA . The nominal resolution at 4500\AA is therefore 15 000. Biases were taken at the start of each night and a series of flat field quartz calibration exposures were taken at the start and end of each night. ThAr arc lamp spectra for wavelength calibration were made at the start, end and at frequent intervals during each night. The spectra were reduced using standard IRAF procedures of bias subtraction, flat field correction and the extraction of the [1-d] spectrum. The wavelength calibration was made using the ThAr arc spectrum that was closest in time to the program spectrum.

The spectra were normalized to the continuum level interactively by using an updated version of the NORMA code (Bonifacio 1989, Castelli & Bonifacio 1990). These normalized spectra were used to derive stellar parameters from the $H\gamma$ -profile and for the comparison with the synthetic spectra.

4.2. ESO-CAT Observations

The southern BHB candidates were observed by Bragaglia with the CAT + CES (Coudé Auxiliary Telescope, 1.4 m diameter + Coudé Echelle Spectrograph) combination at La Silla, Chile, during April and September 1995. This equipment gives a single echelle order which was observed with two different instrumental configurations. In April we used an RCA CCD (ESO #9), 1024 pixels long, covering about 40\AA at a resolution of 0.14\AA (or $R \simeq 30\,000$), while in September the detector was a Loral CCD (ESO #38), 2688×512 pixels, covering about 50\AA at a resolution of 0.11\AA (or $R \simeq 40\,000$). In both cases the spectra were centered on the $\lambda 4481\text{ Mg II}$ line. Integration times ranged from 10 to 70 minutes; the faintest stars were observed twice.

The ESO-CAT spectra also were reduced with standard IRAF procedures. The extraction of the [1-d] spectra from the [2-d] images was performed weighting the pixels according to the variance and without automatic cleaning from cosmic rays. The wavelength calibration also was computed from a series of Thorium arc-spectra and is estimated to be accurate to a few hundredths of an \AA . IRAF tasks were used to clean the spectra from cosmic rays and defects, for flattening and for normalization.

4.3. The measurement of the Kitt Peak (KPNO) and ESO-CAT spectra

In order to be able to compare the spectra with the models, they were transformed to zero velocity using the IRAF *dopcor* routine. Line positions and equivalent widths were obtained from the reduced spectra using the IRAF *splot* routine, approximating (or deblending, if necessary) lines with gaussian functions. When either two KPNO or two ESO-CAT spectra were available for the same star, they were measured independently and the values of the equiv-

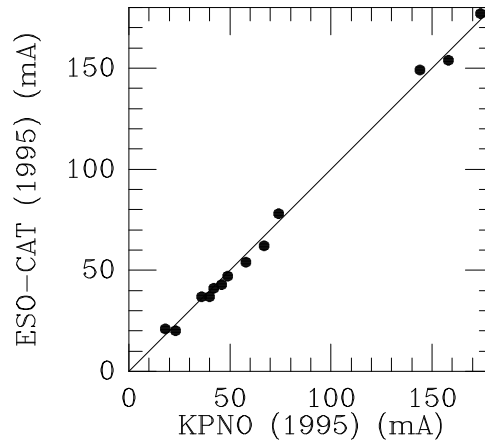


Fig. 5. A comparison of the equivalent widths from the ESO-CAT and Kitt Peak spectra of HD 31943 and HD 180903.

alent widths were averaged. The comparison with the synthetic spectra was made, however, with the spectrum of highest quality in order to compare $H\gamma$ profiles, to derive stellar parameters, to test abundances (derived from the averaged equivalent widths), to test the microturbulent velocity and to derive the rotational velocities. Our measured equivalent widths, together with the derived abundances (Sect. 8), are given in Table 4 and Table 5 for the KPNO and ESO-CAT spectra respectively. The wavelengths and multiplet numbers in these tables are taken from Moore (1945).

Fig. 2 gives a comparison of the equivalent widths that we and other observers obtained from the spectrum of HD 161817. Fig. 2 (a) compares the equivalent widths obtained from the 1994 Kitt Peak spectrum of HD 161817 with those obtained from a spectrum that was taken with the same equipment at the end of the night of 1995 May 03 UT and which has a significantly poorer focus than any of our other program spectra; even in this case, the effect on the equivalent widths appears to be minor. The comparison in (b) is with the early photographic observations of Kodaira (1964) which were made with the Palomar coude spectrograph ($10\text{\AA}/\text{mm}$) and shows a fairly large scatter (presumably because of the low S/N of single photographic exposures) but the systematic differences are small. The comparison in (c) with the more recent photographic observations of Klochkova & Panchuk (1990), however, shows substantial differences in the sense that the equivalent widths of these authors are systematically too large with respect to the present measurements. On the other hand, the systematic agreement of our data for this star with those of Adelman et al. (1987) shown in Fig. 2 (d) is quite good. The Adelman et al. spectrum was derived from 12 co-added photographic spectra ($6.5\text{\AA}/\text{mm}$) and has a resolution of about 25 000; a 100\AA -section of this spectrum is shown in Fig. 3 (above) together with

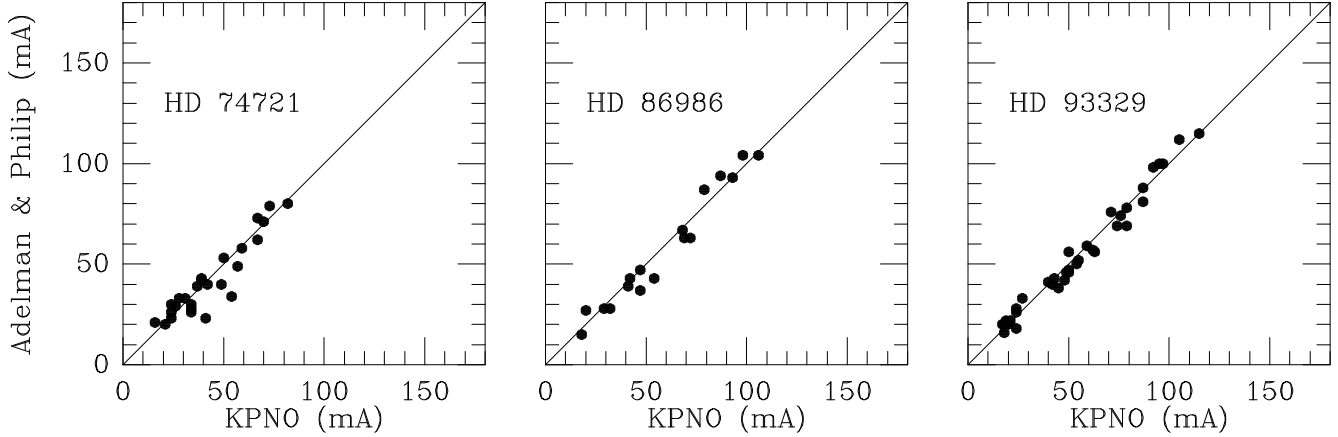


Fig. 4. Comparison of equivalent widths measured by Adelman & Philip (1994, 1996a) for HD 74721, HD 86986 and HD 93329 with those measured from the KPNO spectra.

the KPNO spectrum of 1994 Sept 06 UT (below)⁷. The noise in the KPNO CCD spectrum is such that some of the fainter lines (equivalent widths less than about 30 mÅ) can be quite distorted. Such lines can generally be recognized and omitted from our analysis.

Fig. 4 compares the equivalent widths for HD 74721, HD 86986 and HD 93329 from the KPNO spectra with those measured by Adelman & Philip (1994, 1996a) using the same equipment. The agreement is satisfactory except for the Fe II $\lambda 4555$ and Ti II $\lambda 4563$ lines in HD 74721. The KPNO equivalent widths give abundances that are in agreement with the other lines of these species and were preferred. Otherwise, these various comparisons give no evidence for significant systematic differences between our equivalent widths and those given by Adelman & Philip.

Fig. 5 compares the KPNO equivalent widths of HD 31943 and HD 180903 with those obtained from the higher resolution ESO-CAT spectra; the agreement is very satisfactory. The 28 spectra of the stars in our sample identified by us as BHB stars are shown for the spectral region 4475 to 4490 Å in Fig. 6; they are numbered as in Table 1.

The determination of the chemical composition of the BHB stars requires a knowledge of the parameters that govern the physical conditions in their atmospheres such as the effective temperature (T_{eff}), the surface gravity ($\log g$), the microturbulent velocity (ξ) and also assumptions about convection. These parameters are determined from both spectroscopic and photometric data. The latter require correction for interstellar reddening and this can be determined in several ways. These different methods and the extent to which they agree are discussed in the next section.

5. The interstellar reddening for the program stars

We have estimated the interstellar reddening for our BHB candidates by two direct and two indirect methods. The first direct method makes use of the whole sky map of the dust infrared emission and the second is based on the empirical calibration of the Strömgren colours. The indirect methods use model atmospheres to compare the observed and computed visible spectrophotometric data and the observed and computed UV colour indices.

5.1. The interstellar reddening for the program stars from whole-sky maps

The reddening in the direction of our program stars was estimated from the whole-sky maps of Schlegel et al. (1998, SFD) which give the total line-of-sight reddening ($E(B - V)_{\text{total}}$) as a function of the galactocentric coordinates (l, b). The reddening between the stars and the observer (Table 6, column 6) was derived by multiplying $E(B - V)_{\text{total}}$ by $(1 - \exp(-|z|/h))$ where z is the star's distance above the galactic plane. The value that was assumed for the scale height (h) was taken to increase linearly from 50 pc for stars at a distance of 200 pc to 120 pc at a distance of 600 pc and to remain constant thereafter. The stellar distances (Table 6, column 4) were computed assuming the M_V vs. $(B - V)$ relation given by Preston et al. (1991) with the zero-point modified to give an M_V of +0.60 at $(B - V) = 0.20$ (the blue edge of the instability strip). The mean difference between the $E(B - V)$ found in this way from the SFD maps and those given by Harris (1996) for 16 high-latitude globular clusters is satisfactorily small ($+0.004 \pm 0.003$). At lower latitudes ($\lesssim 30^\circ$), however, the extinction is too patchy for the simple exponential model to be reliable and the reddenings found in this way are much less certain. The least reliable values (Table 6, column 6) are marked with a colon.

⁷ The first spectra of HD 161817 were taken by Albitzky (1933) who noted “The spectrum contains fairly good H lines, strong K line, and a number of faint metallic lines. The Mg 4481 is hardly perceptible and was measured on one plate only.” The Mg II ($\lambda 4481$) line is the strongest line (equivalent width 210 mÅ) in this figure.

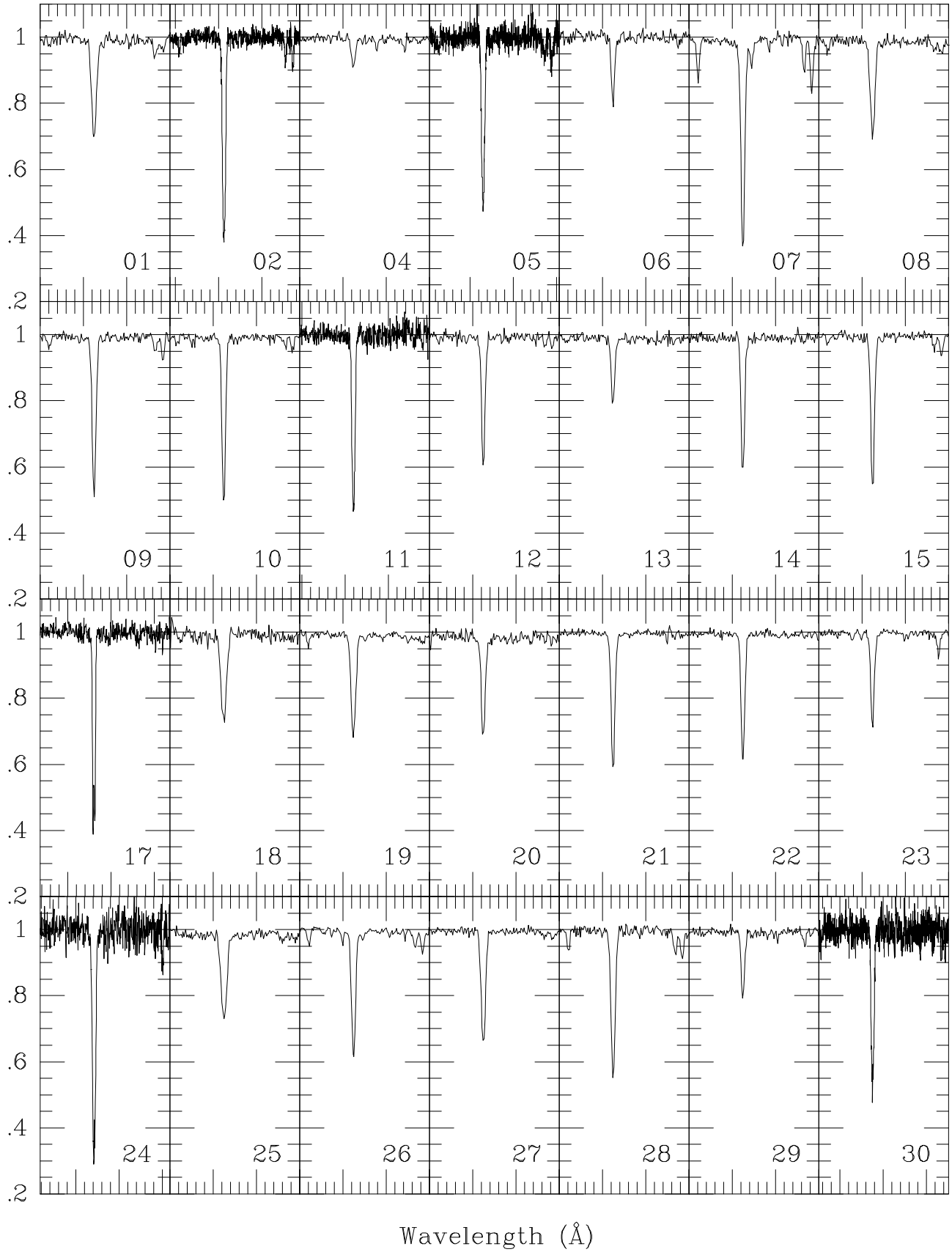


Fig. 6. The spectra of the 28 BHB stars in our sample in the spectral range 4475 to 4490 Å. The stars are numbered as in Table 1.

Table 6. Galactic coordinates, distances, IUE colour ($18 - V$) and a comparison of the extinctions for the program BHB stars by different methods.

Star	l	b	Dist. (pc)	$(18 - V)$	$E(B - V)$					$[M/H]/T_{\text{eff}}/\log g^f$
					SFD ^a	ED ^b	Moon ^c	IUE ^d	IUE ^e	
(1)	(2)	(3)	(4)	(5)	(6)	(7)	(8)	(9)	(10)	(11)
HD 2857	110.0	-67.6	717	1.085	0.042	0.005	0.030	0.008	0.010	-1.50/7 500/2.95
HD 4850	303.8	-69.8	563	0.272	0.016	...	0.000	0.010	0.010	-1.50/8 400/3.10
BD +00 0145	126.8	-60.8	600:	-0.670	0.028	...	0.000	0.024	0.030	-1.50/10 000/4.00
HD 8376	130.8	-30.6	565	0.554	0.051	...	0.035	0.039	0.037	-2.00/8 100/3.20
HD 13780	272.8	-63.0	640	0.651	0.018	...	0.008	0.016	0.015	-1.50/7 930/3.10
HD 14829	180.5	-62.3	715	-0.093	0.024	0.025	0.000	0.023	0.023	-2.00/8 950/3.30
HD 16456	256.3	-63.4	308	...	0.021	...	0.007
HD 31943	247.8	-38.4	317	0.774	0.008	...	0.000	0.011	0.006	-1.00/7 850/3.00
HD 252940	185.0	+03.8	460	1.129	0.168:	...	0.042	0.051	0.06:	-1.75/7 600/3.00
HD 60778	218.2	+09.9	443	0.517	0.054	0.040	0.016	0.027	0.028	-1.50/8 160/3.10
HD 74721	213.5	+31.3	351	-0.042	0.029	0.015	0.000	0.006	0.005	-1.50/8 800/3.30
HD 78913	284.6	-14.0	483	0.175	0.068	...	0.007	0.060	0.062	-1.50/8 870/3.25
HD 86986	221.9	+48.8	274	0.617	0.030	0.005	0.023	0.035	0.025	-1.50/8 000/3.20
HD 87047	196.5	+53.3	633	0.584	0.019	...	0.000	0.000	0.000	-2.50/7 800/3.00
HD 87112	154.7	+47.7	511	-0.602	0.009	...	0.000	0.000	0.000	-1.50/9 700/3.50
HD 93329	235.4	+56.6	386	0.392	0.029	...	0.000	0.014	0.014	-1.50/8 260/3.10
BD +32 2188	190.5	+75.2	4170	-0.872	0.021	0.000:	0.000	0.023
HD 106304	295.3	+21.4	369	-0.401	0.082	...	0.000	0.031	0.031	-1.50/9 600/3.50
BD +42 2309	139.5	+74.7	895	0.025	0.018	0.020	0.000	0.012	0.013	-1.50/8 730/3.30
HD 109995	134.3	+77.5	211	0.198	0.017	0.050	0.000	0.020	0.020	-1.50/8 558/3.15
BD +25 2602	359.2	+85.1	707	...	0.017	...	0.000
HD 117880	316.7	+43.2	358	-0.077	0.087	0.080	0.000	0.066	0.064	-1.50/9 300/3.50
HD 128801	000.8	+58.1	306	-0.791	0.027	...	0.000	0.004	0.004	-1.50/10 135/3.50
HD 130095	332.3	+29.0	241	0.103	0.108:	0.085	0.016	0.060	0.060	-2.00/8 925/3.40
HD 130201	323.4	+12.5	664	0.089	0.103	...	0.015	0.056	0.055	-1.50/8 925/3.50
HD 139961	332.0	+08.0	370	0.316	0.149:	...	0.042	0.058	0.060	-1.50/8 600/3.30
HD 161817	050.4	+24.9	185	0.999	0.073:	0.000	0.000	0.000	0.000	-1.50/7 525/3.00
HD 167105	078.7	+26.9	372	-0.091	0.043	...	0.000	0.030	0.029	-1.50/9 050/3.25
HD 180903	013.6	-16.6	523	1.220	0.076	...	0.103	0.090	0.095	-1.50/7 700/3.10
HD 202759	010.8	-44.3	447	1.285	0.098	0.065	0.063	0.063	0.06:	-2.00/7 465/3.00
HD 213468	355.1	-57.9	939	-0.228	0.017	...	0.000	0.005	0.006	-1.50/9 100/3.25

^a Derived from the whole sky map of Schlegel et al. (1998).^b Derived from the energy distribution.^c Derived from the Strömgren colours using the Moon (1985) code.^d Derived from a comparison of the observed with the theoretical (ATLAS9) $(18 - V)$ colours $(E(B - V)_1)$.^e Derived by comparing the observed $(18 - V)$ vs. $(b - y)$ colours with the corresponding theoretical values $(E(B - V)_2)$.^f The $[M/H]/T_{\text{eff}}/\log g$ that were used to obtain the reddenings that are given in columns (9) and (10).

5.2. Reddening from the intrinsic colour calibration

We used the UVBYLIST code of Moon (1985) to derive the intrinsic Strömgren indices from the observed indices of our program BHB stars by means of empirical calibrations that are taken from the literature.

The stars are divided into eight photometric groups according to their spectral class and a different empirical calibration is used for each group. All our program stars except BD+32 2188 have $2.72 \leq \beta \leq 2.88$ and belong to group 6 (stars of spectral type A3–F0 with luminosity class III–V). We placed BD+32 2188 in group 4 (B0–A0 bright giants).

A complete description of the dereddening procedures can be found in Moon (1985) and also Moon & Dworetzky (1985). Here we recall that for group 6, $(b - y)_0$, and hence the reddening, is calculated from the equations given by Crawford (1979), which relate $(b - y)_0$ to the β , δc_1 , and $\delta m_1(\beta)$ indices. For group 4, a dereddening equation was derived by coupling linear relations between the c_0 and $(u - b)_0$ colours, determined from Table IV of Zhang (1983), with the reddening ratios given by Crawford & Mandwewala (1976):

$$(b - y)_0 = (b - y) - E(b - y)$$

$$m_0 = m_1 + 0.32E(b - y)$$

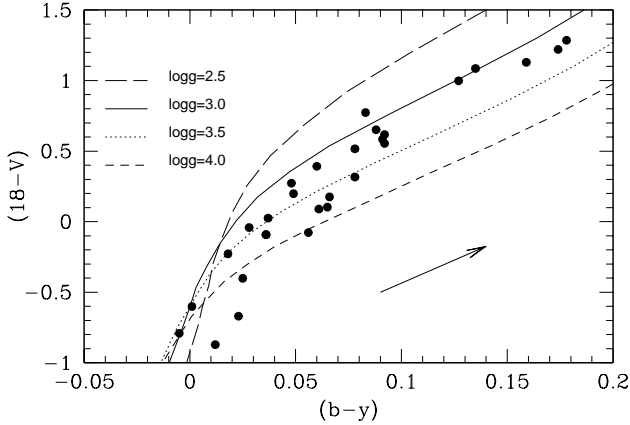


Fig. 7. The theoretical (ATLAS9) colours $(18-V)$ vs $(b-y)$ for $[m/H]=-1.5$ and gravity from 2.5 to 4.0 in steps of 0.5. The arrow indicates the effect of reddening.

$$c_0 = c_1 - 0.20E(b-y)$$

We emphasize, however, that the empirical calibrations used by this method are based on stars of spectral type B0 to M2 that lie on or near the *main sequence*. Hence, for the BHB stars, the reddening, the intrinsic indices, and results from them, should be compared with the corresponding quantities obtained with other methods in order to assess the reliability of this dereddening procedure. The reddening values derived from the UVBYLIST program are given in column 8 of Table 6.

5.3. Reddening from Spectrophotometric Data

Spectrophotometric observations are available (Philip & Hayes 1983, Hayes & Philip 1983) for twelve of our candidate BHB stars. An estimate of the reddening was derived for these stars in the process of obtaining the stellar parameters (Sect. 7) by fitting the observed energy distributions to a grid of computed fluxes. For each star, we dereddened the observed energy distribution for a set of $E(B-V)$ values, sampled at steps of 0.005 mag and starting from 0.000 mag. The adopted reddening law $A(\lambda)$ was taken from Table 1 in Mathis (1990) for $A_V/E(B-V) = 3.1$. For each $E(B-V)$, the stellar parameters are those that give the minimum *rms* (Sect. 7.2). We assumed as the most probable $E(B-V)$, that which gave the minimum *rms* among those given by the fitting procedure. These $E(B-V)$ are listed in column 7 of Table 6.

5.4. Reddening from IUE Ultraviolet Data

It has been shown (Huenemoerder et al. 1984) that far-UV spectra can be useful for classifying BHB stars and for determining their reddening. All of our candidate BHB stars (except HD 16456 and BD+25 2602) have UV IUE low-resolution (6 Å) spectra, that have been previously analysed and discussed (Huenemoerder et al. 1984, Cacciari 1985, Cacciari et al. 1987 and de Boer et al. 1997 and references therein). We felt, however, that we should re-discuss the UV-spectra of these stars, especially the short-wavelength spectra (SWP, 1150-1980 Å), using the data that is in the IUE Final Archive⁸. In this way we could extract all the UV-spectra in a *homogeneous* way using the final IUE flux calibration and image-processing techniques (Nichols & Linsky 1996, Bohlin 1996) and compare them to the latest model atmospheres for metal-poor stars computed by Castelli with the ATLAS9 code and the Opacity Distribution Functions (ODFs) from Kurucz (Castelli 1999).

The region of the UV spectrum that is best reproduced by the model atmospheres of stars with T_{eff} between 7500 K and 10000 K seems to be that in the region of 1800Å (Huenemoerder et al. 1984, Cacciari et al. 1987). The values of the observed fluxes at 1800Å were obtained from the SWP spectra by averaging the flux over a rectangular bandpass 150 Å wide. The UV-colour $(18-V)$ (given in Table 6, column 5) is defined as

$$(18-V) = -2.5(\log F_{1800} - \log F_V)$$

where $\log F_V = -0.4V - 8.456$ (Gray 1992). The UV-flux is strongly affected by interstellar extinction. Consequently, the reddening can be estimated from the $(18-V)$ colour by comparing it with that predicted by a model atmosphere assuming that the temperature and/or gravity are known. We used corrections for reddening that were based on Seaton's (1979) reddening law, which gives

$$E(18-V)/E(B-V) = 4.748$$

on the assumption that $A_V = 3.1E(B-V)$. The recent re-analysis of the interstellar extinction by Fitzpatrick (1999) would give a somewhat higher value (4.85) for this ratio. We also estimated the $(19-V)$ -colour, defined similarly to $(18-V)$, as a check on the consistency of our results. The colours $(18-V)$ and $(19-V)$ sample contiguous parts of the energy distribution and so are highly correlated; $(19-V)$ is closer to the 2200Å feature and can be more noisy because it is near the edge of the energy distribution in the SWP spectra. We verified that both of these colours gave consistent results but only have used the more reliable $(18-V)$ colour so as to avoid duplication.

⁸ The data in the Final Archive was reprocessed by the IUE Project using the latest and most accurate flux calibrations and the most recent image-processing techniques so that no further processing of this data is needed.

We started with preliminary values of T_{eff} , $\log g$ and abundances that had been derived from the model atmosphere analysis. When it was available, we preferred the parameters derived from the $H\gamma$ profile because these are reddening-independent. These stellar parameters were used to calculate an intrinsic $(18 - V)$ colour and the difference between this and the observed $(18 - V)$ colour gives the reddening $E(B - V)$, called here $E(B - V)_1$.

The reddening $E(B - V)$ may also be estimated by comparing the observed $(18 - V)$ vs. $(b - y)$ pairs with those predicted by the models at a given gravity, and is called here $E(B - V)_2$. In Fig 7 we show the program stars and theoretical relations for $[M/H] = -1.5$ and gravities 2.5, 3.0, 3.5 and 4.0 in the $(18 - V)$ vs. $(b - y)$ plane. If these two estimates of the reddening were consistent within ~ 0.02 mag, then we assumed that our initial values of T_{eff} and $\log g$ were reasonably correct. If this was not the case, we repeated the analysis with different initial values. Our finally adopted values for $E(B - V)_1$ and $E(B - V)_2$ are given in columns 9 and 10 of Table 6, where they are compared with the other reddening determinations. The finally adopted values for $[M/H]$, T_{eff} and $\log g$ used to obtain these reddenings are given in column 11 of Table 6. They generally agree with other determinations (Sect. 7). In the second method, the UV data essentially constrain the $\log g$ that is permitted for a given reddening; in particular this strongly discriminates between FHB stars and main sequence stars of higher gravity. The *internal* accuracies of the parameters that are found by this way are estimated to be ± 0.1 in $\log g$ and $\pm 100\text{K}$ in T_{eff} .

We estimate that the typical error in these reddenings that comes from photometric errors and the systematic errors to the absolute visual and UV photometric calibrations is ≤ 0.03 mag. Using only the 20 higher latitude BHB stars where the SFD-derived reddenings (Table 6, column 6) are reliable, the mean value of the SFD reddenings *minus* the mean of the two reddenings derived from the IUE data (Table 6, columns 9 and 10) is $+0.017 \pm 0.004$. The mean difference between the reddenings derived by the intrinsic colour calibration (Sect. 5.2; Table 6, column 11) and the mean of the two reddenings derived from the IUE data is -0.011 ± 0.004 (28 stars).

A detailed comparison between the different reddening estimates is given in Table 6. Clearly systematic differences of the order of a few hundredths of a magnitude in $E(B - V)$ exist between the reddenings derived by the different methods even at high galactic latitudes. At lower latitudes, the differences are much larger because of the greater uncertainties in the reddenings derived from whole sky maps. It does not seem possible to resolve these differences without additional observations (e.g. mapping the extinction in the direction of the BHB stars using the Strömgren photometry of main sequence field stars).

6. The Model Atmosphere analysis

The high-resolution spectra were analyzed with the model atmosphere technique. Stellar parameters were estimated from Strömgren photometry, from spectrophotometry, from $H\gamma$ profiles, from IUE ultraviolet colours and (for nine stars) from $(V - K)$ colours. The estimates obtained by these different methods and the values of the parameters that we adopted are given in Table 7.

Having fixed the model atmosphere, we computed abundances from both the equivalent widths and line profiles for each star observed at KPNO, except for BD +00 0145 and HD 14829. For these two stars and for the BHB stars that were observed at ESO (whose spectra only extended over 50 Å) we estimated the abundances from the equivalent widths alone.

We used model atmospheres and fluxes that were computed by Castelli with an updated version of the ATLAS9 code (Kurucz 1993a). We adopted models for stars with an α -element enhancement $[\alpha/\alpha_{\odot}] = +0.4$ (which is generally appropriate for halo stars). The symbol “a” near the metallicity in column 6 of Table 7 indicates when these models were used. The convective models ($T_{\text{eff}} < 8750\text{K}$) were calculated with the no-overshooting approximation. More details about these models can be found in Castelli et al. (1997) and in Castelli (1999). The synthetic grids of Strömgren indices, Johnson $(V - K)$ indices and $H\gamma$ profiles were also computed by Castelli from the above models. Grids of models, fluxes and colours are available either at the Kurucz website (<http://kurucz.harvard.edu>) or upon request.

We derived abundances from the equivalent widths using the WIDTH code (Kurucz 1993a), modified so that we could derive the Mg abundance from the measured equivalent width of the doublet Mg II 4481 Å. The SYNTHE code (Kurucz 1993b), together with the atomic line lists from Kurucz & Bell (1995), were used to compute the synthetic spectra.

Table 7. Comparison of the stellar parameters obtained by different methods.

Star	Data	$E(B - V)$	$T_{\text{eff}}(\text{K})$	$\log g^{\ddagger}$	[M/H]	Method
HD 2857	(c, (b - y))	0.042 ¹	7 730±120	3.15±0.04	[-1.5a]	interpolation
	(c, (b - y))	0.030 ²	7 650±120	3.10±0.04	"	"
	[(V - K)	(0.022) ³	7 420±95*	(3.1)	"	"]
	En. Distr.	0.005 ⁴	7 400±100	2.8±0.1	"	fit, RMS(min)=0.0110
	UV	0.008 ⁵ , 0.010 ⁶	7 500±100	2.95±0.1	"	
	H γ	...	7 550±150	(3.0)	"	fit, RMS(min)=0.0104
Mean		0.022±0.009	7566±58	3.00±0.08	[-1.5a]	
HD 4850	(a, r)	0.016 ¹	8 610±275	3.15±0.04	[-1.5a]	interpolation
	(c, (b - y))	0.000 ²	8 350±250	3.35±0.05	"	"
	UV	0.010 ⁵ , 0.010 ⁶	8 400±100	3.10±0.1	"	
Mean:		0.009±0.005	8453±80	3.20±0.08	[-1.5a]	
BD +00 145	(a, r)	0.028 ¹	9 740±350	4.05±0.04	[-1.5a]	interpolation
	(a, r)	0.000 ²	9 350±300	4.00±0.05	"	"
	UV	0.024 ⁵ , 0.030 ⁶	10 000±200	4.00±0.2	"	
Mean:		0.018±0.009	9697±189	4.02±0.02	[-1.5a]	
HD 8376	(c, (b - y))	0.051 ¹	8 270±250	3.35±0.05	[-2.5]	interpolation
	(c, (b - y))	0.035 ²	8 110±175	3.25±0.04	"	"
	UV	0.039 ⁵ , 0.037 ⁶	8 100±100	3.20±0.1	[-2.0a]	
	H γ	...	8 050±150	(3.3)	[-2.5]	fit, RMS(min)=0.0081
Mean:		0.041±0.005	8133±48	3.27±0.04	[-2.5]	
HD 13780	(c, (b - y))	0.018 ¹	7 970±150	3.15±0.04	[-1.5a]	interpolation
	(c, (b - y))	0.008 ²	7 890±150	3.10±0.04	"	"
	UV	0.016 ⁵ , 0.015 ⁶	7 930±100	3.10±0.1	"	
Mean:		0.014±0.003	7930±23	3.12±0.02	[-1.5a]	
HD 14829	(a,r)	0.024 ¹	9 010±275	3.35±0.04	[-2.0a]	interpolation
	(c, (b - y))	0.000 ²	8 700±250	3.30±0.05	"	"
	[(V - K)	(0.018) ³	9 040±170*	(3.2)	"	"]
	En. Distr.	0.025 ⁴	9 000±50	3.0±0.1	"	fit, RMS(min)=0.0100
	UV	0.023 ⁵ , 0.023 ⁶	8 950±100	3.20±0.1	"	
Mean:		0.018±0.006	8915±73	3.21±0.08	[-2.0a]	
HD 16456[†]	H γ	...	6 750±150	(2.8)	"	fit, RMS(min)=0.0140
Mean:		...	6750±150	(2.8)	[-1.5a]	
HD 31943	(c, (b - y))	0.008 ¹	8 020±150	3.35±0.04	[-1.0]	interpolation
	(c, (b - y))	0.000 ²	7 950±150	3.30±0.04	"	"
	UV	0.011 ⁵ , 0.006 ⁶	7 850±100	3.00±0.1	"	
	H γ	...	7 750±100	(3.2)	"	fit, RMS(min)=0.0061
Mean:		0.006±0.003	7893±59	3.22±0.11	[-1.0]	
HD 252940	[(c, (b - y))	0.168 ¹	8 660±300	3.65±0.05	[-1.5a]	interpolation]
	(c, (b - y))	0.042 ²	7 490±120	2.90±0.04	"	"
	UV	0.051 ⁵ , 0.06 ⁶	7 600±100	3.00±0.1	[-1.75a]	
	H γ	...	7 600±150	(2.9)	[-1.5a]	fit, RMS(min)=0.0104
Mean:		0.048±0.006	7563±37	2.95±0.05	[-1.5a]	

Table 7. Comparison of the stellar parameters obtained by different methods. (continued)

Star	Data	$E(B - V)$	T_{eff}	$\log g^{\ddagger}$	[M/H]	Method
HD 60778	[(a, r)	0.054 ¹	8 590±275	3.10±0.05	[-1.5a]	interpolation]
	(c, (b - y))	0.016 ²	8 080±200	3.20±0.04	"	"
	[(V - K)	(0.028) ³	8 110±90*	(3.1)	"	"]
	En. Distr.	0.040 ⁴	8 100±100	3.1±0.1	"	fit,RMS(min)=0.0105
	UV	0.027 ⁵ ,0.028 ⁶	8 160±100	3.10±0.1	"	
	H γ	...	7 950±300	(3.1)	"	fit,RMS(min)=0.0072
Mean:		0.028±0.007	8072±44	3.13±0.03	[-1.5a]	
HD 74721	(a, r)	0.029 ¹	9 170±300	3.30±0.04	[-1.5a]	interpolation
	(a, r)	0.000 ²	8 810±300	3.25±0.04	"	"
	[(V - K)	(0.012) ³	8 680±175*	(3.3)	"	"]
	En. Distr.	0.015 ⁴	8 850±50	3.3±0.2	"	fit,RMS(min)=0.0093
	UV	0.006 ⁵ ,0.005 ⁶	8 800±100	3.30±0.1	"	
	H γ	...	(8 850)	3.4±0.1	"	fit,RMS(min)=0.0080
Mean:		0.012±0.006	8908±88	3.31±0.02	[-1.5a]	
HD 78913	[(a, r)	0.068 ¹	9 000±290	3.20±0.04	[-1.5a]	interpolation]
	(c, (b - y))	0.007 ²	8 160±200	3.25±0.04	"	"
	UV	0.060 ⁵ ,0.062 ⁶	8 870±100	3.25±0.1	"	
Mean:		0.034±0.027	8515±355	3.25±0.00	[-1.5a]	
HD 86986	(c, (b - y))	0.030 ¹	8 050±170	3.25±0.04	[-1.5a]	interpolation
	(c, (b - y))	0.023 ²	7 980±170	3.20±0.04	"	"
	[(V - K)	(0.022) ³	7 870±140*	(3.2)	"	"]
	En. Distr.	0.005 ⁴	7 850±50	3.1±0.1	"	fit,RMS(min)=0.0105
	UV	0.035 ⁵ ,0.025 ⁶	8 000±100	3.20±0.1	"	
	H γ	...	7 800±150	(3.2)	"	fit,RMS(min)=0.0085
Mean:		0.022±0.006	7936±47	3.19±0.03	[-1.5a]	
HD 87047	(c, (b - y))	0.019 ¹	7 970±150	3.15±0.04	[-2.5]	interpolation
	(c, (b - y))	0.000 ²	7 790±150	3.05±0.04	"	"
	UV	0.000 ⁵ ,0.000 ⁶	7 800±100	3.00±0.1	"	"
	H γ	...	7 750±100	(3.1)	"	fit,RMS(min)=0.0069
Mean:		0.006±0.006	7828±49	3.07±0.04	[-2.5]	
HD 87112	(a, r)	0.009 ¹	9 810±340	3.45±0.04	[-1.5a]	interpolation
	(a, r)	0.000 ²	9 690±325	3.45±0.04	"	"
	UV	0.000 ⁵ ,0.000 ⁶	9 700±100	3.5±0.1	"	
	H γ	...	(9 750)	3.5±0.1	"	fit,RMS(min)=0.0080
Mean:		0.003±0.003	9733±38	3.48±0.01	[-1.5a]	
HD 93329	(c, (b - y))	0.029 ¹	8 460±300	3.25±0.06	[-1.5a]	interpolation
	(c, (b - y))	0.000 ²	8 130±200	3.15±0.05	"	"
	UV	0.014 ⁵ ,0.014 ⁶	8 260±150	3.1±0.1	"	
	H γ	...	8 100±200	3.0±0.1	"	fit,RMS(min)=0.0046
Mean:		0.014±0.008	8237±82	3.12±0.05	[-1.5a]	
BD +32 2188	(c, β)	0.021 ¹	10 420±100	2.10±0.05	[-1.0]	interpolation
	(c, β)	0.000 ²	10 400±100	2.10±0.04	"	"
	En. Distr.	0.000 ⁴	10 500±500	2.2±0.4	"	fit,RMS(min)=0.0396
	H γ	...	(10 400)	2.1±0.05	"	fit,RMS(min)=0.0085
Mean:		0.007±0.007	10440±30	2.12±0.02	[-1.0]	

Table 7. Comparison of the stellar parameters obtained by different methods. (continued)

Star	Data	$E(B - V)$	T_{eff}	$\log g^{\ddagger}$	[M/H]	Method
HD 106304	(a, r)	0.082 ¹	10 440±300	3.55±0.04	[-1.5a]	interpolation
	(a, r)	0.000 ²	9 200±300	3.45±0.04	"	"
	UV	0.031 ⁵ , 0.031 ⁶	9 600±100	3.5±0.1	"	"
	Mean:	0.038±0.024	9747±365	3.50±0.03	[-1.5a]	
BD +42 2309	(a, r)	0.018 ¹	8 870±300	3.20±0.04	[-1.5a]	interpolation
	(a, r)	0.000 ²	8 650±275	3.20±0.04	"	"
	En. Distr.	0.020 ⁴	9 050±100	3.0±0.2	"	fit,RMS(min)=0.0179
	UV	0.012 ⁵ , 0.013 ⁶	8 730±100	3.3±0.1	"	"
	H γ	...	(8 850)	3.3±0.1	"	fit,RMS(min)=0.0077
	Mean:	0.013±0.004	8825±88	3.20±0.05	[-1.5a]	
HD 109995	(a, r)	0.017 ¹	8 610±300	3.10±0.04	[-1.5a]	interpolation
	(c, (b - y))	0.000 ²	8 300±250	3.25±0.05	"	"
	[(V - K)	(0.022) ³	8 390±235*	(3.15)	"	"]
	En. Distr.	0.050 ⁴	8 900±100	2.9±0.3	"	fit,RMS(min)=0.0190
	UV	0.020 ⁵ , 0.020 ⁶	8 560±200	3.15±0.2	"	"
	H γ	...	8 200±250	3.0±0.1	"	fit,RMS(min)=0.0075
	Mean:	0.022±0.010	8514±123	3.08±0.07	[-1.5a]	
BD +25 2602	(a, r)	0.017 ¹	8 610±275	3.15±0.04	[-2.0a]	interpolation
	(c, (b - y))	0.000 ²	8 320±275	3.25±0.05	"	"
	H γ	...	8 300±300	3.1±0.1	"	fit,RMS(min)=0.0074
	Mean:	0.008±0.008	8410±100	3.17±0.04	[-2.0a]	
HD 117880	(a, r)	0.087 ¹	9 590±325	3.45±0.04	[-1.5a]	interpolation
	[(c, (b - y))	0.000 ²	8 320±220	3.55±0.04	"	"]
	[(V - K)	(0.077) ³	9 380±225*	(3.3)	"	"]
	En. Distr.	0.080 ⁴	9 300±50	3.3±0.1	"	fit,RMS(min)=0.0074
	UV	0.066 ⁵ , 0.0064 ⁶	9 300±100	3.5±0.1	"	"
	H γ	...	8 950±500	3.1±0.2	"	fit,RMS(min)=0.0109
	Mean:	0.077±0.006	9285±131	3.34±0.09	[-1.5a]	
HD 128801	(a, r)	0.027 ¹	10 640±400	3.55±0.04	[-1.5a]	interpolation
	(a, r)	0.000 ²	10 160±400	3.55±0.04	"	"
	UV	0.004 ⁵ , 0.004 ⁶	10 140±200	3.5±0.1	"	"
	H γ	...	(10 300)	3.6±0.1	"	fit,RMS(min)=0.0087
	Mean:	0.010±0.008	10313±163	3.55±0.02	[-1.5a]	
HD 130095	[(a, r)	0.108 ¹	9 650±350	3.35±0.04	[-2.0a]	interpolation]
	[(c, (b - y))	0.016 ²	8 300±250	3.40±0.05	"	"]
	[(V - K)	(0.072) ³	8 990±180*	(3.3)	"	"]
	En. Distr.	0.085 ⁴	9 100±50	3.3±0.1	"	fit,RMS(min)=0.0073
	UV	0.060 ⁵ , 0.060 ⁶	8 920±100	3.4±0.1	"	"
	H γ	...	(9 000)	3.2±0.1	"	fit,RMS(min)=0.0082
	Mean:	0.072±0.012	9010±90	3.30±0.03	[-2.0a]	
HD 130201	[(a, r)	0.103 ¹	9 700±330	3.45±0.04	[-1.5a]	interpolation]
	(c, (b - y))	0.015 ²	8 370±250	3.45±0.05	"	"
	UV	0.056 ⁵ , 0.055 ⁶	8 920±100	3.5±0.1	"	"
	Mean:	0.035±0.020	8645±275	3.48±0.03	[-1.5a]	

7. Stellar parameters

7.1. Stellar parameters from Strömgren photometry

The stellar parameters T_{eff} and $\log g$ were found from the observed Strömgren indices after de-reddening (as discussed in Sect. 5) by interpolation in the $uvby\beta$ synthetic grids. The adopted indices are those listed in boldface in Table 1. Dereddened indices were obtained both from $E(B - V)$ values derived from the SFD whole sky map (Table 6, column 6) and from the $E(B - V)$ derived from the UVBYLIST program of Moon (1985) (Table 6, column 8). The reddening relations given in Sect. 5.2 were used in both cases.

When $T_{\text{eff}} > 8500$ K and $\log g < 3.5$, the $(c, (b - y))$ grid does not give an unambiguous determination of the parameters and the (a, r) grid (Strömgren 1966) is to be preferred. It should be noted that different values for the reddening may be derived for a star by the two methods, so that it may lie in the (a, r) plane according to one reddening determination, and in the $(c, (b - y))$ plane according to the other.

For each star, we started by selecting, from among the available grids of colour indices, the one which had the metallicity closest to that given in the literature or from a preliminary estimate based on the strength of the $\lambda 4481$ Mg II line (KSK). After a new metallicity was found from the model atmosphere analysis, it was used to determine, by interpolation, the colour grid which corresponded to this new metallicity. New parameters were then re-determined. We found that the stellar parameters were, in practice, relatively insensitive to the value used for the metallicity. For this reason, the stellar parameters found from the Strömgren indices and listed in the first two (or three) lines of Table 7 are those relative to the approximate metallicity listed in column 6. At this stage, we also adopted a microturbulent velocity of $\xi = 2.0$ km s⁻¹ for all the stars. In Table 7, the data on the first line for each star correspond to the $E(B - V)$ derived from the SFD whole sky-map (Table 6, column 6), while the data on the second line correspond to the $E(B - V)$ derived using Moon's program (Table 6, column 8). The reddening $E(B - V) = E(b - y)/0.73$ is given in column 3 of Table 7. The specific Strömgren indices that we used to obtain T_{eff} and $\log g$ for each star are given in the second column of Table 7. The errors in the parameters were calculated by assuming an uncertainty of ± 0.015 mag for all Strömgren indices except β for which ± 0.005 mag was adopted. The actual error in β may well be larger than this for some stars as noted in Table 1 and in Sect. 3.

7.2. Stellar parameters from spectrophotometry in the visible

Spectrophotometric observations are available (Philip & Hayes 1983, Hayes & Philip 1983) for some of our candidate BHB stars. Stellar parameters were derived for these

stars by fitting the observed energy distribution to the fluxes of that grid, among those available to us, which had the closest metallicity either to that given in the literature, or to that obtained from a preliminary estimate based on the strength of the $\lambda 4481$ Mg II line, or to that given in a preliminary abundance analysis. The observed energy distribution was dereddened as described in Sect. 5.3. The fitting procedure is that described by Lane & Lester (1984) in which the entire energy distribution is fitted to the model which yields the minimum *rms* difference. The search for the minimum *rms* difference is made by interpolating in the grid of computed fluxes. The computed fluxes are sampled in steps of 50 K or 100 K in T_{eff} depending whether $T_{\text{eff}} \leq 10000$ K or $T_{\text{eff}} > 10000$ K, and in steps of 0.1 dex in $\log g$. The fluxes are actually given in steps of 250 K or 500 K in T_{eff} and in steps of 0.5 dex in $\log g$, so the finer sampling was obtained by linear interpolation.

The parameters derived from the energy distributions are given on the "En. Distr." line in Table 7 and the adopted metallicity is that listed in column 6. The errors in the parameters were estimated from the ranges in T_{eff} and $\log g$ for which $rms = rms(\text{min}) + 50\% rms(\text{min})$. Lane & Lester note that the point-to-point scatter that determines the value of *rms* may be less important in their data than the calibration errors over large ranges of wavelength. In our data the main uncertainty in deriving T_{eff} and $\log g$ from the energy distribution probably comes from the spectrophotometric observations being available at relatively few wavelengths. This makes it difficult to get accurate results when they are fitted to the computed spectra.

7.3. Stellar parameters from $H\gamma$

For stars cooler than about 8000 K, the $H\gamma$ profile is a good temperature indicator because it is almost independent of gravity, while for hotter stars with T_{eff} between 8000 K and 10000 K it depends on both T_{eff} and $\log g$. Above 10000 K, $H\gamma$ becomes a good gravity indicator, because it is almost independent of temperature.

In order to derive the stellar parameters from the $H\gamma$ profiles given by the KPNO spectra, we fitted the observed profiles (normalized to the continuum level) to the grids of profiles computed with the BALMER9 code (Kurucz, 1993a). For each star, we used the grid computed for a microturbulent velocity $\xi = 2$ km s⁻¹ and the metallicity closest to that derived for the star in a preliminary abundance analyses. We found that the fit was insensitive to the adopted value of ξ .

We used an interactive routine to omit all the lines of other elements which affect the $H\gamma$ profile, and by linear interpolation, we derived the residual intensities $R_{\text{obs}}(i)$ of $H\gamma$ for each $\lambda(i)$ sampled in the observed spectrum. We then used the same fitting procedure as that used to derive the parameters from the energy distributions. For

Table 7. Comparison of the stellar parameters obtained by different methods. (continued)

Star	Data	$E(B - V)$	T_{eff}	$\log g^{\ddagger}$	[M/H]	Method
HD 139961	[(a, r)	0.149 ¹	9 840±350	3.30±0.04	[-1.5a]	interpolation]
	(c, (b - y))	0.042 ²	8 350±250	3.30±0.05	"	"
	UV	0.058 ⁵ , 0.060 ⁶	8 600±100	3.3±0.1	"	"
	H γ	...	8 600±250	3.1±0.1	"	fit,RMS(min)=0.0098
	Mean:	0.051±0.008	8517±83	3.23±0.07	[-1.5a]	
HD 161817	[(c, (b - y))	0.073 ¹	8 120±150	3.50±0.04	[-1.5a]	interpolation]
	(c, (b - y))	0.000 ²	7 510±120	3.00±0.04	"	"
	[(V - K)	(0.000) ³	7 410±45*	(3.00)	"	"]
	En. Distr.	0.000 ⁴	7 550±200	3.0±0.2	"	fit,RMS(min)=0.0262
	UV	0.000 ⁵ , 0.000 ⁶	7 520±100	3.0±0.1	"	"
	H γ	...	7 550±100	(3.00)	"	fit,RMS(min)=0.0078
Mean:		0.000±0.000	7533±10	3.00±0.00	[-1.5a]	
HD 167105	(a, r)	0.043 ¹	9 270±300	3.25±0.04	[-1.5a]	interpolation
	(a, r)	0.000 ²	8 730±300	3.25±0.04	"	"
	UV	0.030 ⁵ , 0.029 ⁶	9 050±100	3.25±0.1	"	"
	H γ	...	9 050±500	3.4±0.2	"	fit,RMS(min)=0.0063
Mean:		0.024±0.013	9025±111	3.29±0.04	[-1.5a]	
HD 180903	[(c, (b - y))	0.076 ¹	7 530±120	2.90±0.04	[-1.5a]	interpolation]
	(c, (b - y))	0.103 ²	7 750±120	3.10±0.04	"	"
	UV	0.090 ⁵ , 0.095 ⁶	7 700±100	3.1±0.1	"	"
	H γ	...	7 600±100	(3.1)	"	fit,RMS(min)=0.0092
Mean:		0.098±0.005	7683±44	3.10±0.00	[-1.5a]	
HD 202759	(c, (b - y))	0.098 ¹	7 790±120	3.35±0.04	[-2.0a]	interpolation
	(c, (b - y))	0.063 ²	7 510±120	3.05±0.04	"	"
	En. Distr.	0.065 ⁴	7 300±100	2.8±0.1	"	fit,RMS(min)=0.0141
	UV	0.063 ⁵ , 0.06 ⁶	7 460±100	3.0±0.1	"	"
	H γ	...	7 550±150	(3.0)	"	fit,RMS(min)=0.0128
Mean:		0.072±0.009	7522±79	3.05±0.11	[-2.0a]	
HD 213468	(a, r)	0.017 ¹	9 280±320	3.30±0.04	[-1.5a]	interpolation
	(a, r)	0.000 ²	9 060±300	3.30±0.04	"	"
	UV	0.005 ⁵ , 0.006 ⁶	9 100±100	3.25±0.1	"	"
Mean:		0.008±0.005	9147±68	3.28±0.02	[-1.5a]	

[‡] If $T_{\text{eff}} < 8000$ K, H γ is almost independent of the gravity and $\log g$ is then given in parentheses. The gravities used to derive T_{eff} from the T_{eff} , $\log g$ & $(V - K)$ grid are also given in parentheses and were not used to obtain the mean gravity.

[†] RR Lyrae variable at phase 0.42 (Sect. 10.7).

* The quoted errors in these T_{eff} correspond to the range in $E(B - V)$ between columns 6 & 8 in Table 6.

¹ $E(B - V)$ taken from SFD map (Table 6, column 6).

² $E(B - V)$ derived from Strömgren colours using the Moon (1985) code (Table 6, column 8).

³ $E(B - V)$ is the mean of the values given in columns 6 & 8 of Table 6.

⁴ $E(B - V)$ was adjusted to obtain the best fit between the model and the observed Energy Distribution.

⁵ $E(B - V)$ was derived by comparing the observed and theoretical $(18 - V)$ colours for the T_{eff} , $\log g$ & [M/H] shown.

⁶ $E(B - V)$ was derived by comparing the observed and theoretical $(18 - V)$ vs. $(b - y)$ for the T_{eff} , $\log g$ & [M/H] shown.

each star, the parameters T_{eff} and $\log g$ are those which give the minimum *rms* difference.

For stars cooler than 8000 K, this procedure gives T_{eff} , but not $\log g$, because the H γ profile is not sensi-

tive to gravity for these temperatures. Therefore, to derive T_{eff} for these stars, we adopted the average $\log g$ from the Strömgren photometry and UV colours, since small differences in $\log g$ do not change the value of T_{eff} .

For stars with T_{eff} between 8000 K and 10000 K both T_{eff} and $\log g$ can be obtained by the fitting procedure, but the situation is less satisfactory because some ambiguity occurs in this range. For example, for $[M/H] = -1.5$, the $H\gamma$ profile is almost the same for $T_{\text{eff}} = 8800$ K, $\log g = 3.0$ as for $T_{\text{eff}} = 9500$ K, $\log g = 3.4$. This means that very small differences in the reduction procedure may give very different values for the parameters. Therefore, when the parameters derived from the fitting procedure were in reasonably agreement with other determinations, we have given both T_{eff} and $\log g$. Otherwise we fixed either T_{eff} or $\log g$ and calculated the other parameter. The stellar parameters found in this way are given on the “ $H\gamma$ ” line in Table 7. We give in parenthesis the parameters that were fixed in advance. As for the energy distribution, the errors in the parameters were estimated from the ranges in T_{eff} and $\log g$ for which $rms = rms(\text{min}) + 50\% rms(\text{min})$.

The main error in deriving T_{eff} and $\log g$ from $H\gamma$ comes from the uncertainty in the normalization of the KPNO spectra; this is largely because of a small non-linear distortion in the spectra which means that it is not a straightforward task to decide where the wings of $H\gamma$ start. The uncertainty in T_{eff} produced by the extraction procedure of the unblended $H\gamma$ profile is of the order of 50 K.

7.4. Stellar parameters from IUE data

As we discussed in Sect. 5, the parameters derived from the ultraviolet fluxes are those which lead to the most consistent values of reddening when one compares the observed $(18 - V)$ colours and also the observed $(18 - V)$ vs. $(b - y)$ colours with the corresponding theoretical values. The parameters found in this way are on the “UV” lines in Table 7.

As a further check, we compared the whole UV-observed energy distributions, for the stars that have both short- and long-wavelength IUE data, with model energy distributions computed with the adopted parameters given in Table 7. We did not find systematic discrepancies between the models and the observed data at 1600 Å and shorter wavelengths, as was found by Huenemörder et al. (1984) and Cacciari et al. (1987) using the 1979 Kurucz models. For more than half of these stars (HD 2857, HD 4850, HD 13780, HD 14829, HD 31943, HD 74721 and HD 93329) the observed and calculated energy distributions match rather well over the entire IUE wavelength range. For three stars (HD 78913, BD +00 0145 and HD 130201), the UV data suggest hotter temperatures than those adopted in Table 7. For three other stars (HD 8376, HD 60778 and HD 252940), the discrepancies may be caused by incorrect values of the adopted stellar parameters and/or uncertainties in the IUE and Strömgren photometry. A detailed investigation, that compares the observed and synthetic UV energy distributions using the latest model atmospheres, would be

Table 8. Systematic differences (Δ) from mean of T_{eff} obtained by different methods

Method	No. of Stars [‡]	Systematic Difference from mean (Δ)	Dispersion (rms)
(1)	(2)	(3)	(4)
$c((b - y))^1$	8	$+152 \pm 26$ K	69 K
$(a, r)^1$	12	$+198 \pm 54$ K	180 K
$c((b - y))^2$	18	-73 ± 30 K	122 K
$(a, r)^2$	8	-218 ± 64 K	169 K
En Distr	10	$+27 \pm 60$ K	180 K
UV	25	-10 ± 26 K	129 K
$H\gamma$	14	-80 ± 26 K	95 K
$(V - K)$	7	-75 ± 49 K	120 K

[‡] Omitting HD 117880, HD 130095 & HD 139961.

¹ $E(B - V)$ taken from SFD map (Table 6, column 6).

² $E(B - V)$ taken from Strömgren colours using Moon (1985) UVBYLIST program (Table 6, column 8).

of interest but is beyond the scope of this paper. Meanwhile, we are confident that the use of the $(18 - V)$ colour index gives results for the reddening and physical parameters which are consistent with and give the same degree of uncertainty as those that would be derived by using the entire IUE energy distributions.

7.5. The Effective Temperatures from $(V - K)_0$.

The $(V - K)$ colours are available for nine of our candidate BHB stars (Arribas & Martinez Roger 1987). These $(V - K)$ colours are listed in Table 1. For seven of these stars, $(V - K)$ colours had previously been given by Carney (1983). The mean difference between these two sets of colours (Carney *minus* Arribas & Martinez Roger) is 0.016 ± 0.005 ; this corresponds to a temperature difference of ~ 50 K; presumably the systematic error in these colours is of this order. The largest source of error in deriving temperatures in this way is likely to come from the correction for reddening. We assumed that $E(V - K) = 2.72 E(B - V)$ (Cohen et al. 1999) and took the $E(B - V)$ to be the mean of the $E(B - V)$ derived from the other methods given in column 3 of Table 7. We assumed the mean $\log g$ from the other determinations, and derived T_{eff} by interpolation in the T_{eff} , $\log g$ and $(V - K)_0$ grid. These temperatures are given in Table 7 and their errors are scaled from the estimated errors in $E(B - V)$; they were not used in deriving the mean T_{eff} but gave a useful independent check on the temperatures obtained by other methods (see Table 7). We see that the systematic difference between our adopted mean T_{eff} and the T_{eff} derived from $(V - K)$ is only slightly larger than that expected from the likely systematic errors in the $(V - K)$ colours.

7.6. The comparison of the stellar parameters determined by the different methods.

Table 7 gives, for each star, the straight means of $E(B - V)$, T_{eff} , and $\log g$ together with the errors of the means. In nearly all cases, the extinction derived from the SFD maps exceeds that derived by using the Moon UVBYLIST program (Table 6) and the use of the SFD extinctions with the $(c, (b - y))$ data gives higher T_{eff} than those found by other methods. This difference is most pronounced for low-latitude stars (HD 252940, HD 60778, HD 78913, HD 130095, HD 130201, HD 139961, HD 161817 and HD 180903) whose computed extinction depends upon an uncertain model of the local distribution of the interstellar extinctions. We have therefore felt justified in rejecting the stellar parameters that were derived using the SFD maps for these low-latitude stars. We also excluded the parameters determined from the Strömgren indices according to the Moon UVBYLIST program for the stars HD 117880 and HD 130095, because of the excessive difference between the reddening derived from the Moon code and that from the other determinations. These excluded parameters (and those derived from $(V - K)$) are enclosed in square brackets in Table 7.

The differences from these straight means were then computed for each method. The average of these differences (Δ) for T_{eff} are given for each method in Table 8. The dispersions given in column 4 of Table 8 are of the same order as the error estimates of the T_{eff} given in column 4 of Table 7 but there are significant differences. Thus the Energy Distribution method has among the smallest errors in Table 7 but has one of the largest dispersions in Table 8. This, together with the undoubted presence of systematic errors associated with each method has stopped us from using the error estimates for any attempt at weighting the T_{eff} in Table 7; we have therefore adopted the straight means for the parameters given in this Table.

8. Abundances

8.1. Abundances from KPNO and ESO-CAT spectra

Our first estimate of the abundances (using the mean stellar parameters given in Table 7) was made by fitting the measured equivalent widths (W_λ) of the apparently unblended lines to the computed ones. In the case of the spectra observed at Kitt Peak⁹, we tried to determine the microturbulent velocity (ξ) by assuming that, for a given element, the abundance is independent of the equivalent widths. The uncertainty, however, both in the equivalent widths of the weak lines and in the $\log gf$ values (especially for the lines of Ti II, which are the most numerous) severely limits this method of obtaining ξ . We therefore, in addition, determined ξ by comparing the observed spectra

against a series of synthetic spectra in which ξ was sampled in steps of 1.0 km s^{-1} ; in a few cases an intermediate step of 0.5 km s^{-1} was used.

In the case of BD +00 0145 and HD 14829 and for the stars observed at ESO we assumed a microturbulent velocity ξ of 2.0 km s^{-1} , since there were too few lines in their spectra to allow us to derive ξ .

In computing the synthetic spectra, we used either the mean abundance derived from the equivalent widths for species with more than one measured line (e.g. Fe I, Fe II, and Ti II) or the abundance computed from a single line if only one line of a species was available (e.g. Ba II $\lambda 4554$).

The synthetic spectra were computed at a resolving power of 500 000 and then were degraded to 15 000 (the nominal resolution of the Kitt Peak spectra) using a gaussian instrumental profile. The computed spectra were then broadened by the rotational velocity ($v \sin i$) that is given in column 2 of Table 15. This $v \sin i$ was derived by fitting the observed profile of the Mg II 4481 Å to the computed profile assuming the Mg abundance that had been derived from the measured equivalent width. No macroturbulent velocity was considered.

The comparison of our observed spectra with the synthetic spectra showed that some of the lines in our original list should be discarded either because they were blended or because they were too weak. The WIDTH program was now used to recompute new abundances from the equivalent widths (W_λ) of the remaining lines using the value of ξ that had been determined from the synthetic spectra. We made several iterations using both the comparison of the observed and the computed W_λ and the comparison of the observed and synthetic spectra until the abundances obtained by the two methods were consistent. In the course of the successive iterations we changed the ξ and the metallicity of the models so that they were as close as possible to the values that we derived from the abundance analysis.

The measured equivalent widths (W_λ), the adopted $\log gf$, their sources, and the logarithmic abundances relative to the *total number of atoms* are given for the individual lines for each star in Table 4 for the KPNO spectra and in Table 5 for the ESO-CAT spectra. Table 9 lists, for each star, the model parameters, the microturbulent velocity and the average abundances derived from the measured equivalent widths of the individual lines. We derived the barium abundance from the Ba II 4554.033 Å line. For a few stars, we used only the synthetic spectra, while for some others we used the equivalent width method in addition. Both values are given in Table 9 (that from the synthetic spectra is identified with the superscript S). The slight systematic difference between the abundances obtained by the two methods may be related to the placement of the continuum level which was fixed independently by Kinman for the measurement of the KPNO equivalent widths and by Castelli for the normalization of the whole observed spectrum.

⁹ except for BD +00 0145 and HD 14829 for which only the Mg II 4481 Å line was measured.

Table 9. Abundances derived from the KPNO and CAT spectra.

	HD 2857 KPNO	HD 4850 CAT	BD +00 145 KPNO	HD 8376 KPNO	HD 13780 CAT
Model	7 550/3.0/[-1.5a]	8 450/3.2/[-1.5a]	9 700/4.0/[-1.5a]	8 150/3.3/[-2.5a]	7 950/3.1/[-1.5a]
$\xi(\text{km s}^{-1})$	3.00	(2.00)	(2.00)	1.00	(2.00)
Mg II	-5.76 (1)	-5.10(1)	-6.46 (1)	-6.86 (1)	-5.58 (1)
Ca I	-7.16 (1)
Ti II	-8.19 \pm 0.23 (14)	-7.65 \pm 0.04 (4)	...	-9.12 \pm 0.14(5)	-7.90 \pm 0.17 (4)
Cr I	-8.10 (1)
Cr II	-7.92 (1)
Fe I	-6.29 \pm 0.24 (6)	-5.86 (1)	...	-7.49 \pm 0.06(2)	-5.97 (1)
Fe II	-6.25 \pm 0.17 (9)	-5.76 \pm 0.05 (2)	-6.01 \pm 0.1 (2)
Ba II	-11.72 (1)
	HD 14829 KPNO	HD 16456 ¹ KPNO	HD 16456 ¹ CAT	HD 31943 KPNO	HD 31943 CAT
Model	8 900/3.2/[-2.0a]	6 750/(2.8)/[-1.5a]	(7500)/(3.0)/[-1.5a]	7 900/3.2/[-1.0a]	7 900/3.2/[-1.0a]
$\xi(\text{km s}^{-1})$	(2.00)	3.00	(3.00)	4.00	4.00
Mg II	-6.47 (1)	- 5.87 (1)	-5.85 (1)	- 4.90 (1)	-4.91 (1)
Ca I	...	-7.22 \pm 0.02 (2)	...	-6.66 \pm 0.06 (3)	-6.53 (1)
Ti II	...	-8.36 \pm 0.30 (14)	-8.31 \pm 0.17(4)	-7.67 \pm 0.21 (20)	-7.68 \pm 0.17 (4)
Cr I	-7.55 (1)	...
Cr II	...	-7.73 (1)	...	-7.26 (1)	...
Fe I	...	-6.25 \pm 0.07 (6)	-6.19 \pm 0.06 (3)	-5.58 \pm 0.14 (8)	-5.47 \pm 0.02 (3)
Fe II	...	-6.24 \pm 0.12 (12)	-6.19 \pm 0.03 (2)	-5.50 \pm 0.10 (13)	-5.49 \pm 0.05 (2)
Ba II	...	-11.44 (1)	...	-11.15 (1)	...
	HD 252940 KPNO	HD 60778 KPNO	HD 74721 KPNO	HD 78913 CAT	HD 86986 KPNO
Model	7 550/2.95/[-1.5a]	8 050/3.1/[-1.5a]	8 900/3.3/[-1.5a]	8 500/3.25/[-1.5a]	7 950/3.2/[-1.5a]
$\xi(\text{km s}^{-1})$	3.50	3.00	4.00	(2.00)	2.50
Mg II	-5.91 (1)	- 5.40 (1)	-5.64 (1)	-5.43 (1)	-5.72 (1)
Ca I	-7.12 (1)	-7.07 (1)
Sc II	-10.54 (1)	...	-10.08 (1)
Ti II	-8.27 \pm 0.19 (14)	-8.14 \pm 0.24 (15)	-8.11 \pm 0.13(13)	-8.23 (1)	-8.32 \pm 0.17 (4)
Cr II	-7.85 (1)	-7.79 (1)	-7.64 (1)	...	-7.79 (1)
Fe I	-6.33 \pm 0.12 (6)	-6.03 \pm 0.21 (6)	-5.95 \pm 0.10 (5)	...	-6.36 \pm 0.10 (4)
Fe II	-6.30 \pm 0.09 (6)	-6.02 \pm 0.13 (12)	-5.97 \pm 0.08 (9)	...	-6.34 \pm 0.10 (7)
Ba II	-11.84 (1)	-11.76 (1) -11.61 ^S (1)	-11.85 (1), -11.71 ^S (1)
	HD 87047 KPNO	HD 87112 KPNO	HD 93329 KPNO	BD +32 2188 KPNO	HD 106304 CAT
Model	7 850/3.1/[-2.5a]	9 750/3.5/[-1.5a]	8 250/3.1/[-1.5a]	10450/2.1/[-1.0]	9 750/3.5/[-1.5a]
$\xi(\text{km s}^{-1})$	2.00:	2.00:	2.00	1.00	(2.00)
Mg II	-6.47 (1)	-5.55(1)	-5.27 (1)	-5.50 \pm 0.05 (2)	-5.28 (1)
Ca I
Sc II	-10.25 \pm 0.03 (2)
Ti II	-8.89 \pm 0.12 (8)	-8.19 \pm 0.11 (7)	-7.84 \pm 0.19 (14)	...	-8.29 (1)
Cr II	...	-7.62 (1)	-7.51 (1)	-7.41 (1)	...
Fe I	-7.01 \pm 0.11 (5)	-5.92 (1)	-5.86 \pm 0.08 (6)
Fe II	-7.01 \pm 0.04 (2)	-6.08 \pm 0.11 (5)	-5.87 \pm 0.06 (12)	-5.65 \pm 0.18 (10)	...
Ba II	-11.27 (1)

Table 9. Abundances derived from the KPNO and CAT spectra.(continued)

	BD +42 2309 KPNO	HD 109995 KPNO	BD +25 2602 KPNO	HD 117880 KPNO	HD 128801 KPNO
Model	8 800/3.2/[-1.5a]	8 500/3.1/[-1.5a]	8 400/3.2/[-2.0a]	9 300/3.3/[-1.5a]	10 300/3.55/[-1.5a]
$\xi(\text{km s}^{-1})$	2.00	3.00	4.00	2.00:	2.00
Mg II	-5.66 (1)	-5.84 (1)	-6.15 (1)	-5.51 (1)	-5.55 (1)
Ca I
Ti II	-8.15 \pm 0.13 (6)	-8.31 \pm 0.12 (10)	-8.63 \pm 0.14(8)	-8.27 \pm 0.20 (9)	-8.23 \pm 0.10 (8)
Cr II	-8.02 (1)	-7.73 (1)	-7.77 (1)
Fe I	-6.13 \pm 0.22 (4)	-6.24 \pm 0.12 (4)	-6.52 \pm 0.10 (5)	-6.13 \pm 0.03 (3)	-6.01 \pm 0.05 (2)
Fe II	-6.20 \pm 0.11 (3)	-6.28 \pm 0.13 (7)	-6.53 \pm 0.02 (3)	-6.23 \pm 0.07 (6)	-5.97 \pm 0.08 (6)
<hr/>					
	HD 130095 KPNO	HD 130095 CAT	HD 130201 CAT	HD 139961 KPNO	HD 139961 CAT
Model	9 000/3.3/[-2.0a]	9 000/3.3/[-2.0a]	8 650/3.5/[-1.0a]	8 500/3.2/[-1.5a]	8 500/3.2/[-1.5a]
$\xi(\text{km s}^{-1})$	2.00	2.00	(2.00)	3.00	3.00
Mg II	-6.11 (1)	-6.12 (1)	-4.66 (1)	-5.80 (1)	-5.79 (1)
Ti II	-8.72 \pm 0.18 (9)	-8.86 (1)	-7.82 \pm 0.16(2)	-8.29 \pm 0.16 (9)	-8.41 (1)
Cr II	-8.06 (1)	-7.78 (1)	...
Fe I	-6.40 (1)	-6.31 \pm 0.04 (4)	...
Fe II	-6.42 \pm 0.15 (4)	...	-5.54 (1)	-6.20 \pm 0.17 (6)	...
<hr/>					
	HD 161817 KPNO	HD 167105 KPNO	HD 180903 KPNO	HD 180903 CAT	HD 202759 KPNO
Model	7 550/3.0/[-1.5a]	9 050/3.3/[-1.5a]	7 700/3.1/[-1.5a]	7 700/3.1/[-1.5a]	7 500/3.05/[-2.0a]
$\xi(\text{km s}^{-1})$	3.00	3.00	3.00	3.00	2.0
Mg II	-5.69 (1)	-5.77 (1)	-5.34 (1)	-5.26 (1)	-6.33 (1)
Ca I	-6.99 (1)	...	-6.70 \pm 0.36 (3) -6.90 ^S
Sc II	-10.08 \pm 0.35 (3)	...	-10.98 \pm 0.24 (2)
Ti II	-8.13 \pm 0.24 (14)	-8.20 \pm 0.14 (11)	-7.89 \pm 0.33(20)	-7.84 \pm 0.01 (3)	-8.74 \pm 0.25 (12)
Cr I	-8.02 (1)	...	-7.99 (1)	...	-8.58 (1)
Cr II	...	-7.80 (1)	-7.69 (1)	...	-8.12 (1)
Fe I	-6.06 \pm 0.12 (6)	-6.08 \pm 0.05 (3)	-5.99 \pm 0.14 (8)	-6.02 \pm 0.02 (2)	-6.67 \pm 0.05 (5)
Fe II	-6.12 \pm 0.07 (10)	-6.12 \pm 0.12 (8)	-5.96 \pm 0.10 (9)	-6.00 \pm 0.03 (2)	-6.73 \pm 0.12 (8)
Ba II	-11.60 (1)	...	-11.46 (1), -11.31 ^S (1)	...	-12.62 (1) -12.52 ^S (1)
<hr/>					
	HD 202759 CAT	HD 213468 CAT			
Model	7 500/3.05/[-2.0a]	9 150/3.3/[-1.5a]			
$\xi(\text{km s}^{-1})$	2.00	(2.00)			
Mg II	-6.38 (1)	- 5.71 (1)			
Ti II	-8.80 \pm 0.18 (4)	-8.04 \pm 0.36 (3)			
Fe I	-6.57 (1)	...			
Fe II	-6.68 \pm 0.08 (2)	...			

^S Abundances derived from the synthetic spectrum analysis¹ RR Lyrae variable CS Eri at phase 0.42. A further discussion is given in Section 10.7

Table 10 summarizes the abundances relative to the solar values together with the [Mg/Fe] and [Ti/Fe] ratios. The solar abundances, relative to the total number of atoms, are taken from Grevesse et al. (1996). Their logarithmic values are -4.46 for Mg, -5.68 for Ca, -8.87 for Sc, -7.02 for Ti, -6.37 for Cr, -4.54 for Fe, and -9.91 for

Ba. A few of them are also given in the last line of Table 10 for reference.

The ESO-CAT abundances, although based on only a few lines, show excellent agreement with those derived from the KPNO spectra for the non-variable stars HD 31943, HD 130095, HD 139961 and HD 180903 and

Table 10. The adopted parameters and abundances relative to the solar values.

Star	T_{eff} (K)	$\log g$	ξ (km/s)	[Fe/H]	[Mg/H]	[Ti/H]	[Ba/H]	[Mg/Fe]	[Ti/Fe]	[Fe/H] ^a
(1)	(2)	(3)	(4)	(5)	(6)	(7)	(8)	(9)	(10)	(11)
HD 2857 ^K	7550	3.00	3.0	[-1.73]	[-1.30]	[-1.17]	[-1.84]	[+0.43]	[+0.56]	[-1.70]
HD 4850 ^C	8450	3.20	(2.0)	[-1.27]	[-0.64]	[-0.63]	...	[+0.63]	[+0.64]	[-1.18]
BD +00 0145 ^K	9700	4.00	(2.0)	...	[-2.00]	[-2.45]
HD 8376 ^K	8150	3.30	1.0	[-2.95]	[-2.40]	[-2.10]	...	[+0.55]	[+0.85]	[-2.82]
HD 13780 ^C	7950	3.10	(2.0)	[-1.45]	[-1.12]	[-0.88]	...	[+0.33]	[+0.57]	[-1.53]
HD 14829 ^K	8900	3.20	(2.0)	...	[-2.01]	[-2.39]
HD 16456 ^K	6750	2.80	3.0	[-1.70]	[-1.41]	[-1.34]	[-1.56]	[+0.29]	[+0.36]	[-1.82]
HD 16456 ^C	7500	3.00	(3.0)	[-1.65]	[-1.39]	[-1.29]	...	[+0.26]	[+0.36]	[-1.80]
HD 31943 ^K	7900	3.20	4.0	[-1.04]	[-0.44]	[-0.65]	[-1.25]	[+0.60]	[+0.39]	[-0.97]
HD 31943 ^C	"	"	"	[-0.94]	[-0.45]	[-0.66]	...	[+0.59]	[+0.28]	[-0.98]
HD 252940 ^K	7550	2.95	3.5	[-1.77]	[-1.45]	[-1.25]	[-1.90]	[+0.32]	[+0.52]	[-1.80]
HD 60778 ^K	8050	3.10	3.0	[-1.49]	[-0.94]	[-1.12]	[-1.70]	[+0.55]	[+0.37]	[-1.34]
HD 74721 ^K	8900	3.30	4.0	[-1.42]	[-1.18]	[-1.09]	...	[+0.24]	[+0.33]	[-1.48]
HD 78913 ^C	8500	3.25	(2.0)	...	[-0.97]	[-1.21]	[-1.43]
HD 86986 ^K	7950	3.20	2.5	[-1.81]	[-1.26]	[-1.30]	[-1.80]	[+0.55]	[+0.51]	[-1.66]
HD 87047 ^K	7850	3.10	2.0:	[-2.47]	[-2.01]	[-1.87]	...	[+0.46]	[+0.60]	[-2.43]
HD 87112 ^K	9750	3.50	2.0:	[-1.46]	[-1.09]	[-1.17]	...	[+0.37]	[+0.29]	[-1.56]
HD 93329 ^K	8250	3.10	2.0	[-1.32]	[-0.81]	[-0.82]	[-1.39]	[+0.51]	[+0.50]	[-1.30]
BD +32 2188 ^K	10450	2.10	1.0	[-1.11]	[-1.04]	[+0.07]	...	[-1.45]
HD 106304 ^C	9750	3.50	(2.0)	...	[-0.82]	[-1.21]	[-1.34]
BD +42 2309 ^K	8800	3.20	2.0	[-1.63]	[-1.20]	[-1.13]	...	[+0.43]	[+0.50]	[-1.62]
HD 109995 ^K	8500	3.10	3.0	[-1.72]	[-1.38]	[-1.29]	...	[+0.34]	[+0.43]	[-1.70]
BD +25 2602 ^K	8400	3.20	4.0	[-1.98]	[-1.69]	[-1.61]	...	[+0.29]	[+0.37]	[-1.98]
HD 117880 ^K	9300	3.30	2.0:	[-1.64]	[-1.05]	[-1.25]	...	[+0.59]	[+0.39]	[-1.51]
HD 128801 ^K	10300	3.55	2.0	[-1.45]	[-1.09]	[-1.21]	...	[+0.36]	[+0.24]	[-1.56]
HD 130095 ^K	9000	3.30	2.0	[-1.87]	[-1.65]	[-1.70]	...	[+0.22]	[+0.17]	[-2.04]
HD 130095 ^C	"	"	"	...	[-1.66]	[-1.84]	[-2.05]
HD 130201 ^C	8650	3.50	(2.0)	[-1.00]	[-0.20]	[-0.80]	...	[+0.80]	[+0.20]	[-0.86]
HD 139961 ^K	8500	3.20	3.0	[-1.71]	[-1.34]	[-1.22]	...	[+0.37]	[+0.49]	[-1.68]
HD 139961 ^C	"	"	3.0	...	[-1.33]	[-1.39]	[-1.66]
HD 161817 ^K	7550	3.00	3.0	[-1.55]	[-1.23]	[-1.11]	[-1.76]	[+0.32]	[+0.44]	[-1.64]
HD 167105 ^K	9050	3.30	3.0	[-1.56]	[-1.31]	[-1.18]	...	[+0.25]	[+0.38]	[-1.66]
HD 180903 ^K	7700	3.10	3.0	[-1.43]	[-0.88]	[-0.87]	[-1.40]	[+0.55]	[+0.56]	[-1.32]
HD 180903 ^C	"	"	"	[-1.47]	[-0.80]	[-0.82]	...	[+0.67]	[+0.65]	[-1.27]
HD 202759 ^K	7500	3.05	2.0	[-2.16]	[-1.87]	[-1.72]	[-2.00]	[+0.29]	[+0.44]	[-2.35]
HD 202759 ^C	"	"	"	[-2.08]	[-1.92]	[-1.78]	...	[+0.16]	[+0.30]	[-2.40]
HD 213468 ^C	9150	3.30	(2.0)	...	[-1.25]	[-1.02]	[-1.67]
Sun	$\log(N_{\text{elem}}/N_{\text{tot}})$			Fe=-4.54	Mg=-4.46	Ti=-7.02	Ba=-9.91			

^K: KPNO spectra; ^C: CAT spectra^a Derived from Mg II λ 4481 (see text).

for the low-amplitude variable HD 202759. The case of the larger amplitude type-c variable HD 16456 (CS Eri) is discussed in Sect. 10.7.

For the stars whose T_{eff} exceeds about 8500 K (or about half the stars in our sample), the He I λ 4471 line is visible in our spectra. Its strength agrees with that predicted by the synthetic spectrum for a solar helium abundance.

8.2. The [Fe/H] abundance as a function of the equivalent width of Mg II λ 4481 line and the colour index $(B - V)_0$

In most halo stars, [Mg/Fe] can be assumed either to be constant or a slowly-varying monotonic function of [Fe/H] (see Sect. 10.5). If we have the photometric information, we can derive the stellar parameters and then determine [Mg/H] from the equivalent width of the Mg II λ 4481 line even in quite low resolution spectra; [Fe/H] can then be

derived by assuming an appropriate value for $[\text{Mg}/\text{Fe}]$; in this paper we assume $[\text{Mg}/\text{Fe}] = 0.43$.

Even if only $(B - V)_0$ is available, one can estimate $[\text{Fe}/\text{H}]$ from the the equivalent width W of the $\text{Mg II } \lambda 4481$ doublet and the intrinsic colour. Using the data and $[\text{Fe}/\text{H}]$ abundances that we derived from our KPNO spectra we found the following expression:

$$[Fe/H] = -3.350 + 0.01119W - 0.00001315W^2 - 0.30(B - V)_0$$

where $(B - V)_0$ was obtained by using the mean extinctions given in boldface in column 3 of Table 7¹⁰. $[\text{Fe}/\text{H}]$ derived from the above equation is listed in the last column of Table 10. The *rms* difference between our measured $[\text{Fe}/\text{H}]$ and those obtained from this equation is ± 0.12 for the range $-0.05 \leq (B - V)_0 \leq 0.17$. Systematic differences can occur between equivalent widths measured at very different spectral resolutions. Our relation strictly applies only to spectra whose resolution is comparable to those discussed in this paper; it may be less accurate if used with equivalent widths derived from lower resolution spectra.

9. Uncertainties

In this section we consider the effect on our abundances of uncertainties in T_{eff} , $\log g$, and the microturbulent velocity ξ . We also consider errors in $\log gf$ and NLTE effects.

9.1. Uncertainty in the the stellar parameters T_{eff} , $\log g$

The quantitative dependence of the derived abundances on differences $\Delta T_{\text{eff}} = \pm 100$ K and $\Delta \log g = \pm 0.1$ dex in the stellar parameters is given for the stars HD 161817, HD 139961, HD 167105, and HD 87112 in Table 11. These stars are representative of stars having T_{eff} around 7500 K, 8500 K, 9000 K, and 9750 K respectively. It is seen that the uncertainty in T_{eff} affects the abundances more than the uncertainty in $\log g$. Furthermore, the species most affected by uncertainties in the parameters are Cr I, Fe I and Ba II. Their abundance changes by about 0.1 dex for $\Delta T_{\text{eff}} = \pm 100$ K. The effect on $\text{Mg II } \lambda 4481$ is small and decreases with increasing T_{eff} .

9.2. Uncertainty in ξ

The value of ξ was assumed for the spectra of the two stars BD 00+00 145 and HD 14829 and for all the ESO-CAT spectra because there were too few lines in these spectra to determine this quantity. Table 12 gives the abundances of the different species in these stars for microturbulent velocities $\xi = 2$ km s⁻¹, 3 km s⁻¹ and 4 km s⁻¹. For a change $\Delta \xi = 1$ km s⁻¹, the abundance derived from the $\text{Mg II } \lambda 4481$ line changes by about 0.2 dex for the stars observed

Table 11. Abundance changes produced by uncertainties of ± 100 K in T_{eff} and ± 0.1 in $\log g$

Star	Elem	$\Delta \log \epsilon$		Net error
		ΔT_{eff} ± 100	$\Delta \log g$ ± 0.1	
(1)	(2)	(3)	(4)	(5)
HD 161817	Mg II	± 0.04	± 0.04	0.06
T_{eff} 7533 K	Ca I	± 0.08	± 0.02	0.08
$\log g$ 3.00	Ti II	± 0.04	± 0.04	0.06
	Cr I	± 0.09	± 0.01	0.09
	Fe I	± 0.08	± 0.01	0.08
	Fe II	± 0.03	± 0.03	0.04
	Ba II	± 0.09	± 0.01	0.09
HD 139961	Mg II	± 0.00	± 0.02	0.02
T_{eff} 8517 K	Ti II	± 0.06	± 0.02	0.06
$\log g$ 3.23	Cr II	± 0.04	± 0.02	0.04
	Fe I	± 0.10	± 0.03	0.10
	Fe II	± 0.04	± 0.02	0.04
HD 167105	Mg II	± 0.01	± 0.01	0.01
T_{eff} 9025 K	Ti II	± 0.07	± 0.01	0.07
$\log g$ 3.29	Cr II	± 0.04	± 0.02	0.04
	Fe I	± 0.10	± 0.04	0.11
	Fe II	± 0.04	± 0.02	0.04
HD 87112	Mg II	± 0.01	± 0.01	0.01
T_{eff} 9733 K	Ti II	± 0.06	± 0.01	0.06
$\log g$ 3.48	Cr II	± 0.03	± 0.02	0.04
	Fe I	± 0.09	± 0.04	0.10
	Fe II	± 0.03	± 0.03	0.04

at ESO and about 0.05 dex for the two weaker-lined stars observed at KPNO (BD +00 145 and HD 14829). The abundance derived from the Ti II lines is also affected by the value of ξ ; the change varies from 0.2 dex for HD 4850 and HD 13780 to 0.05 dex for HD 106304. The effect of ξ on the Fe I and Fe II abundances is very small in all these stars.

9.3. Errors in $\log gf$

The errors in $\log gf$ can be a significant source of uncertainty if only a few lines of a species are available for measurement. This can happen if the star is very metal-poor (e.g. HD 008376) so that only the strongest lines are measurable or, as with the ESO-CAT spectra, the observed waveband is not large. We inferred the presence of these errors in $\log gf$ as follows.

Our first estimate of the abundance was made by fitting the measured equivalent widths (W_λ) of the apparently unblended lines to those computed by Kurucz's WIDTH program. We therefore have an abundance for each line and the difference between this abundance and the mean for that species in a given star is called $\Delta[\text{m}/\text{H}]$.

¹⁰ One may replace the $(B - V)_0$ term by $-0.44(b - y)_0$.

Table 12. The effect of the microturbulent velocity ξ on the abundances

Star	Elem	$\log(N_{elem}/N_{tot})$		
		$\xi=2.0$	$\xi=3.0$	$\xi=4.0$
HD 4850	Mg II	-5.10	-5.34	-5.53
	Ti II	-7.65	-7.86	-7.95
	Fe I	-5.86	-5.87	-5.87
	Fe II	-5.76	-5.80	-5.82
BD +00 0145	Mg II	-6.46	-6.51	-6.54
HD 13780	Mg II	-5.48	-5.69	-5.82
	Ti II	-7.90	-8.11	-8.20
	Fe I	-5.97	-5.98	-5.60
	Fe II	-6.01	-6.04	-6.06
HD 14829	Mg II	-6.40	-6.47	-6.53
HD 78913	Mg II	-5.43	-5.64	-5.78
	Ti II	-8.23	-8.41	-8.50
HD 106304	Mg II	-5.28	-5.49	-5.64
	Ti II	-8.23	-8.27	-8.29
HD 130201	Mg II	-4.66	-4.86	-5.06
	Ti II	-7.82	-7.94	-8.00
	Fe II	-5.54	-5.60	-5.63
HD 213468	Mg II	-5.71	-5.87	-6.00
	Ti II	-7.90	-7.94	-7.96
	Fe I	-4.28	-4.36	-4.40

This quantity, when averaged over all our program stars, ($\langle \Delta[m/H] \rangle$) is shown in Fig 8 for both the Fe II and Ti II lines. It shows little correlation with equivalent width (the W_λ on the left of Fig. 8 are those for HD 93329 which has an intermediate T_{eff}).

$\langle \Delta[m/H] \rangle$ was also computed (for the same lines) from the BHB star data of Lambert et al. (1992) and is called $\langle \Delta[m/H] \rangle_{\text{LMS}}$. It is seen that there is a correlation between the values of $\langle \Delta[m/H] \rangle$ determined from our data and those of Lambert et al.; moreover the range in this quantity is markedly greater for the Ti II lines than for the Fe II ones. This scatter in $\langle \Delta[m/H] \rangle$ is greater than can be accounted for by measuring errors (the vertical error bars) and must be caused by a factor that is intrinsic to each species and which is common to both our calculations and those of Lambert et al. It seems most likely that it is caused by errors in the assumed $\log gf$.

9.4. Non-LTE effects

The models used to derive our abundances assume LTE conditions. In hot stars, however, UV radiation can cause the Fe I states to be underpopulated while the Fe II lines

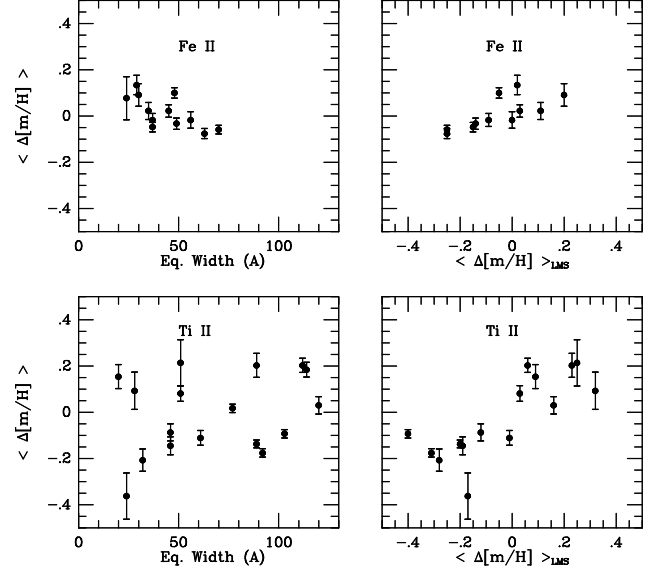


Fig. 8. $\Delta[m/H]$ is the difference between the abundance derived from a given line and the mean abundance of that species for that star. $\langle \Delta[m/H] \rangle$ is the mean value of this quantity for each [Fe II] line (above) and [Ti II] line (below). This mean is plotted against the equivalent width (on the left) and against the same quantity from the BHB spectra of Lambert et al. (1992) (on the right).

are relatively unaffected; the effect is expected to increase with decreasing metallicity. Lambert et al. (1992) tried to allow for this effect by adjusting their stellar parameters so as to make $[\text{Fe I}] - [\text{Fe II}] = -0.2$. Cohen & McCarthy (1997), however, made no non-LTE corrections in deriving the abundances of BHB stars in M 92. The T_{eff} of their stars were in the range 7500 K to 9375 K and were derived from their $(B - V)$ and $(V - K)$ colours. They found a mean value for $\langle [\text{Fe I}] - [\text{Fe II}] \rangle$ of only -0.08 ; this suggests that non-LTE effects are not significant. The abundances, moreover, which they found for their BHB stars were in excellent agreement with those previously found for red giants in the same cluster. We find $\langle [\text{Fe I}] - [\text{Fe II}] \rangle = 0.01 \pm 0.01$ for the 27 spectra where we measured both Fe I and Fe II lines. We therefore feel that it is unlikely that our iron abundances are significantly compromised by non-LTE effects. Our barium abundances (Table 9) were derived from the Ba II $\lambda 4554.03$ line alone and gave a mean LTE abundance of $[\text{Ba}/\text{Fe}]$ from nine stars of -0.08 ± 0.05 ; hyperfine broadening was not taken into account and significant non-LTE effects may be expected for this line (Mashonkina & Bikmaev 1996, Belyakova et al. 1998).

9.5. Convection

For the coolest stars of our sample ($T_{\text{eff}} < 8000$ K) there may be a problem with the treatment of the convection in the model atmospheres. Uncertainties of the order of 200 K in T_{eff} can be expected in the sense that T_{eff} is

higher for the mixing-length parameter $l/H = 1.25$ that we adopted than for the lower value $l/H = 0.5$ suggested by Fuhrmann, Axer & Gehern (1993, 1994). Also, a different convection theory, like that of Canuto & Mazzitelli (1992) leads to a very low convection (or no convection) in stars hotter than 7000 K, so that T_{eff} derived by adopting this theory may be lower than that derived by us. We feel, however, that more accurate observations that allow a more precise location of the continuum and more discussions on the theories adopted to compute the Balmer profiles are needed in order to confirm the superiority of other convections over that adopted by us. The effect of convection on the colour indices and Balmer profiles, and therefore on the T_{eff} derived from them, has been discussed by Smalley & Kupka (1997), Van't Veer-Menneret & Megessier (1996), Castelli et al. (1997), and Gardiner et al. (1999).

10. Discussion

10.1. Comparison with previous observers.

Table 13 compares model parameters and abundances found by us (KCCBHV) with those given by other authors. Stellar abundances are relative to the solar values from Grevesse et al. (1996), as given at the end of Table 10. Parameters from de Boer et al. (1997) (BTS) are only averages of previous determinations taken from the literature. Takeda & Sadakane (1997) estimated the stellar parameters of HD 161817 from the literature. They obtained a microturbulent velocity $\xi = 4 \text{ km s}^{-1}$ from an analysis of O I lines in this star and suggested that ξ is depth dependent.

The mean differences between our parameters and abundances and those found by Adelman & Philip (1990, 1994, 1996a) for the nine stars we have in common are:

$$\begin{aligned} \langle \Delta[\text{Fe}/\text{H}] \rangle &= +0.08 \pm 0.05 \quad (\pm 0.14) \\ \langle \Delta[\text{Mg}/\text{H}] \rangle &= -0.02 \pm 0.14 \quad (\pm 0.35) \\ \langle \Delta[\text{Ti}/\text{H}] \rangle &= +0.16 \pm 0.05 \quad (\pm 0.14) \\ \langle \Delta T_{\text{eff}} \rangle &= +331 \text{ K} \pm 75 \text{ K} \quad (\pm 212 \text{ K}) \\ \langle \Delta \log g \rangle &= +0.10 \pm 0.10 \quad (\pm 0.27) \\ \langle \Delta \xi \rangle &= +1.0 \pm 0.4 \quad (\pm 1.0) \end{aligned}$$

where the numbers in parentheses are the *rms* differences between the individual determinations. The most significant difference is in T_{eff} and this may well be traceable to different assumptions for interstellar reddening. The largest of these is the 800 K difference in T_{eff} for HD 130095 for which there is a large range in the different estimates of $E(B - V)$. In spite of this, the differences between the abundance estimates for this star are quite small. For further comments on HD 130095 see Sect. 10.6.

Gray et al. (1996) give stellar parameters for BHB stars that were determined from Philip's Strömgren photometry, classification-dispersion spectra and spectral synthesis. The mean differences between our parameters and theirs for the ten stars in common are:

$$\begin{aligned} \langle \Delta[\text{Fe}/\text{H}] \rangle &= -0.26 \pm 0.05 \quad (\pm 0.16) \\ \langle \Delta T_{\text{eff}} \rangle &= +40 \text{ K} \pm 91 \text{ K} \quad (\pm 272 \text{ K}) \\ \langle \Delta \log g \rangle &= -0.09 \pm 0.02 \quad (\pm 0.06) \end{aligned}$$

The systematic difference between our T_{eff} and those of Gray et al. are much smaller than for those given by Adelman & Philip. The abundance estimates of Gray et al. from their low resolution spectra, however, average 0.2 to 0.3 dex more metal rich than ours.

10.2. Comparison of BHB abundances with those of other types of halo stars.

Excluding BD +32 2188, BD +00 0145 and HD 16456, we have 28 stars that from their stellar parameters, abundances, $v \sin i$ and kinematics have a very high probability of being BHB stars. HD 202759 has been classified as a type c RR Lyrae star, but its V -amplitude is so low ($< 0.1 \text{ mag}$), and its T_{eff} is so high (7500 K), that it has been included with the BHB stars. The $[\text{Fe}/\text{H}]$ of these 28 stars lie in the range -0.99 (for HD 31943) to -2.95 (for HD 8376) with a mean value of -1.67 ± 0.08 and an *rms* dispersion (σ) about this mean of $\pm 0.42^{11}$. We compare these parameters with those of other types of halo stars in Table 14. The small group of nearby red horizontal branch stars are taken from Pilachowski et al. (1996). The nearby RR Lyrae stars include those with abundances by Clementini et al. (1995) and by Lambert et al. (1996). The red giants are those within 600 pc from the sample given by Chiba & Yoshi (1998). The halo globular clusters are those listed by Armandroff (1989). The first sample is a subset of 21 of these clusters whose $[\text{Fe}/\text{H}]$ has been given by Carretta & Gratton (1997). The second sample contains all those in Armandroff's list, using Carretta & Gratton's abundances for 21 of the clusters while for the remainder, the abundances given by Armandroff (which are on the Zinn & West (1984) scale) were converted to the system of Carretta & Gratton using the quadratic relation given in their paper¹². The halo clusters, on the average, appear to be 0.1 or 0.2 dex more metal-rich than the field halo stars. On the Zinn & West scale, they would have had more comparable metallicities. The red giant sample contains a greater fraction of very metal-poor stars than the other groups. Thus, 30% of the red giants have $[\text{Fe}/\text{H}] \leq -2.00$ while only between 5 and 10% of the globular clusters are this metal-poor; this difference is significant at better than the 1% level. This is possibly because many of the red giants were discovered in the objective-prism surveys of Bond (1970, 1980)

¹¹ The 24 BHB stars for which we derived abundances from high resolution spectra have a mean $[\text{Fe}/\text{H}]$ of -1.66 ± 0.09 . The four BHB stars for which an abundance was estimated from the Mg II ($\lambda 4481$) line have a mean $[\text{Fe}/\text{H}]$ of -1.71 ± 0.27

¹² The most metal-poor cluster, NGC 5053, lies outside the range of this relation. This makes the metal-poor limit of this cluster sample uncertain but scarcely affects its mean value.

Table 13. Comparison of stellar parameters and abundances from different authors

Star	T_{eff} (K)	$\log g$	ξ km s^{-1}	[Fe/H]	[Mg/H]	[Ti/H]	[Ba/H]	Source
(1)	(2)	(3)	(4)	(5)	(6)	(7)	(8)	(9)
HD 2857	7550	3.00	3.0	[−1.73]	[−1.30]	[−1.17]	[−1.84]	KCCBHV
	7700	3.10	...	[−1.5]	GCP
HD 14829	8900	3.20	...	[−2.39]	[−2.01]	KCCBHV
	8700	3.30	...	[−2.0]	GCP
HD 60778	8050	3.10	3.0	[−1.49]	[−0.94]	[−1.12]	[−1.70]	KCCBHV
	8600	3.30	...	[−1.0]	GCP
HD 74721	8900	3.30	4.0	[−1.42]	[−1.18]	[−1.09]	...	KCCBHV
	8600	3.30	1.4	[−1.40]	[−0.96]	[−1.00]	...	AP96
	8600	3.30	...	[−1.5]	GCP
HD 86986	7950	3.20	2.5	[−1.81]	[−1.26]	[−1.30]	[−1.80]	KCCBHV
	7800	3.10	2.2	[−1.80]	[−1.21]	[−1.35]	[−2.15]	AP96
	8050	3.20	...	[−1.5]	GCP
HD 93329	8250	3.10	2.0	[−1.32]	[−0.81]	[−0.82]	[−1.39]	KCCBHV
	8150	3.10	2.4	[−1.40]	[−0.96]	[−0.98]	[−1.65]	AP96
BD +42 2309	8800	3.20	2.0	[−1.63]	[−1.20]	[−1.13]	...	KCCBHV
	8400	3.30	...	[−1.5]	GCP
HD 109995	8500	3.10	3.0	[−1.72]	[−1.38]	[−1.29]	...	KCCBHV
	8150	3.25	1.7	[−1.89]	[−1.28]	[−1.39]	...	AP94,AP96
	8300	3.20	...	[−1.5]	GCP
	8300	3.15	BTS
HD 128801	10300	3.55	2.0	[−1.45]	[−1.09]	[−1.21]	...	KCCBHV
	10250	3.40	0.0	[−1.26]	[−0.79]	[−1.33]	...	AP94,AP96
HD 117880	9300	3.30	2.0	[−1.64]	[−1.05]	[−1.25]	...	KCCBHV
	9200	3.40	...	[−1.5]	GCP
HD 130095	9000	3.30	2.0	[−1.87]	[−1.65]	[−1.70]	...	KCCBHV
	8300	3.45	2.0	[−2.03]	[−1.55]	[−2.09]	...	AP94,AP96
	8950	3.40	...	[−1.5]	GCP
	8800	3.40	BTS
HD 139961	8500	3.20	3.0	[−1.71]	[−1.34]	[−1.22]	...	KCCBHV
	8750	3.30	BTS
HD 161817	7550	3.00	3.0	[−1.55]	[−1.23]	[−1.11]	[−1.76]	KCCBHV
	7225	2.80	2.3	[−1.66]	[−1.98]	[−1.43]	[−2.01]	AP94,AP96
	7600	3.10	...	[−1.2]	GCP
	7500	2.95	BTS
HD 167105	7500	3.00	4.0	[~−1.5]	TS
	9050	3.30	3.0	[−1.56]	[−1.31]	[−1.18]	...	KCCBHV
	8550	3.30	2.0	[−1.80]	...	[−1.42]	...	AP94,AP96
HD 202759	7500	3.05	2.0	[−2.16]	[−1.87]	[−1.72]	[−2.00]	KCCBHV
	7000	2.30	0.6	[−2.36]	...	[−1.85]	...	AP90
	7400	3.10	PB

KCCBHV: this paper; AP90, AP94, AP96: Adelman & Philip (1990; 1994; 1996a); GCP: Gray et al. (1996)

BTS: de Boer et al. (1997); PB: Przybylski & Bessell (1974); TS: Takeda & Sadakane (1997)

which, while being kinematically unbiased, tended to accentuate the discovery of the most metal-poor stars. The large subdwarf samples of Ryan & Norris (1991), although they contain stars in the range $+0.01 \geq [\text{Fe}/\text{H}] \geq -3.70$ and presumably include thick disk stars, have a maximum frequency in $[\text{Fe}/\text{H}]$ at -1.65 . This is similar to what we find for the field halo stars but not for the halo globular clusters where the maximum frequency is ~ 0.3 dex more metal-rich. Thus, although the $[\text{Fe}/\text{H}]$ abundances which we have derived for the BHB stars is in general agreement

with those found for other local halo stars, they are appreciably more metal-poor than those of the halo globular clusters. This discrepancy requires further investigation¹³.

¹³ Current abundance estimates of late-type halo stars are generally based on LTE analyses. The problem of NLTE effects in these stars is discussed by Gratton et al. (1999) and by Thévenin & Idiart (1999).

Table 14. Comparison of the distribution of $[\text{Fe}/\text{H}]$ in our BHB stars with that of other samples of halo stars.

Type & No. of stars	$[\text{Fe}/\text{H}]$		
	Range	Mean	σ
BHB stars ¹ (28)	-0.99 to -2.95	-1.67 ± 0.08	± 0.42
RHB stars ² (14)	-1.17 to -2.26	-1.62 ± 0.11	± 0.40
RR Lyrae ³ (39)	-1.11 to -2.49	-1.61 ± 0.06	± 0.35
R. Giants ⁴ (46)	-0.92 to -2.82	-1.78 ± 0.07	± 0.50
Halo \oplus ⁵ (21)	-0.96 to -2.16	-1.50 ± 0.08	± 0.35
Halo \oplus ⁶ (76)	-0.79 to -2.71	-1.40 ± 0.04	± 0.35

¹ BHB stars (this paper).² Pilachowski et al. (1996).³ Halo RR Lyraes (see text).⁴ Chiba & Yoshii (1998) (Red Giants within 600 pc).⁵ Halo globular clusters (see text).⁶ Halo globular clusters (see text).

10.3. Comparison with ZAHB models.

The T_{eff} and $\log g$ that we adopted for the analysis of the Kitt Peak and ESO-CAT spectra (Table 10) are plotted in Fig. 9. The 28 stars that have a high probability of being BHB stars are plotted as filled circles and the c-type RR Lyrae star HD 16456 as a filled triangle. For comparison we show the ZAHB models of Dorman et al. (1993) with $[\text{m}/\text{H}] = -1.48$ and $[\text{O}/\text{Fe}] = 0.6$, the models of Straniero et al. (1998, priv. comm.) with $[\text{m}/\text{H}] = -1.3$ (equivalent to $[\text{m}/\text{H}] = -1.6$ with α -enhancement +0.4, see Salaris et al. 1993) and the He-enhanced models of Sweigert (1997, 1999) ($\Delta X_{\text{mix}} = 0.0$ and 0.10^{14} with $[\text{m}/\text{H}] = -1.56$). We also show models by Bono & Cassisi (1999, priv. comm.) for $[\text{Fe}/\text{H}] = -1.7$ and -2.5 ; these illustrate the small metallicity dependence that is present. The agreement is generally satisfactory except for HD 130201 whose T_{eff} is not very well determined. A similar plot for the BHB stars in globular clusters (both metal-poor and the metal-rich NGC 6388, NGC 6441, NGC 362, and 47 Tuc) has been given in Fig. 8 of the recent review by Moehler (1999). At $\log T_{\text{eff}} = 3.95$, the metal-poor globular cluster BHB have $\log g$ in the range 2.90 to 3.44 and are mostly concentrated in the range 3.10 to 3.40. We have eleven BHB with $\log T_{\text{eff}}$ in the range 3.93 to 3.97 and their mean $\log g$ is 3.27, so there is good agreement between the field and cluster BHB stars in the T_{eff} vs $\log g$ plot. Both field and cluster BHB stars tend to lie slightly above the ZAHB, suggesting either that some evolution is present or that some He-enhancement is required. The difference is, however, comparable with the errors in the computed gravities so that no definitive conclusion is possible.

¹⁴ ΔX_{mix} is a measure of the amount of helium that is mixed into the envelope of the red giant precursor of the HB star.

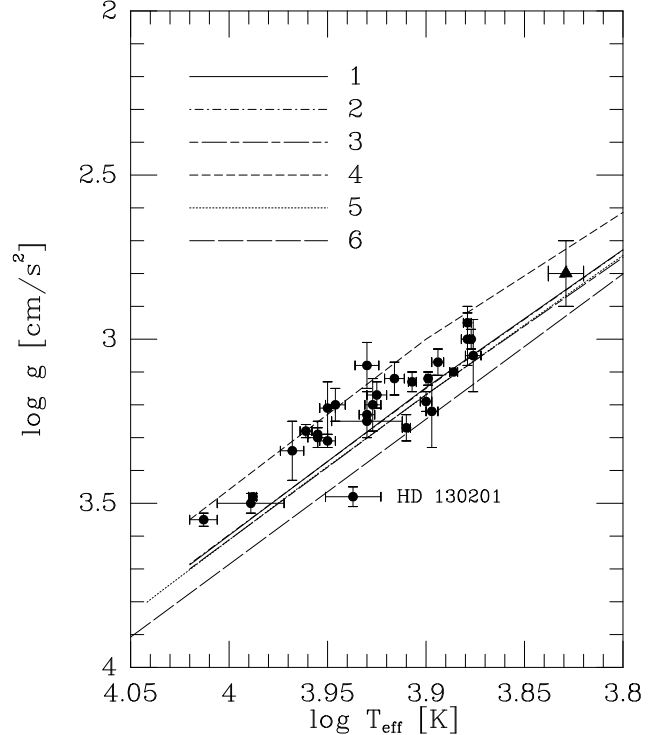


Fig. 9. The 28 BHB stars (filled circles) and the RR Lyrae star HD 016456 (filled triangle) in the $\log T_{\text{eff}} - \log g$ plane using the mean values given in Table 11. The lines show the ZAHB O-enhanced models of Dorman et al. (1993) (1) and the models of Straniero et al. (priv. comm.) (2) and the He-enhanced models of Sweigert (1997, 1999) for $\Delta X_{\text{mix}} = 0.00$ (3) and $\Delta X_{\text{mix}} = 0.10$ (4). The models of Bono & Cassisi for $[\text{Fe}/\text{H}] = -2.5$ and -1.7 are shown by (5) and (6) respectively.

10.4. Projected rotational velocities ($v \sin i$)

Peterson et al. (1983) measured the projected rotational velocities ($v \sin i$) of eight of the brighter field BHB stars from echelle spectra (resolution of 24 000) and found rotations of up to 30 km s^{-1} . Peterson (1983, 1985a and 1985b) also measured the $v \sin i$ of HB stars in the globular clusters M3, M5, M13, M4 and NGC 288. More recently, the $v \sin i$ of 67 HB stars in M3, M5, M13 and NGC 288 have been measured by Peterson et al. (1995, hereafter PRC). Also, Cohen & McCarthy (1997) have determined $v \sin i$ for 5 HB stars in M92 from HIRES Keck spectra. Behr et al. (2000) have also measured $v \sin i$ for stars in M13. Rotations of up to 40 km s^{-1} were found in both M13 and M92 for HB stars whose T_{eff} were less than 11 000 K. PRC could find no correlation between $(B - V)$ and $v \sin i$. Cohen & McCarthy suspected a possible trend of $v \sin i$ with abundance.

The resolution of most of our spectra (15 000) is not enough for us to make definitive measurements of $v \sin i$, but we can distinguish quite easily between stars with a $v \sin i$ of less than 15 km s^{-1} and those with a $v \sin i \sim$

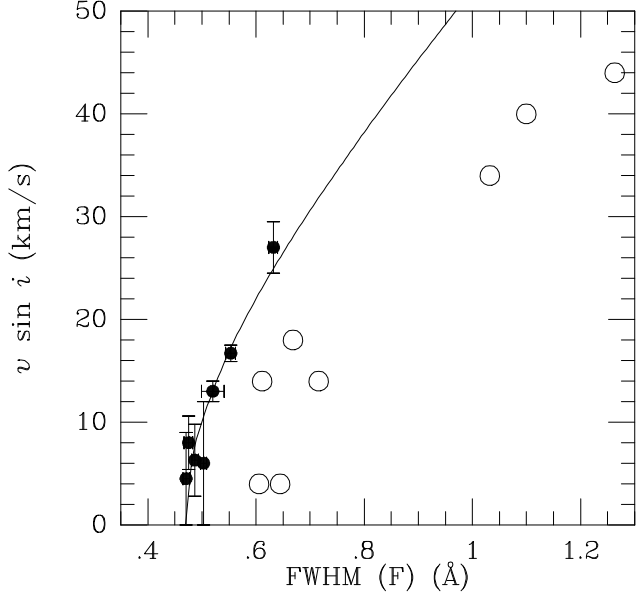


Fig. 10. A plot of $v \sin i$ against the FWHM of the Mg II $\lambda 4481$ doublet for BHB stars observed by Peterson, Tarbell & Carney (1983) (filled circles) and IAU standards (open circles). The adopted calibration is shown by the curve.

30 km s^{-1} . We chose to use the Mg II ($\lambda 4481$) line¹⁵ and measured its FWHM (F) with the IRAF routine that employs a simple gaussian fit. The $v \sin i$ of seven field BHB stars observed by Peterson et al. (1983) were used to convert the FWHM to $v \sin i$ with the relation:

$$v \sin i = 59.0 \times \sqrt{(F^2 - K)}$$

where F is in Å and the constant K is 0.221 for the Kitt Peak spectra and 0.151 for the ESO CAT spectra. The fit for the Kitt Peak spectra is shown in Fig 10. A number of early-type stars whose $v \sin i$ are given in the IAU Transactions (1991) were also observed and they are shown by open circles. Their $v \sin i$ follow the same trend with F as the calibrating BHB stars (filled circles) but their $v \sin i$ are systematically lower for a given F . The reason for this discrepancy is not understood but we have chosen to follow the calibration defined by the observations of Peterson et al. (1983) because our main interest is to compare our $v \sin i$ with those obtained by PRC for the BHB stars in globular clusters. We point out, however, that the use of our relation for $v \sin i > 30 \text{ km s}^{-1}$ does involve a small extrapolation beyond the range of the calibration. Had we used a calibration based on the IAU standards, our computed $v \sin i$ would have been about 60% of those given in Table 15.

¹⁵ This close doublet was used by Slettebak (1954) for his study of the rotational velocities of stars of spectral types B8 to A2. The line was also used by Glaspey et al. (1989) to derive $v \sin i$ for two HB stars in NGC 6752. The line is strong over a wide range of spectral types and is essentially unblended.

Table 15. The rotational velocity ($v \sin i$) for BHB star candidates[†] (determined from the Mg II $\lambda 4481$ line). The Strömgen index β for the same stars determined both photometrically and from our spectra.

Star (1)	$v \sin i^1$ (km s ⁻¹) (2)	$v \sin i^2$ (km s ⁻¹) (3)	β^a (4)	β^b (5)
HD 2857	28	30	2.787	2.779
HD 4850	...	14	2.846	...
HD 8376	20	10	2.835	2.837
HD 13780	...	14	2.816	...
HD 14829	...	07	2.858	...
HD 16456	15	14
HD 31943	13	16	2.814	2.806
HD 252940	25	24	2.768	2.776
HD 60778	15	11	2.834	2.835
HD 74721	10	02	2.859	2.856
HD 78913	...	14	2.842	...
HD 86986	15	04	2.825	2.827
HD 87047	12	00	2.797	2.810
HD 87112	10	03	2.840	2.823
HD 93329	15	07	2.825	2.832
BD +32 2188	05	00	2.633	2.592
HD 106304	...	10	2.845	...
BD +42 2309	35	35	2.844	2.856
HD 109995	27	25	2.848	2.852
BD +25 2602	20	12	2.850	2.855
HD 117880	15	13	2.855	...
HD 128801	14	04	2.816	2.800
HD 130095	12	07	2.855	2.847
HD 130201	...	16	2.860	...
HD 139961	35	39	2.858	2.852
HD 161817	17	17	2.746	2.777
HD 167105	22	21	2.849	2.856
HD 180903	20	17	2.800	2.789
HD 202759	15	07	2.770	2.759
HD 213468	...	12	2.849	...

¹ Determined from synthetic spectra.

² Determined from FWHM of line (Sect. 9.4).

[†] Omitting BD +00 0145 because of the poor quality of the spectrum.

^a Adopted photometric value (Table 1)

^b Determined from H γ (Sect. 3).

In Fig 11(b), we compare the $v \sin i$ that were determined from the FWHM of the Mg II line with the estimates of the rotational broadening that were obtained in fitting the observed and computed Mg II line profiles. There is a good correlation between the two for $v \sin i \gtrsim 15 \text{ km s}^{-1}$; for smaller $v \sin i$, the fractional errors in the estimates are greater and so there is a poorer correlation. In any case, we should not expect the two quantities to be identical since the $v \sin i$ determined from the Mg II line have been forced onto the system of another observer, whereas the rotational broadenings deduced from the model in-

Table 16. Mean $v \sin i$ and deprojected rotational velocities in field and cluster stars

System	No. of Stars	$\overline{v \sin i}$	\bar{v} km s ⁻¹	$\sqrt{(v - \bar{v})^2}$
(1)	(2)	(3)	(4)	(5)
Field BHB stars (this paper)	28	14.0	17.8	10.3
Clusters M3 ^a , M13 ^a , M92 ^b & NGC 288 ^a	72	13.6	17.3	9.0
Clusters M3 ^a , & NGC 288 ^a	38	10.3	13.1	3.8
Clusters M13 ^a & M92 ^b	34	17.3	22.0	10.7

^a Data from Peterson et al. (1995).^b Data from Cohen & McCarthy (1997).

volve different assumptions. In Fig 11 (a) we compare the $v \sin i$ that were obtained from the ESO-CAT spectra with those obtained for the same seven stars (six BHB stars and HD 140194) with the KPNO coude feed. The good agreement between these independent estimates of $v \sin i$ fully supports the conclusion that our data can be used to distinguish between stars with a $v \sin i \sim 30$ km s⁻¹ and those of lower rotational velocity.

The dependence of $v \sin i$ on the metallicity is shown in panel (a) of Fig 12. Although the six most metal-weak stars have lower than average $v \sin i$, it is not thought that these data show any *significant* trend of $v \sin i$ with metallicity. The middle and lower panels of Fig 12 show plots of $v \sin i$ against $(B - V)_0$ for the HB stars in globular clusters (middle) and for our field BHB (below). The distributions in the clusters and in the field are similar and in neither case is there a trend seen between $v \sin i$ and colour.

The interpretation of the observed distribution of $v \sin i$ in terms of a randomly oriented population has been discussed by Chandrasekhar & Münch (1950) and by Brown (1950). Brown, in particular, points out that the true distribution of rotational velocities can only be determined from relatively large samples. It is possible to put some constraints on the true distribution using the expressions given by Chandrasekhar & Münch for the mean and mean square deviation of this distribution (their equation (20)). Table 16 gives the mean projected rotational velocity ($\overline{v \sin i}$), the mean true rotational velocity (\bar{v}) and the root mean square deviation of this true rotational velocity ($\sqrt{(v - \bar{v})^2}$) in km s⁻¹ for our sample of field BHB stars and for various samples of globular cluster HB stars. Bearing in mind that our measured $v \sin i$ undoubtedly have somewhat larger observational errors than those of the globular cluster HB stars, the $\overline{v \sin i}$, \bar{v} and $\sqrt{(v - \bar{v})^2}$ of our sample well match the whole sample of globular cluster HB stars. This suggests that the two subgroups of globular clusters with low \bar{v} and $\sqrt{(v - \bar{v})^2}$ (M3 & NGC 288) and high \bar{v} and $\sqrt{(v - \bar{v})^2}$ (M13 & M92) are fairly equally represented in the field. None of these samples show significant evidence for skewness so the characterization of the true velocity distribution in terms of \bar{v} and $\sqrt{(v - \bar{v})^2}$ is

sufficient. It is to be noted that the $\sqrt{(v - \bar{v})^2}$ of the low velocity group must be very largely produced by observational error so that the intrinsic dispersion in this subgroup must be very low.

10.5. Abundances of the α -elements.

It is well known that the α -elements are more abundant relative to iron in metal-poor halo stars than in disk stars with solar abundances (Wheeler et al. 1989). The exact form of this enhancement may differ somewhat from element to element. Thus Boesgaard et al. (1999) have found a linear relation between [O/H] and [Fe/H] in the range $0.0 > [\text{Fe}/\text{H}] > -3.0$, but the relation is less well-defined for other α -elements such as Mg and Ti. The mean abundances of these two elements (relative to iron) are given in Table 17 for the BHB stars in our sample and for a number of other samples of metal-poor stars of similar metallicity. All of these other samples are late-type halo stars except for the old metal-poor selection taken from the thick-disk stars of Edvardsson et al. (1993) and the halo RR Lyrae sample of Clementini et al. (1995). Some systematic differences may be expected between the abundance ratios found for the different samples because they are derived from different lines of these elements and also different ionization states and undoubtedly systematic errors are present in their assumed $\log gf$. Also, the abundance determined from the Mg II $\lambda 4481$ line can be quite sensitive to the assumed microturbulent velocity (Table 12). Under these circumstances, we consider that the α -element enhancement in our BHB sample is in reasonable agreement with other recent determinations for halo stars.

10.6. BHB Binaries and HD 130095.

Binaries may be expected among halo stars and a discussion of their possible effect on the abundances has been given by Edvardsson et al. (1993) and Clementini et al. (1999). We have no direct evidence from the spectra that there are any binaries in our sample except that HD 130095 may have a variable radial velocity although it does not appear to vary in light (ESA Hipparcos Cat-

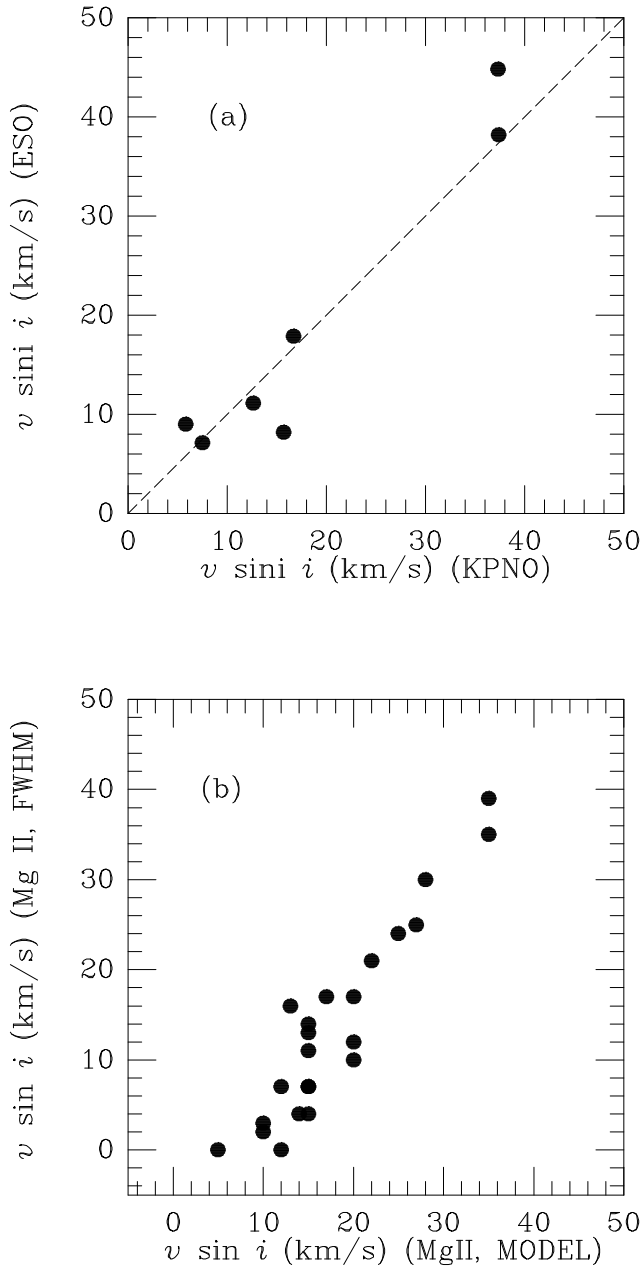


Fig. 11. **a** A comparison of the $v \sin i$ obtained (using the FWHM of the Mg II doublet) from spectra taken with the ESO-CAT (ordinate) with those obtained from spectra of the same stars taken with the Kitt Peak coude feed (abscissa). **b** A comparison of the $v \sin i$ obtained (using the FWHM of the Mg II doublet) for the Kitt Peak coude feed spectra (ordinate) with that determined from the same line using the synthetic spectra. (abscissa).

alogue 1997, Stetson 1991). Although the published radial velocities of this star (Table 18) show a spread of over 50 km s^{-1} , more than half of these velocities lie in a 5 km s^{-1} range centered on $+63 \text{ km s}^{-1}$. It does not seem entirely impossible that HD 130095 has a constant velocity of $+63 \text{ km s}^{-1}$ and that the errors of the velocities that

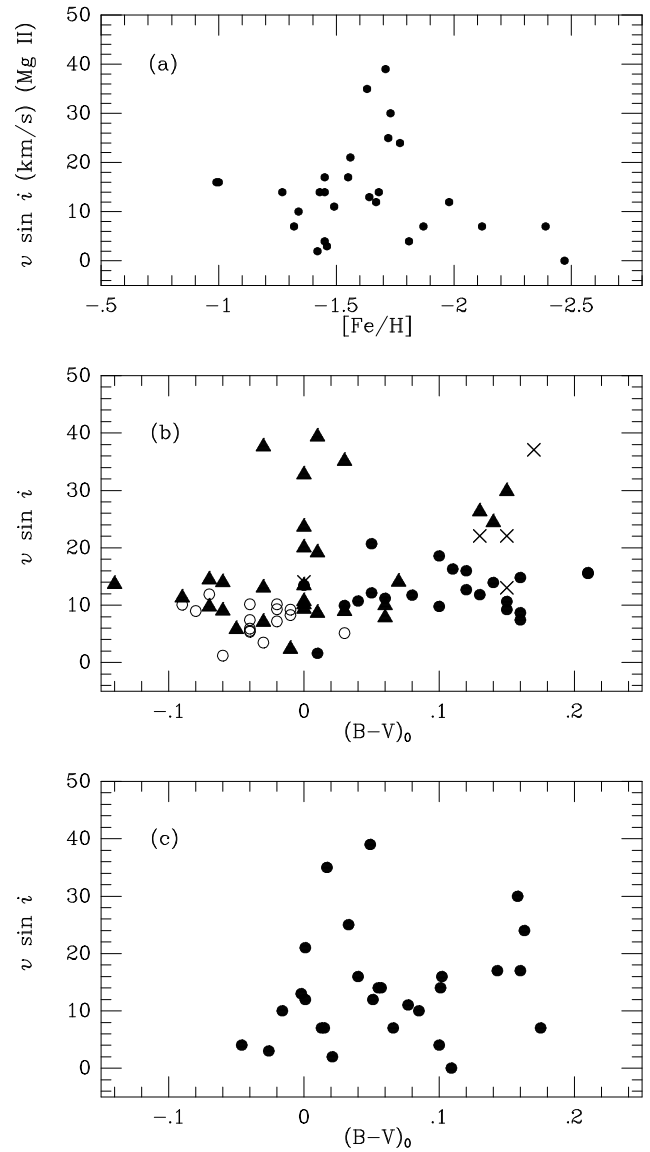


Fig. 12. **a** A plot of $v \sin i$ (ordinate) against $[\text{Fe}/\text{H}]$ (abscissa) for our field BHB stars. **b** A plot of $v \sin i$ (ordinate) against $(B-V)_0$ (abscissa) for BHB stars in the globular clusters NGC 288 (open circles), M3 (filled circles) and M13 (filled triangles) from Peterson et al. (1995) and also M92 (crosses) from Cohen & McCarthy (1997). **c** A plot of $v \sin i$ (ordinate) against $(B-V)_0$ (abscissa) for our field BHB stars.

are outside this range have been greatly underestimated. If, however, the spread is real, then a period of about seven months seems to be possible, although far from certain. Now if P is the period in years, a is the semi-major axis of the orbit (in A.U.) and m_1 and m_2 are the masses of the two components (in M_\odot), then

$$a^3 = P^2 \times (m_1 + m_2)$$

If we assume equal components with a combined mass of $1.2 M_\odot$, then the semi-major axis will be 0.74 A.U. ;

Table 17. Mean values of [Mg/Fe] and [Ti/Fe] from various sources.

<[Mg/Fe]>	<[Ti/Fe]>	<[Fe/H]>	No.	Ref.
+0.43±0.03	+0.44±0.03	-1.66	24	(1)
+0.33±0.02	+0.23±0.02	-0.68	19	(2)
+0.37±0.05	+0.32±0.02	-1.60	8	(3)
...	+0.28±0.02	-1.62	11	(4)
+0.30±0.01	...	-1.86	60	(5)
+0.48±0.02	+0.42±0.02	-2.13	20	(6)
+0.42±0.03	+0.27±0.02	-2.15	9	(7)
+0.23±0.03	+0.20±0.03	-1.60	11	(8)
+0.37±0.02	+0.30±0.02	-1.09	16	(9)

- (1) BHB stars (this paper).
(2) Edvardsson et al. (1993) (Thick disk: Age ≥ 10 Gyr; Orbital Ecc. ≥ 0.35; [Fe/H] ≤ -0.50).
(3) Clementini et al. (1995) (halo RR Lyraes).
(4) Gratton & Sneden (1991) (metal-poor dwarfs and giants).
(5) Pilachowski et al. (1996) (halo giants).
(6) Magain (1989) (halo dwarfs).
(7) Nissen et al. (1994) (metal-poor dwarfs and subgiants).
(8) Stephens (1999) (halo dwarfs: eccentric orbit).
(9) Clementini et al. (1999) (Hipparcos stars: [Fe/H] ≤ -0.50).

Table 18. Radial velocities of HD 130095.

Date (UT)	Radial velocity (km s ⁻¹)	Source
1960 Apr 23	+46.0	(1)
1963 Feb 13	+73	(2)
1963 Mar 01	+64	(2)
1963 May 19	+55	(2)
1964 Apr 28	+61.0	(1)
1964 May 28	+42.9	(1)
1969 May 23	+63	(2)
...	+65±2.4	(3)
1980 Jul	+83±6	(4)
1982 Apr 08	+64.3±1.0	(5)
1982 Apr 17	+65.0±1.0	(5)
...	+96±2	(6)
1995 Apr 29	+65.6±0.8	(7)
1995 May 03	+66.0±0.7	(8)

- (1) Przybylski & Kennedy (1965b)
(2) Hill (1971)
(3) Greenstein & Sargent (1974)
(4) Kodaira & Philip (1984)
(5) Peterson et al. (1983)
(6) Adelman & Philip (1990)
(7) This paper (ESO-CAT)
(8) This paper (KPNO coudé feed)

this is somewhat larger than the radius of the red giant progenitor of the HB star ($\sim 100R_{\odot}$). The other component might possibly be an equally metal-poor subdwarf ([Fe/H] = -2.0) whose lines would not be easily detectable in the spectrum of HD 130095. Such a star would be much less luminous than but of comparable mass to the HB star.

Such a companion would not be particularly bright in the infrared and so would not have been discovered in the survey for infrared-bright companions of halo stars by Carney (1983).

It is known (Smart 1931) that

$$A \sin i = 6875 P (\alpha + \beta) \sqrt{(1 - e^2)}$$

where A is the semi-axis major (in km), T is the period (in days), e is the orbital eccentricity and $(\alpha + \beta)$ is the velocity amplitude. If we assume a velocity amplitude of 50 km s⁻¹, then we find

$$\sin i = 1.5 \times \sqrt{(1 - e^2)}$$

which requires that $e > 0.75$. Thus the published radial velocities are not incompatible with HD 130095 being a binary, but it does seem highly desirable to make new velocity measurements over a period of several months so that the reality of the variability can be confirmed and a period established. The star is relatively bright ($V = 8.15$) and at declination -27° ; the observations would most easily be made in the southern hemisphere.

10.7. The RR Lyrae variable CS Eri (HD 16456)

Solano et al. (1997) observed CS Eri (HD 16456) with an Image Tube spectrograph (resolving power 19 000) on the SAAO 1.9-m telescope at Sutherland in July, 1995. They determined abundances by assuming a microturbulent velocity (ξ) of 3.6 km s⁻¹ and a $\log g$ of 2.75. A summary of their observations and ours is given in Table 19. Solano et al. found the phases of their observations from the ephemeris of CS Eri given in the General Catalogue of Variable Stars (Kholopov et al. 1985) (column 2 of Table 19). We have calculated phases for all the observations using the more recent ephemeris given in the Hipparcos Catalogue (1997) (column 3 of Table 19)¹⁶. The effective temperatures which are given by Solano et al. and also the one which we derived from the Kitt Peak spectrum are given in column 4. CS Eri is intermediate in metallicity and amplitude to the two c-type variables T Sex ($\Delta V = 0.42$ mag) and TV Boo ($\Delta V = 0.60$ mag) and has a similar period. Using the T_{eff} given for these stars by Liu & Janes (1990), we deduce that the maximum and minimum T_{eff} for CS Eri should be 7475 K and 6725 K respectively.

¹⁶ The radial velocities indicate that these phases are reasonably correct. DH Peg is a c-type RR Lyrae star that has a V -amplitude of 0.51 mag that is only slightly smaller than the V -amplitude (0.55 mag) of CS Eri. Jones, Carney & Latham (1988) have determined a precise radial velocity curve for DH Peg so that the difference between the radial velocity and the γ -velocity at each phase is known and this may be scaled by the V -amplitudes to predict the corresponding differences for CS Eri. From these differences we derive γ -velocities of -145.2 and -150.3 km s⁻¹ for CS Eri from the Kitt Peak and ESO-CAT spectra respectively. These agree well with the γ -velocity of -147 km s⁻¹ given by Solano et al. (1997).

Table 19. Spectroscopic observations of CS Eri (HD 16456).

Source	Phase		T_{eff}	$[\text{Fe}/\text{H}]^a$	$[\text{Fe}/\text{H}]^b$	Rad. vel. (km s ⁻¹)
	Gen. Catalogue	Hipparcos				
Solano et al.	0.12	0.20	6928	-1.36
Solano et al.	0.31	0.39	6679	-1.45
This Paper (Kitt Peak)	...	0.42	6750 ^c	-1.70	-1.69	-139.8
This Paper (ESO-CAT)	...	0.94	(7500) ^c	-1.65	-1.65	-158.9

^a from the equivalent widths of both the Fe I and Fe II lines.

^b from the equivalent widths of the Fe II lines only.

^c $\log g = 3.0$

This minimum T_{eff} is in good agreement with the T_{eff} determined from the Kitt Peak spectrum which was taken near minimum (phase 0.42). The abundance deduced from the ESO-CAT spectrum (phase 0.92, near maximum) assuming $T_{\text{eff}} = 7500$ K agrees well with that deduced from the Kitt Peak spectrum; their mean is $[\text{Fe}/\text{H}] = -1.67$. Table 20 also gives the $[\text{Fe}/\text{H}]$ that was derived for the Fe II lines alone since, at the T_{eff} of RR Lyrae stars, the strengths of these lines are less sensitive both to T_{eff} and NLTE effects than those of Fe I (Fernley & Barnes, 1997). Our abundances for $[\text{Fe}/\text{H}]$ are therefore ~ 0.2 dex lower than those found by Solano et al. (1997).

11. Summary and Conclusions

The purpose of this paper is to determine stellar parameters (e.g. $v \sin i$, T_{eff} & $\log g$) and chemical abundances that will allow us to isolate a local sample of BHB stars by their physical properties. All of our sample of thirty one candidate stars appear to belong to the halo, but BD +32 2188 (a post-AGB star), BD +00 0145 (a possible cool sdB star) and HD 16456 (the RR Lyrae star CS Eri) are not BHB stars. HD 202759, although classified as an RR Lyrae star (AW Mic), has such a low V -amplitude (< 0.1 mag) and high T_{eff} (7500 K) that it has been included with the BHB stars. Our spectra of HD 14829, HD 78913, HD 106304 and HD 213468 were not of sufficient quality for a complete abundance analysis although we were able to estimate $[\text{Fe}/\text{H}]$ from their Mg II ($\lambda 4481$) lines.

Of the twenty eight stars which we classify as BHB stars, the most doubtful is HD 139961 because it has the largest $v \sin i$ and also an unusually low orbital eccentricity (0.22)¹⁷. It is also NSV 7204 in the New Catalogue of Suspected Variable stars, Kukarkin et al. (1982). Corben et al. (1972) found a range of 0.08 magnitudes in V over six observations. The 85 observations of this star in the ESA Hipparcos catalogue, however, show a range of only 0.05 magnitudes; this corresponds to an *rms* deviation of only 0.01 magnitudes. Its colour, moreover, does

not put it near the edge of the instability strip, so that its variability seems questionable. *The existence of stars such as HD 139961 shows how difficult the classification of BHB stars can be and how necessary it is to use all available criteria.* When large numbers of stars are to be surveyed, simpler methods may have to suffice but one must then expect to get more misclassifications. Thus, Wilhelm et al. (1999) classify BHB stars with broad band UBV colours, Balmer-line widths and the Ca II (K-line) equivalent widths. Among the 18 stars in common with our sample, they classify the broad-lined A-star HD 203563 as an FHB star and their $[\text{Fe}/\text{H}]$ average 0.32 ± 0.08 more metal-poor than ours with individual stars differing from our $[\text{Fe}/\text{H}]$ by as much as 0.8 and 0.9 dex.

Projected rotational velocities ($v \sin i$) were determined for each star by calibrating the FWHM of the Mg II ($\lambda 4481$) line against the $v \sin i$ of seven of the stars in our sample that had previously been determined from echelle spectra by Peterson et al. (1983). No obvious trend of $v \sin i$ was found with either $(B - V)_0$ or abundance. A simple analysis of the $v \sin i$ (following Chandrasekhar & Munch 1950) shows that the deprojected distributions of these rotational velocities are similar to those found in globular clusters. Both have a \bar{v} of ~ 17 km s⁻¹ that is intermediate between that of the high rotational velocity clusters (M13 and M92) and the low rotational clusters (M3 and NGC 288).

BD +00 0145, HD 14829, HD 78913, HD 106304 and HD 213468 should be reobserved since we did not obtain spectra of sufficient quality for a complete analysis. Improved equivalent widths and $v \sin i$ could be obtained for all our BHB stars by using a higher resolution and a larger waveband (e.g. by using an echelle spectrograph) so that more lines would be available. Improved abundances, however, require a better understanding of the physical conditions in the stellar atmospheres and more accurate gf values as well as more certain determinations of the interstellar extinctions. In this latter connection, more reliable determinations of the extinction would be possible if $(V - K)$ colours were available for our entire sample. It is possible that HD 130095 is a binary. Its reported velocity

¹⁷ to be discussed in forthcoming paper with Christine Allen.

variations should be checked so that (if these are real) a period can be derived.

As we noted earlier, many of our BHB stars were selected from the early type stars that were found in surveys for high proper motion; our sample may therefore be expected to have a kinematic bias. This bias (*inter alia*) will be examined in a following paper, where we shall compare the galactic orbits of these BHB stars with those of other nearby halo stars.

Acknowledgements. We thank Saul Adelman for making his spectrum of HD 161817 available to us and also Giuseppe Bono and Santino Cassisi for providing their ZAHB models before publication. We also thank Allen Sweigart for sending us his He-enhanced models in electronic form. We are grateful to John Glaspey for helpful comments on a provisional draft of this paper and the referee (Klaas de Boer) for questioning the validity of models for representing far-UV spectra of BHB stars and for many suggestions for improving the style and readability of the paper. We are pleased to acknowledge the use of the IUE Final Archive which is sponsored and operated by NASA/ESA. This research has made use of the Simbad database, operated at CDS, Strasbourg, France.

Appendix A: Comments on other possible BHB star candidates.

Philip & Adelman (1993) found 19 BHB star candidates by searching the Hauck & Mermilliod photometric catalogue (1980) for stars with the appropriate Strömgren indices (e.g. one of their criteria was that the c_1 index should exceed 1.15). Bragaglia et al. (1996) made preliminary measurements of the $v \sin i$ of fourteen of these stars and noted that their rotations were mostly too large for them to be BHB stars. Adelman & Philip (1996b) obtained high resolution spectra of seven of these stars (HD 15042, HD 42999, HD 47706, HD 48567, HD 49224, HD 67426 & HD 79566) and also concluded that their rotational velocities were too high for them to be BHB stars. Of the remaining seven stars observed by Bragaglia et al., five (HD 53042, HD 67542, HD 128855, HD 181119 & HD 185174) have $v \sin i$ greater than 60 km s^{-1} . Two, however, (HD 83751 and HD 140194) have $v \sin i \sim 30 \text{ km s}^{-1}$ which is within the range of rotations observed for BHB stars; both stars have Population I kinematics¹⁸ and roughly solar abundances; thus in spite of their low $v \sin i$, they are unlikely to be BHB stars. The remaining five of the nineteen candidates listed by Philip & Adelman were not observed by us but some comments can be made on the probability that they are BHB stars. HD 100548 was classified as G8 III by Upgren (1962) from its objective prism spectrum. The photometry of this star listed in the Hauck & Mermilliod catalogue (1980) appears to be spurious because the star is not found among those in the listed reference (Drilling & Pesch 1973). Three of the remaining

stars (HD 94509, HD 120401 & HD 304325) have very low galactic latitudes ($b \leq 3^\circ$) while HD 123664 is likely to be a member of the Scorpio-Centaurus Association (Glaspey 1972, Slawson et al. 1992). It therefore seems unlikely that any of Philip & Adelman's nineteen BHB star candidates have a high probability of being BHB stars. Their work was valuable, however, because it has shown the need to use criteria in addition to Strömgren photometry in the identification of these stars.

Listed below are a number of other stars that have sometimes been suggested to be BHB stars; this list is not intended to be exhaustive. Spectra of one of them (BD +33 2171) should be obtained since its classification is doubtful from the available data. The others are almost certainly not BHB stars.

HD 52057 Stetson (1991). Kilkenny & Hill (1975) classified the star as B6 and almost certainly subluminal.

HD 57336 FHB 24 in Philip (1984). Huenemoerder et al. (1984) noted that the star has Population I metal-line characteristics. It is broad-lined.

BD +33 2171 FHB 2 in Philip (1984). Its colour ($B - V$) = +0.276 is too red for it to be a BHB star if the reddening given by the STD maps (1998) ($E(B - V) = 0.021$) is correct. The $v \sin i$ of 42 km s^{-1} is also somewhat high for a BHB star.

HD 176387 Stetson (1991) is the RR Lyrae star MT Tel.

HD 203563 Stetson (1991) is broad-lined.

HD 214539 Stetson (1991). Feast et al. (1955) discovered its very high radial velocity ($+333 \text{ km s}^{-1}$) and Przybylski (1969) found it to be metal-poor and considered it to be an HB star. A two-sigma upper limit to its Hipparcos parallax (ESA 1997), however, means that it cannot be closer than 735 pc which would give it an M_V of -2.1 or brighter so that it cannot be a HB star.

References

- Adelman S.J., Hill G., 1987, MNRAS 226, 581
- Adelman S.J., Philip A.G.D., 1990, MNRAS 247, 132
- Adelman S.J., Philip A.G.D., 1992, MNRAS 254, 539
- Adelman S.J., Philip A.G.D., 1994, MNRAS 269, 579
- Adelman S.J., Philip A.G.D., 1996a, MNRAS 280, 285
- Adelman S.J., Philip A.G.D., 1996b, Baltic Astronomy 5, 117.
- Adelman S.J., Philip A.G.D., 1996c, In: Formation of the Galactic Halo ... Inside and Out. Morrison H., Sarajedini A. (eds.) ASP Conference Ser. Vol. 92, ASP, San Francisco, p. 347
- Adelman S.J., Fisher W.A., Hill G., 1987, Publ. Dom. Astrophys. Obs. XVI, 203
- Albitzky V., 1933, Poulkova Obs. Circ. No. 7
- Alexander J.B., Carter B.S., 1971, Roy. Greenwich Obs. Bull. 169, 351
- Altmann M., de Boer K.S., 2000, A&A 353, 135
- Armandroff T.E., 1989, AJ 97, 375
- Arnold R.A., Gilmore G., 1992, MNRAS 257, 225
- Arribas S., Martinez Roger C., 1987, A&AS 70, 303
- Beers T.C., Wilhelm R., Doinidis S.P., Mattson C.J., 1996, ApJS 103, 433

¹⁸ The radial velocities of HD 83751 and HD 140194 are $+13.5$ and $+1.2 \text{ km s}^{-1}$ respectively.

- Behr B.B., Cohen J.G., McCarthy J.K., Djorgovski S.G., 1999, *ApJ* 517, L135
- Behr B.B., Djorgovski S.G., Cohen J.G., et al., 2000, *ApJ* 528, 849
- Belyakova E.V., Mashonkina L.I., Sakhibullin N.A., 1998, In: *Modern Problems of Stellar Evolution*. Wiebe D.S. (ed.) Geos, Moscow, p. 253
- Boesgaard A.M., King J.R., Delyannis C.P., Vogt S.S., 1999, *AJ* 117, 492
- Bohlin R.C., 1996, *AJ* 111, 1743
- Bond H.E., 1970, *ApJS* 22, 117
- Bond H.E., 1980, *ApJS* 44, 517
- Bonifacio P., 1989, NORMA: A Program for the Normalization of Spectra. University of Trieste, Astronomy Department, Internal Rep. 20-Apr-1989
- Bonifacio P., Castelli F., Hack M., 1995, *A&AS* 110, 441
- Bragaglia A., Cacciari C., Harmer D., Kinman T.D., Valdes F., 1996, In: *Formation of the Galactic Halo Inside and Out* Morrison H., Sarajedini A. (eds.) ASP Conference Ser. Vol. 92, ASP, San Francisco, p. 175
- Brown A., 1950, *ApJ* 111, 366
- Bridges J.M., Kornblith R.L., 1974, *ApJ* 192, 793
- Burbidge E.M., Burbidge G.R., 1956, *ApJ* 124, 116
- Cacciari C., 1985, *A&AS* 61, 407
- Cacciari C., Malagnini M.L., Morossi C., Rossi L., 1987, *A&A* 183, 314
- Caloi V. 1999, *A&A* 343, 904
- Canuto V.M., Mazzitelli I., 1992, *ApJ* 389, 724
- Carney B.W., 1983, *AJ* 88, 623
- Carretta E., Gratton R.G., 1997, *A&AS* 121, 95
- Castelli F., 1999, *A&A* 346, 564
- Castelli F., Bonifacio P., 1990, *A&AS* 84, 259
- Castelli F., Gratton R.G., Kurucz R.L., 1997, *A&A* 318, 841
- Chandrasekhar S., Münch G., 1950, *ApJ* 111, 142
- Chiba M., Yoshii Y., 1998, *AJ* 115, 168
- Clementini G., Carretta E., Gratton R.G., et al., 1995, *AJ* 110, 2319
- Clementini G., Gratton R.G., Carretta E., Sneden C., 1999, *MNRAS* 302, 22
- Cohen, J.G., McCarthy, J.K., 1997, *AJ* 113, 1353
- Cohen J.G., Gratton R.G., Behr B.B., Carretta E., 1999, *ApJ* 523, 739
- Corben P.M., Carter B.S., Banfield R.M., Harvey G.M., 1972, *MNASSA* 31, 1 & 2, 7
- Cousins A.W.J., 1972, *MNASSA* 31, 75
- Cowley C.R., 1958, *AJ* 63, 484
- Crawford D.L., 1979, *AJ* 84, 1858
- Crawford D.L., Mandwewala N., 1976, *PASP* 88, 917
- de Boer K.S., Tucholke H.-J., Schmidt J.H.K., 1997, *A&A* 317, L23
- Dorman B., Rood R.T., O'Connell R.W., 1993, *ApJ* 419, 596
- Drilling J.S., Pesch P., 1973, *AJ* 78, 47
- Edvardsson B., Andersen J. Gustafsson B., et al., 1993, *A&A* 275, 101
- ESA 1997, *The Hipparcos & Tycho Catalogues*. (ESA SP-1200) (Noordwijk: ESA)
- Feast M.W., Thackeray A.D., Wesselink A.J., 1955, *Mem. R. Astron. Soc.* 67, 51
- Fernley J., Barnes T.G., 1997, *A&AS* 125, 313
- Flynn C., Sommer-Larsen J., 1988, *MNRAS* 235, 175
- Fitzpatrick E.L., 1999, *PASP* 111, 63
- Fuhr J.R., Martin G.A., Wiese W.L., 1988, *J. Phys. Chem. Ref. Data* 17, Suppl. No. 4
- Fuhrmann K., Axer M., Gehren T., 1993, *A&A* 271, 451
- Fuhrmann K., Axer M., Gehren T., 1994, *A&A* 285, 585
- Gardiner R. B., Kupka F., Smalley B., 1999, *A&A* 347, 876
- Glaspey J.W., 1972, *AJ* 77, 474
- Glaspey J.W., Michaud G., Moffat A.F.J., Demers S., 1989, *ApJ* 339, 926
- Graham J.A., Doremus C., 1968, *AJ* 73, 226
- Gratton R.G., Sneden C., 1991, *A&A* 241, 501
- Gratton R.G., Carretta E., Eriksson K., Gustafsson B., 1999, *A&A* 350, 955
- Gray D.F., 1992, *The Observations and Analysis of Stellar Photospheres*. Cambridge Univ. Press, Cambridge, p. 184
- Gray R.O., Olsen E.H., 1991, *A&AS* 87, 541
- Gray R.O., Corbally C.J., Philip A.G.D., 1996, *AJ* 112, 2291
- Green E.M., Morrison H.L., 1993, In: *The Globular Cluster-Galaxy Connection*. Smith G.H., Brodie J.P., (eds.) ASP Conf. Series, Vol. 48, ASP San Francisco, p. 318
- Green E.M., Liebert J., Peterson R.C. 1996 In: *Formation of the Galactic Halo Inside and Out*. Morrison H.L., Sarajedini A., (eds.) ASP Conference Ser. Vol. 92, ASP San Francisco, p. 184
- Greenstein J.G., Eggen O.J., 1966, In: *Vistas in Astronomy* 8, Beer A., Strand K. Aa., (eds.) Oxford, Pergamon, p. 63
- Greenstein J.G., Sargent A.I., 1974, *ApJS* 28, 157
- Grevesse N., Noels A., Sauval A.J., 1996, In: *Cosmic Abundances*. Holt S.S., Sonneborn G., (eds.) ASP Conf. Series, Vol. 99, ASP San Francisco, p. 117
- Grundahl F., Catelan M., Landsman W.B., Stetson P.B., Andersen M.I., 1999, *ApJ* 524, 242
- Harris W.E., 1996, *AJ* 112 1487
- Hayes D.S., Philip A.G.D., 1983, *ApJS* 53, 759
- Hauck B., Mermilliod M., 1980, *A&AS* 40, 1
- Hauck B., Mermilliod M., 1998, *A&AS* 129, 431
- Hill P.W., 1971, *MemRAS* 75, 1
- Hill G., Barnes J.V., Hilditch R.W., 1982, *Publ. Dom. Ap. Obs.* 16, 111
- Huenemoerder D.P., de Boer K.S., Code A.D., 1984, *AJ* 89, 851
- IAU Trans., 1991, Vol XXIB, Bergeron, J., (ed.) Kluwer, Dordrecht, p. 275
- Joner M.D., Taylor B.J., 1997, *PASP* 109, 1122
- Jones R.V., Carney B.W., Latham D.W., 1988, *ApJ* 326, 312
- Kholopov P.N., Samus N.N., Frolov M.S., et al., 1985, *General Catalogue of Variable Stars*. Nauka, Moscow
- Kilkenny D., 1984, *MNRAS* 211, 969
- Kilkenny D., Hill P.W., 1975, *MNRAS* 173, 625
- Kilkenny D., Muller S., 1989, *SAAO Circ.* 13, 69
- Kinman T.D., 1998, *PASP* 110, 1277
- Kinman T.D., Allen C., 1996, In: *Formation of the Galactic Halo Inside and Out*. Morrison H.L., Sarajedini A., (eds.) ASP Conference Ser. Vol. 92, ASP San Francisco, p. 36
- Kinman T.D., Suntzeff N.B., Kraft R.P., 1994, *AJ* 108, 1722 (KSK)
- Klemola A.R., 1962, *AJ* 67, 740
- Klochko V.G., Panchuk V.E., 1990, *Bulletin of the Special Astrophysical Observatory: North Caucasus* 26, 23 (Allerton Press Translation Series).
- Kodaira K., 1964, *Zeits. für Astrophys.* 59, 139

- Kodaira K., Philip A.G.D., 1984, *ApJ* 278, 208
- Kukarkin B.V., et al., 1982, *New Catalogue of Suspected Variable Stars*. Nauka: Moscow
- Kurucz R.L., 1993a, *ATLAS9 Stellar Atmospheres Programs and 2 km/s grid*, CD-ROM No 13
- Kurucz R.L., 1993b, *SYNTHS Spectrum Synthesis Programs and Line Data*, CD-ROM No 18
- Kurucz R.L., Bell B., 1995, *Atomic Line List*, CD-ROM No 23
- Kurucz R.L., Peytremann E., 1975, *SAO Special Report* 362
- Lambert D.L., McWilliam A., Smith V.V., 1992, *ApJ* 386, 685
- Lambert D.L., Heath J.E., Lemke M., Drake J., 1996, *ApJS* 103, 183
- Lane M.C., Lester J.B., 1984, *ApJ* 281, 723
- Liu T., Janes K.A., 1990, *ApJ* 354, 273
- Luyten W.J., 1957 “A Search for Faint Blue Stars” IX, The Lund Press, Minneapolis
- MacConnell D.J., Frye R.L., Bidelman W.P., Bond H.E., 1971, *PASP* 83, 98
- Majewski S.R., 1999 In: *Globular Clusters*. Martínez Roger C., Perez Fournón I., Sánchez F., (eds.) Cambridge Univ. Press, p. 91
- Magain P., 1989, *A&A* 209, 211
- Martin G.A., Fuhr J.R., Wiese W.L., 1988, *J. Phys. Chem. Ref. Data* 17, Suppl. No. 3
- Mashonkina L.I., Bikmaev I.F., 1996, *Astronomy Reports* 40, 94
- Mathis J.S., 1990, *ARA&A* 28, 37
- Miles B.M., Wiese W.L., 1969, *NBS Technical Note* 474
- Mitchell K.J., Saffer R.A., Howell S.B., Brown T.M. 1998, *MNRAS* 295, 225
- Moehler S., 1999, *RvMA* 12 in press (astro-ph/9812147)
- Moehler S., Sweigart A.V., Landsman W.B., Heber U., Cate-lan M., 1999, *A&A* 346, L1
- Moon T.T., 1985, *Comm. Univ. London Obs.* No 78
- Moon T.T., Dworetzky M.M., 1985, *MNRAS* 217, 305
- Moore C.E., 1945, *Contrib. Princeton Univ. Obs.* 20 (A Multiple Table of Astrophysical Interest)
- Nichols J.S., Linsky J.L., 1996, *AJ* 111, 517
- Nissen P.E., Gustafsson B., Edvardsson B., Gilmore G., 1994, *A&A* 285, 440
- Oja T., 1987, *A&AS* 71, 561
- Oke J.B., Greenstein J.G., Gunn J.E., 1966, In: *Stellar Evolution*. Stein R.G., Cameron A.G.W., (eds.) Plenum, New York, p. 399
- Peterson R.C., 1983, *ApJ* 275, 737
- Peterson R.C., 1985a, *ApJ* 289, 320
- Peterson R.C., 1985b, *ApJ* 294, L35
- Peterson R.C., Tarbell T.D., Carney B.W., 1983, *ApJ* 265, 972
- Peterson R.C., Rood R.T., Crocker D.A., 1995, *ApJ* 453, 214
- Philip A.G.D., 1967, *ApJ* 148, L143
- Philip A.G.D., 1969, *AJ* 74, 209
- Philip A.G.D., 1984, *Contr. of the Van Vleck Obs.* 2, 1
- Philip A.G.D., 1994, In: *Hot Stars in the Galactic Halo*. Adelman S.J., Upgren A.R., (eds.) Cambridge Univ. Press, p. 41
- Philip A.G.D., Tift L.E., 1971, *AJ* 76, 567
- Philip A.G.D., Adelman S.J., 1993, In: *Workshop on Databases for Galactic Structure*. Philip A.G.D., Hauck B., Upgren A.R., (eds.) L. Davis Press, Schenectady, p. 245
- Philip A.G.D., Hayes D.S., 1983, *ApJS* 53, 751
- Philip A.G.D., Hayes D.S., Adelman S.J., 1990, *PASP* 102, 649
- Pier J.R., 1983, *ApJS* 53, 791
- Pilachowski C.A., Sneden C., Kraft R.P., 1996, *AJ* 111, 1689
- Preston G.W., Shectman S.A., Beers T.C., 1991, *ApJ* 375, 121
- Przybylski A., 1969, *MNRAS* 146, 71
- Przybylski A., 1970, *MNRAS* 151, 197
- Przybylski A., 1971, *MNRAS* 153, 111
- Przybylski A., Bessell M.S., 1974, *PASP* 86, 403
- Przybylski A., Kennedy P.M., 1965a, *MNRAS* 129, 63
- Przybylski A., Kennedy P.M., 1965b, *MNRAS* 131, 95
- Rich R.M., Sosin C., Djorgovski S.G., et al., 1997, *ApJ* 484, L25
- Roman N.G., 1955a, *ApJS* 2, 195
- Roman N.G., 1955b, *Publ. David Dunlap Obs.* 2, 97
- Röser S., Bastian U., 1991, *PPM Star Catalogue*. Spektrum, Heidelberg
- Ryan S.G., Norris J.E., 1991, *AJ* 101, 1865
- Salaris M., Chieffi A., Straniero O., 1993, *ApJ* 414, 580
- Schlegel D.J., Finkbeiner D.P., Davis M., 1998, *ApJ* 500, 525 (SFD)
- Schönberner D., 1983, *ApJ* 272, 708
- Seaton M.J., 1979, *MNRAS* 187, 73
- Slawson R.W., Hill R.J., Landstreet J.D., 1992, *ApJS* 82, 117
- Slettebak A., 1952, *ApJ* 115, 576
- Slettebak A., 1954, *ApJ* 119, 146
- Slettebak A., Stock J., 1959, *Astr. Abh. Hamburg* 5, 1
- Slettebak A., Bahner K., Stock J., 1961, *ApJ* 134, 195
- Sluis A.P.N., Arnold R.A., 1998, *MNRAS* 297, 732
- Smalley B., Kupka F., 1997, *A&A* 328, 349
- Smart W.M., 1931, *Spherical Astronomy*. Cambridge Univ. Press, p. 364
- Solano E., Garrido R., Fernley J., Barnes T.G., 1997, *A&AS* 125, 321
- Sommer-Larsen J., Christensen P.R., 1986, *MNRAS* 219, 537
- Sommer-Larsen J., Christensen P.R., Carter D., 1989, *MNRAS* 238, 225
- Stephens A., 1999, *AJ* 117, 1771.
- Stetson P.B., 1991, *AJ* 102, 589
- Strömgren B., 1966, *ARA&A* 4, 433
- Sweigart A.V., 1997, *ApJ* 474, L23
- Sweigart A.V., 1999, In “The 3rd Conf. on Faint Blue Stars” Philip A.G.D., Liebert J., Saffer R.A., (eds.) (Schenectady, L. Davis Press) p. 3
- Takeda Y., Sadakane K., 1997, *Publ. Astron. Soc. Japan* 49, 571
- Terndrup D.M., Peterson R.C., Sadler E.M., Walker A.R., 1999, In “The Stellar Content of Local Group Galaxies” IAU Symposium No. 192, Whitelock P., Cannon R., (eds.) Astr. Soc. Pacific: San Francisco, p. 395
- Thévenin F., Idiart T.P., 1999, *ApJ* 521, 753
- Upgren A.R., 1962, *AJ* 67, 37
- van’t Veer-Menneret C., Mégessier C., 1996, *A&A* 309, 879
- Wallerstein G., Hunziker W., 1964, *ApJ* 140, 214
- Wheeler J.C., Sneden C., Truran J.W., 1989, *ARA&A* 27, 279
- Wiese W.L., Smith M.W., Miles B.M., 1969, *NSRDS-NBS* 22 Vol. II
- Wiese W.L., Fuhr J.R., 1975, *J. Phys. Chem. Ref. Data* 4 263
- Wilhelm R., Beers T.C., Gray R.O., 1999, *AJ* 117, 2308
- Zhang E.-H., 1983, *AJ* 88, 825
- Zinn R., West M.J., 1984, *ApJS* 55, 45

Table 4. Line wavelengths, equivalent widths (in mÅ), and abundances for the stars observed at KPNO

λ (Å)	Species	Mult. no.	$\log gf$	HD 2857		HD 8376		HD 16456		HD 31943		HD 252940	
				W_λ	$\log \epsilon$	W_λ	$\log \epsilon$	W_λ	$\log \epsilon$	W_λ	$\log \epsilon$	W_λ	$\log \epsilon$
4 481.21	Mg II	(4)	-0.978	200	-5.76	051	-6.86	147	-5.87	355	-4.90	189	-5.91
4 318.652	Ca I	(5)	-0.208	041	-7.24	025	-6.74
4 434.960	Ca I	(4)	-0.029	026	-7.16	058	-7.20	045	-6.62	029:	-7.12
4 455.887	Ca I	(4)	-0.510	018	-6.61
4 246.829	Sc II	(7)	+0.320	112	-10.54
4 325.010	Sc II	(15)	-0.440
4 400.355	Sc II	(14)	-0.510
4 287.893	Ti II	(20)	-2.020	027	-8.22	062	-8.10	067	-7.49
4 290.222	Ti II	(41)	-1.120	129	-7.86
4 300.052	Ti II	(41)	-0.770	143	-7.78	030	-8.89	143	-8.15	178	-7.52	140	-8.06
4 301.928	Ti II	(41)	-1.160	054:	-8.62	082:	-8.66	104:	-7.95	082:	-8.35
4 312.861	Ti II	(41)	-1.160	065:	-8.47	083	-8.63	116	-7.82	068	-8.49
4 386.858	Ti II	(104)	-1.260	14:	-8.17	036	-7.52
4 394.057	Ti II	(51)	-1.590	048:	-8.60	049	-8.02
4 395.031	Ti II	(19)	-0.660	158	-7.71	026	-9.17	151	-8.21	180	-7.69	144:	-8.19
4 395.848	Ti II	(61)	-2.170	078:	-7.64	039	-7.55
4 399.767	Ti II	(51)	-1.270	084	-8.10	102	-7.81	070	-8.32
4 411.080	Ti II	(115)	-1.060	037	-7.34
4 417.718	Ti II	(40)	-1.430	064:	-8.22	082	-8.40	104	-7.69	082:	-8.09
4 443.802	Ti II	(19)	-0.700	125	-8.24	022	-9.23	119	-8.71	156	-7.96	122	-8.46
4 450.487	Ti II	(19)	-1.450	047	-8.49	066	-8.64	082	-7.93	048	-8.51
4 464.458	Ti II	(40)	-2.080	027	-8.12	061	-8.02	058	-7.48	025	-8.18
4 468.493	Ti II	(31)	-0.600	138	-8.09	024	-9.26	139	-8.44	174	-7.81	136	-8.34
4 488.319	Ti II	(115)	-0.820	042	-7.50
4 501.270	Ti II	(31)	-0.750	121	-8.23	121	-8.60	158	-7.86	106	-8.56
4 529.465	Ti II	(82)	-2.030	038	-7.47
4 533.966	Ti II	(50)	-0.770	022	-9.06	194	-7.31	137	-8.09
4 563.761	Ti II	(50)	-0.960	103	-8.20	122	-8.29	148	-7.69	104	-8.30
4 571.971	Ti II	(82)	-0.530
4 274.803	Cr I	(1)	-0.231	041	-8.10	062	-7.56
4 558.659	Cr II	(44)	-0.660	041	-7.92	069	-7.73	094	-7.26	050	-7.85
4 260.479	Fe I	(152)	-0.020	118	-5.58	066	-6.33
4 271.764	Fe I	(42)	-0.164	122	-6.24
4 325.765	Fe I	(42)	-0.010	099:	-6.48	150	-5.81	109	-6.47
4 383.547	Fe I	(41)	+0.200	132	-6.26	0.15:	-7.56	173	-6.12	183	-5.68	138	-6.40
4 404.752	Fe I	(41)	-0.142	097	-6.42	009:	-7.43	145	-6.26	150	-5.72	108	-6.40
4 415.125	Fe I	(41)	-0.615	088	-6.04	110	-6.35	127	-5.48	088	-6.11
4 447.722	Fe I	(68)	-1.342	017:	-5.92	032	-6.19	026	-5.43
4 476.021	Fe I	(350)	-0.570	008:	-6.61	044	-6.25	049	-5.41
4 494.568	Fe I	(68)	-1.136	039	-6.31	036	-5.49
4 273.317	Fe II	(27)	-3.340	042	-5.47
4 296.567	Fe II	(28)	-3.010	031	-6.03	043	-6.10	072:	-5.38
4 303.166	Fe II	(27)	-2.490	066	-6.32	116	-5.48
4 385.381	Fe II	(27)	-2.570	026	-6.51	051	-6.37	095	-5.56	042	-6.27
4 416.817	Fe II	(27)	-2.600	029:	-6.43	045	-6.42	093	-5.54
4 489.185	Fe II	(37)	-2.970	047	-6.00	067	-5.39
4 491.401	Fe II	(37)	-2.700	050	-6.20	074	-5.57
4 508.283	Fe II	(38)	-2.210	056	-6.37	077	-6.35	114	-5.69	064	-6.32
4 515.337	Fe II	(37)	-2.480	055	-6.11	058	-6.33	104	-5.52	050	-6.22
4 520.225	Fe II	(37)	-2.600	041	-6.22	062	-6.18	099	-5.47	046	-6.18
4 522.634	Fe II	(38)	-2.030	074	-6.33	099	-6.25	140	-5.61	078	-6.36
4 541.523	Fe II	(38)	-3.050	027	-6.97	032	-6.12	064	-5.33
4 555.890	Fe II	(37)	-2.290	055	-6.33	079	-6.26	133	-5.44	048	-6.46
4 554.033	Ba II	(1)	+0.170	038	-11.72	115	-11.44	062	-11.17	036	-11.84

Table 4. Line wavelengths, equivalent widths (in mÅ), and abundances for the stars observed at KPNO (continued)

λ (Å)	Species	Mult. no.	$\log gf$	HD 60778		HD 74721		HD 86986		HD 87047		HD 87112	
				W_λ	$\log \epsilon$	W_λ	$\log \epsilon$	W_λ	$\log \epsilon$	W_λ	$\log \epsilon$	W_λ	$\log \epsilon$
4 481.21	Mg II	(4)	-0.978	265	-5.40	250	-5.64	203	-5.72	95	-6.47	204	-5.55
4 318.652	Ca I	(5)	-0.208
4 434.960	Ca I	(4)	-0.029	018	-7.07
4 455.887	Ca I	(4)	-0.510
4 246.829	Sc II	(7)	+0.320
4 325.010	Sc II	(15)	-0.440
4 400.355	Sc II	(14)	-0.510	010:	-10.08
4 287.893	Ti II	(20)	-2.020	028	-7.93
4 290.222	Ti II	(41)	-1.120	089	-7.97	050	-7.96	068	-8.18	033:	-8.75
4 300.052	Ti II	(41)	-0.770	112	-8.01	082	-7.96	098	-8.09	052	-8.77	030	-8.02
4 301.928	Ti II	(41)	-1.160	034	-8.13	042	-8.51
4 312.861	Ti II	(41)	-1.160	061	-8.25	037	-8.08	047	-8.43
4 386.858	Ti II	(104)	-1.260
4 394.057	Ti II	(51)	-1.590	024	-8.35
4 395.031	Ti II	(19)	-0.660	120	-8.08	073	-8.23	106	-8.14	057	-8.88	031	-8.18
4 395.848	Ti II	(61)	-2.170
4 399.767	Ti II	(51)	-1.270	046	-8.30	024	-8.16	041	-8.37
4 411.080	Ti II	(115)	-1.060
4 417.718	Ti II	(40)	-1.430	051	-8.12	031	-7.92	054	-8.07
4 443.802	Ti II	(19)	-0.700	092	-8.43	070	-8.23	079	-8.53	048	-8.99	019	-8.41
4 450.487	Ti II	(19)	-1.450	046	-8.23	021	-8.16	029	-8.51
4 464.458	Ti II	(40)	-2.080	051	-7.48
4 468.493	Ti II	(31)	-0.600	103	-8.35	067	-8.33	087	-8.48	049	-9.05	035	-8.14
4 488.319	Ti II	(115)	-0.820
4 501.270	Ti II	(31)	-0.750	089	-8.39	059	-8.27	080	-8.44	040	-9.06	023	-8.24
4 529.465	Ti II	(82)	-2.030
4 533.966	Ti II	(50)	-0.770	114	-7.97	083	-7.93	096	-8.10	049	-8.80	024:	-8.13
4 563.761	Ti II	(50)	-0.960	077	-8.26	054	-8.05	070	-8.30	039	-8.79	015	-8.19
4 571.971	Ti II	(82)	-0.530
4 274.803	Cr I	(1)	-0.231
4 558.659	Cr II	(44)	-0.660	040	-7.79	030	-7.64	039	-7.79	016	-7.62
4 260.479	Fe I	(152)	-0.020	024	-5.80
4 271.764	Fe I	(42)	-0.164	049	-5.86	028:	-7.12
4 325.765	Fe I	(42)	-0.010	083	-6.28	039	-6.07	069	-6.48	032	-7.12
4 383.547	Fe I	(41)	+0.200	110	-6.20	067	-6.03	093	-6.41	056	-7.00	021	-5.92
4 404.752	Fe I	(41)	-0.142	077	-6.26	039	-5.97	072	-6.35	033	-7.00
4 415.125	Fe I	(41)	-0.615	047	-6.20	019	-6.82
4 447.722	Fe I	(68)	-1.342	009	-5.84
4 476.021	Fe I	(350)	-0.570	019	-5.79
4 494.568	Fe I	(68)	-1.136	014	-5.83
4 273.317	Fe II	(27)	-3.258
4 296.567	Fe II	(28)	-3.010	029:	-5.88
4 303.166	Fe II	(27)	-2.490	056	-6.00	028	-6.06
4 385.381	Fe II	(27)	-2.570	037	-6.13	034	-5.83	020	-6.47
4 416.817	Fe II	(27)	-2.600	037	-6.11	026	-5.94	032	-6.18	009:	-6.15
4 489.185	Fe II	(37)	-2.970	030	-5.81
4 491.401	Fe II	(37)	-2.700	035	-5.99	016:	-6.04
4 508.283	Fe II	(38)	-2.210	063	-6.10	042	-6.02	035	-6.47	013:	-7.05	018	-6.12
4 515.337	Fe II	(37)	-2.480	045	-6.07	034	-5.89	029	-6.32	017:	-5.90
4 520.225	Fe II	(37)	-2.600	048	-5.93	024	-5.97	026	-6.28
4 522.634	Fe II	(38)	-2.030	070	-6.20	057	-6.03	060	-6.28	022	-6.97	022	-6.20
4 541.523	Fe II	(38)	-3.050	024	-5.84
4 555.890	Fe II	(37)	-2.290	049	-6.21	041	-5.98	037	-6.38	018	-6.05
4 554.033	Ba II	(1)	+0.170	016:	-11.76	016:	-11.85

Table 4. Line wavelengths, equivalent widths (in mÅ), and abundances for the stars observed at KPNO (continued)

λ (Å)	Species	Mult. no.	$\log gf$	HD 93329		BD +32 2188		BD +42 2309		HD 109995		BD +25 2602	
				W_λ	$\log \epsilon$	W_λ	$\log \epsilon$	W_λ	$\log \epsilon$	W_λ	$\log \epsilon$	W_λ	$\log \epsilon$
4 390.585	Mg II	(10)	-0.530	14	-5.55
4 481.21	Mg II	(4)	-0.978	252	-5.27	191	-5.45	203	-5.66	206	-5.84	169	-6.15
4 318.652	Ca I	(5)	-0.280
4 434.960	Ca I	(4)	-0.029	018	-6.74
4 455.887	Ca I	(4)	-0.510
4 246.829	Sc II	(7)	+0.320	074	-10.28
4 325.010	Sc II	(15)	-0.440
4 400.355	Sc II	(14)	-0.510	019	-10.22
4 287.893	Ti II	(20)	-2.020	020:	-7.97
4 290.222	Ti II	(41)	-1.120	087	-7.63	043	-8.02	058	-8.08	035:	-8.47
4 300.052	Ti II	(41)	-0.770	115	-7.38	048	-8.28	082	-8.13	052	-8.59
4 301.928	Ti II	(41)	-1.160	036	-8.35
4 312.861	Ti II	(41)	-1.160	059	-8.06	035	-8.35	021:	-8.68
4 386.858	Ti II	(104)	-1.260	018	-7.73
4 394.057	Ti II	(51)	-1.590
4 395.031	Ti II	(19)	-0.660	114	-7.58	058	-8.30	082	-8.32	087	-8.42
4 395.848	Ti II	(61)	-2.170
4 399.767	Ti II	(51)	-1.270	054	-7.99
4 411.080	Ti II	(115)	-1.060
4 417.718	Ti II	(40)	-1.430	050	-7.95	023	-8.32
4 443.802	Ti II	(19)	-0.700	095	-7.96	073	-8.39	047	-8.80
4 450.487	Ti II	(19)	-1.450	045	-8.07	019	-8.47
4 464.458	Ti II	(40)	-2.080	019	-7.90
4 468.493	Ti II	(31)	-0.600	105	-7.81	065	-8.23	078	-8.40	055	-8.77
4 488.319	Ti II	(115)	-0.820
4 501.270	Ti II	(31)	-0.750	092	-7.96	042	-8.79
4 529.465	Ti II	(82)	-2.030
4 533.966	Ti II	(50)	-0.770	067	-7.96	071	-8.24	055	-8.53
4 563.761	Ti II	(50)	-0.960	087	-7.77	045	-8.13
4 571.971	Ti II	(82)	-0.530
4 274.803	Cr I	(1)	-0.231
4 558.659	Cr II	(44)	-0.660	050	-7.50	024	-7.41	021:	-8.02
4 260.479	Fe I	(152)	-0.020	040	-6.12	018:	-6.40
4 271.764	Fe I	(42)	-0.164	079	-5.82	032:	-6.11	056	-6.09	037:	-6.51
4 325.765	Fe I	(42)	-0.010	076	-5.95	020	-6.45	041	-6.36	038	-6.58
4 383.547	Fe I	(41)	+0.200	097	-5.80	052	-6.13	065	-6.35	054	-6.68
4 404.752	Fe I	(41)	-0.142	079	-5.80	046	-5.84	048	-6.17	040	-6.45
4 415.125	Fe I	(41)	-0.615	050:	-5.80
4 447.722	kfe	(68)	-1.342
4 476.021	Fe I	(350)	-0.570
4 494.568	Fe II	(68)	-1.136
4 296.567	Fe II	(28)	-3.010	024:	-5.87	019	-5.56
4 303.166	Fe II	(27)	-2.490	055	-5.83	045	-5.39	027	-6.26
4 385.381	Fe II	(27)	-2.570	043	-5.90	030	-5.65	019	-6.31
4 416.817	Fe II	(27)	-2.600	048	-5.79	027	-5.69	021	-6.23
4 489.185	Fe II	(37)	-2.970	024:	-5.83	020	-5.50
4 491.401	Fe II	(37)	-2.700	027:	-6.02	034	-5.47
4 508.283	Fe II	(38)	-2.210	062	-5.90	033	-5.90	024	-6.33	024	-6.51
4 515.337	Fe II	(37)	-2.480	049	-5.85	025	-5.84	024	-6.07	020	-6.33	014:	-6.54
4 520.225	Fe II	(37)	-2.600	042	-5.87	030	-5.60	029	-6.04
4 522.634	Fe II	(38)	-2.030	071	-5.94	039	-5.93	041	-6.19	047	-6.31	034:	-6.55
4 541.523	Fe II	(38)	-3.050	021:	-5.81	020	-5.41
4 555.890	Fe II	(37)	-2.290	063	-5.83	032	-5.84	023:	-6.50
4 554.033	Ba II	(1)	+0.170	025	-11.27

Table 4. Line wavelengths, equivalent widths (in mÅ), and abundances for the stars observed at KPNO (continued)

λ (Å)	Species	Mult. no.	$\log gf$	HD 167105		HD 180903		HD 202759		Sources [†] of $\log gf$
				W_λ	$\log \epsilon$	W_λ	$\log \epsilon$	W_λ	$\log \epsilon$	
4 390.585	Mg II	(10)	-0.530	KP
4 481.21	Mg II	(4)	-0.978	208	-5.77	261	-5.34	100	-6.33	NBS1
4 318.652	Ca I	(5)	-0.208	026	-6.88	NBS1
4 434.960	Ca I	(4)	-0.029	028	-7.03	NBS1
4 455.887	Ca I	(4)	-0.510	050	-6.20	NBS1
4 246.829	Sc II	(7)	+0.320	155	-9.61	044:	-11.20	MFW
4 325.010	Sc II	(15)	-0.440	028	-10.44	019:	-10.73	MFW
4 400.355	Sc II	(14)	-0.510	038	-10.19	NBS2
4 287.893	Ti II	(20)	-2.020	038	-7.93	MFW
4 290.222	Ti II	(41)	-1.120	037	-8.02	158	-7.09	049:	-8.65	MFW
4 300.052	Ti II	(41)	-0.770	060	-8.04	159	-7.42	076	-8.54	MFW
4 301.928	Ti II	(41)	-1.160	078	-8.22	023	-9.09	MFW
4 312.861	Ti II	(41)	-1.160	018	-8.34	094	-8.03	034	-8.85	MFW
4 386.858	Ti II	(104)	-1.260	028	-7.73	MFW
4 394.057	Ti II	(51)	-1.590	023	-8.55	MFW
4 395.031	Ti II	(19)	-0.660	051	-8.33	141	-7.92	078	-8.70	MFW
4 395.848	Ti II	(61)	-2.170	014	-8.19	MFW
4 399.767	Ti II	(51)	-1.270	064	-8.24	031	-8.76	MFW
4 411.080	Ti II	(115)	-1.060	019	-7.77	MFW
4 417.718	Ti II	(40)	-1.430	019:	-8.07	083	-7.91	MFW
4 443.802	Ti II	(19)	-0.700	047	-8.35	128	-8.10	062	-8.95	MFW
4 450.487	Ti II	(19)	-1.450	067	-8.14	MFW
4 464.458	Ti II	(40)	-2.080	040	-7.79	MFW
4 468.493	Ti II	(31)	-0.600	051	-8.36	144	-7.91	067	-8.92	MFW
4 488.319	Ti II	(115)	-0.820	020:	-8.03	MFW
4 501.270	Ti II	(31)	-0.750	042	-8.35	132	-7.97	063	-8.84	MFW
4 529.465	Ti II	(82)	-2.030	031	-7.69	MFW
4 533.966	Ti II	(50)	-0.770	052	-8.12	161	-7.37	066	-8.69	MFW
4 563.761	Ti II	(50)	-0.960	036	-8.17	124	-7.81	049	-8.79	MFW
4 571.971	Ti II	(82)	-0.530	059:	-8.05	MFW
4 274.803	Cr I	(1)	-0.231	040:	-7.99	019	-8.58	MFW
4 558.659	Cr II	(44)	-0.660	019	-7.80	054	-7.69	028	-8.12	MFW
4 260.479	Fe I	(152)	-0.020	072	-6.11	FMW
4 271.764	Fe I	(42)	-0.164	070:	-6.67	FMW
4 325.765	Fe I	(42)	-0.010	032	-6.02	113	-6.16	070	-6.73	FMW
4 383.547	Fe I	(41)	+0.200	042	-6.15	144	-5.93	090	-6.62	FMW
4 404.752	Fe I	(41)	-0.142	024:	-6.07	108	-6.15	072	-6.60	FMW
4 415.125	Fe I	(41)	-0.615	103	-5.71	038:	-6.70	FMW
4 447.722	Fe I	(68)	-1.342	013	-5.95	FMW
4 476.021	Fe I	(350)	-0.570	023	-5.97	BK
4 494.568	Fe I	(68)	-1.136	020:	-5.96	FMW
4 273.317	Fe I	(27)	-3.258	FMW
4 296.567	Fe II	(28)	-3.010	FMW
4 303.166	Fe II	(27)	-2.490	018:	-6.21	018	-6.81	FMW
4 385.381	Fe II	(27)	-2.570	012	-6.28	051	-6.04	017	-6.73	FMW
4 416.817	Fe II	(27)	-2.600	016:	-6.11	059	-5.92	FMW
4 489.185	Fe II	(37)	-2.970	006:	-6.20	FMW
4 491.401	Fe II	(37)	-2.700	014:	-6.03	046	-5.93	FMW
4 508.283	Fe II	(38)	-2.210	075	-6.07	029	-6.74	FMW
4 515.337	Fe II	(37)	-2.480	059	-6.00	018:	-6.74	FMW
4 520.225	Fe II	(37)	-2.600	026	-5.86	068	-5.79	014:	-6.77	FMW
4 522.634	Fe II	(38)	-2.030	038	-6.18	096	-5.99	041	-6.71	FMW
4 541.523	Fe II	(38)	-3.050	032	-5.81	010:	-6.45	FMW
4 555.890	Fe II	(37)	-2.290	030	-6.06	071	-6.05	020	-6.89	FMW
4 554.033	Ba II	(1)	+0.170	051:	-11.46	008::	-12.62	NBS3

Table 4. Line wavelengths, equivalent widths (in mÅ), and abundances for the stars observed at KPNO (continued)

[†] Sources of $\log gf$: KP (Kurucz & Peytremann 1975); NBS1 (Wiese, Smith & Miles 1969);
 NBS2 (Wiese & Fuhr 1975); NBS3 (Miles & Wiese 1969);
 MFW (Martin, Fuhr & Wiese 1988); FMW (Fuhr, Martin & Wiese 1988); BK (Bridges & Kornblith 1974).

Table 5. Line wavelengths, equivalent widths (in mÅ), and abundances for the stars observed with the ESO-CAT.

λ	Species	Mult. no.	$\log gf$	HD 4850		HD 13780		HD 16456		HD 31943		HD 78913	
				W_λ	$\log \epsilon$	W_λ	$\log \epsilon$	W_λ	$\log \epsilon$	W_λ	$\log \epsilon$	W_λ	$\log \epsilon$
4 481.2	Mg II	(4)	-0.978	272	-5.10	224	-5.58	192	-5.85	354	-4.91	232	-5.43
4 455.887	Ca I	(4)	-0.510	021	-6.53
4 464.458	Ti II	(40)	-2.080	023	-7.66	026	-7.89	029	-8.10	054	-7.52
4 468.493	Ti II	(31)	-0.600	109	-7.59	117	-7.71	115	-8.47	177	-7.77	075	-8.23
4 488.319	Ti II	(115)	-0.820	020	-7.65	022	-7.82	015	-8.19	041	-7.51
4 501.270	Ti II	(31)	-0.750	098	-7.69	089	-8.18	104	-8.49	154	-7.91
4 466.570	Fe I	(2)	-0.590	008	-5.86	015	-5.97	017	-6.26	043	-5.48
4 476.021	Fe I	(350)	-0.570	020	-6.19	047	-5.44
4 494.568	Fe I	(68)	-1.136	020	-6.11	037	-5.48
4 489.185	Fe II	(37)	-2.970	025	-5.71	026	-5.90	023	-6.16	062	-5.45
4 491.401	Fe II	(37)	-2.700	032	-5.82	028	-6.11	033	-6.22	078	-5.53

λ	Species	Mult. no.	$\log gf$	HD 106304		HD 130095		HD 130201		HD 139961		HD 180903	
				W_λ	$\log \epsilon$	W_λ	$\log \epsilon$	W_λ	$\log \epsilon$	W_λ	$\log \epsilon$	W_λ	$\log \epsilon$
4 481.2	Mg II	(4)	-0.978	234	-5.28	142	-6.12	332	-4.66	211	-5.79	271	-5.26
4 464.458	Ti II	(40)	-2.080	017	-7.66	037	-7.84
4 468.493	Ti II	(31)	-0.600	030	-8.29	022	-8.86	082	-7.98	076	-8.41	149	-7.82
4 488.319	Ti II	(115)	-0.820	025	-7.85
4 466.570	Fe I	(2)	-0.590	021	-6.01
4 476.021	Fe I	(350)	-0.570	020	-6.04
4 489.185	Fe II	(37)	-2.970	025	-6.03
4 491.401	Fe II	(37)	-2.700	040	-5.54	043	-5.98

λ	Species	Mult. no.	$\log gf$	HD 202759		HD 213468	
				W_λ	$\log \epsilon$	W_λ	$\log \epsilon$
4 481.2	Mg II	(4)	-0.978	094	-6.38	193	-5.71
4 464.458	Ti II	(40)	-2.080	012	-8.52	013	-7.53
4 468.493	Ti II	(31)	-0.600	067	-8.92	045	-8.32
4 488.319	Ti II	(115)	-0.820	004	-8.79
4 501.270	Ti II	(31)	-0.750	055	-8.98	040	-8.27
4 466.570	Fe I	(2)	-0.590	009	-6.57
4 489.185	Fe II	(37)	-2.970	009	-6.60
4 491.401	Fe II	(37)	-2.700	011	-6.75